Modeling a controlled-sourced, multichemical plume undergoing natural attenuation

by

Caitlin Anne Martin

A thesis
presented to the University of Waterloo
in fulfilment of the
thesis requirement for the degree of
Master of Science
in
Earth Sciences

Waterloo, Ontario, Canada, 2004

I hereby declare that I am the sole author of this thesis. This is a true copy of the thesis, including any required final revisions, as accepted by my examiners.

I understand that my thesis may be made electronically available to the public.

Abstract

Sampling of an emplaced creosote source installed below the water table at CFB Borden was conducted over a period of ten years, with over nine thousand samples taken from approximately 250 multilevel samplers. This extensive dataset was used in several attempts to model the multi-chemical plumes emanating from this emplaced source, and to further understand the chemical and biological processes affecting these plumes and their natural attenuation.

An aerobic microcosm study of naphthalene, 1-methylnaphthalene and acenaphthene was conducted in order to determine the possibility of interactions between these three chemicals. All three chemicals degraded within the eight days of the study, and the degradation of naphthalene and 1-methylnaphthalene was not affected by the presence of any of the three chemicals studied. Acenaphthene degraded more quickly when naphthalene was present in the microcosm.

The programs Visual MODFLOW and RT3D were used to model the transport and degradation of naphthalene at CFB Borden. Both a first order rate reaction module and a multiple electron acceptor reaction module were used, and contaminant mass was introduced to the model through a fence of observed concentrations. Good results were found at early time with the multiple electron acceptor reaction package, however at late time the model did not match to observations.

The program BIONAPL/3D was used in a similar attempt to model the transport and degradation of naphthalene. Naphthalene mass was introduced to the model through a fence of observed concentrations, and multiple electron acceptors were used to degrade this chemical. Results were good at early time, but at late time the model did not match observations.

BIONAPL was then used to simulate the dissolution of the original source NAPL. Several chemicals of interest were examined: naphthalene, m-xylene, 1-methylnaphthalene and acenaphthene. Naphthalene and m-xylene dissolved from the source at rates similar to observations, however the dissolution of 1-methylnaphthalene and acenaphthene was not as well modeled. As with the Visual MODFLOW model, the BIONAPL model which best matched observations generally worked well at early times, but did not at late times.

The models were not able to successfully simulate many processes that occur in the field, such as chemical and biological interactions and NAPL source dissolution. Mismatches between the models and observations are likely due to these reasons. It may be that we do not fully understand these processes, so we are unable to model them.

Acknowledgments

Thanks first of all to my supervisor, Jim Barker, who offered me a project that let me make good use of my analytical skills. His ability to understand my piles of graphs and keep me focused on the "big picture" for this project has been greatly appreciated.

Thanks to Waterloo Hydrogeologic Inc. for helping to fund my work through the NSERC Industrial Postgraduate Scholarship program, and for offering me the use of their company resources in my modeling work. Thanks especially to Hugh McCreadie, my guide through the Visual MODFLOW part of my work, for always being available for a quick discussion about my problem of the day, and for encouraging me to work to the best possible solution. Thanks also to Miln Harvey for helping me to wrap up my lab exercise, and to Nilson Guiguer for agreeing to support my studies. I am also grateful for the friendliness shown to me by all the employees at WHI.

Thanks also to Barb Butler for her help and advice in designing the microcosm experiment, and to Marianne VanderGriendt for her attention to detail in setting up and running the experiment. Thanks to Claudia Naas and Michelle Fraser for collecting the sand and water samples from CFB Borden, and to Michelle again for helping out in the lab whenever she could.

John Molson has been a tremendous help with the BIONAPL modeling part of my study. He has been generous with his time and source code, explaining how the model works, and modifying the program to allow me to collect the data I needed, or to represent the source in a new way. Whenever he was on campus, he tried to find time to discuss the problems I was having with the model, and to offer suggestions and advice.

Dedication

To Jean-Luc - for always being my best friend. Your support, love, and patience have meant everything to me over the years, and your passion for learning has inspired me. Here's to finally living our adventures together in the same city!

Contents

List of Figures

List of Tables

Chapter 1

Introduction

1.1 Background - creosote emplaced source

In the summer of 1991, a coal tar creosote source was emplaced below the water table at Canadian Forces Base (CFB) Borden, upgradient of an existing dense network of multilevel wells. The resulting groundwater plume was allowed to develop under natural gradient conditions, and was sampled intensively over a period of ten years.

Coal tar creosote consists of over 200 organic compounds, and at this site, the various compounds separated chromatographically to form single compound plumes. Several different plume behaviours were observed: some compounds leached quickly from the source and disappeared rapidly, some took a very long time to develop and are still growing, and others grew, peaked in size and extent, and began to retreat during the time frame of the monitoring [8].

CFB Borden is an extremely well studied site. The aquifer is a glaciofluvially deposited sand, consisting of a complex distribution of beds and lenses of fine-, medium- and coarse-grained sand. Locally, the aquifer is very heterogeneous, but on a larger scale the aquifer is reasonably uniform. The hydrogeologic character of the site sand is well known, having been studied by MacFarlane et al. [5], Sudicky et al. [12], Mackay et al. [6] and others. Properties of the aquifer are summarized in Table 1.1. Groundwater velocity through the sand averaged $9\,\mathrm{cm}\,/\,\mathrm{d}$ and was nearly horizontal, in a predominantly northerly direction, varying between N11W and N50E over the first two years of monitoring. The gradient varied from 0.002 to 0.0053 over the first two years of monitoring, with a time-weighted average of 0.0039.

Parameter	**Method/Result**	**Source**
Mineralogy	analysis of bulk sample by X-ray diffraction: quartz 58%, feldspars 19%, carbonates 14%, amphiboles 7%, chlorite 2%	Mackay et al. (1986)
Porosity	volume weighted arithmetic mean of 36 samples: 0.33	Mackay et al. (1986)
Bulk density	volume weighted arithmetic mean of 36 samples: 1.81g/cm^3	Mackay et al. (1986)
Solids density	volume weighted arithmetic mean of 36 samples: 2.71g/cm^3	Mackay et al. (1986)
Organic carbon content	average of 0.02%; ranging from 0.01% to 0.09%	Mackay et al. (1986)
Hydraulic conductivity	-slug tests at 26 points; mean of $7x10^{-5}$ m/s -falling head permeameter tests with 1279 samples; overall geometric mean of $9.75x10^{-5}$ m/s	Mackay et al. (1986) Sudicky (1986)
Depth to water table	varies with time from ground surface to 1.5 m below grade	Linderfelt and Wilson (1994)
Hydraulic gradient	ranged from 0.002 to 0.0053 over first two years of current study period; time weighted average of 0.0039	Linderfelt (pers. comm.)
Groundwater flow direction	ranged from N11W to N50E over first two years of current study period; predominant flow direction was N21E	Linderfelt (pers. comm.)
Groundwater velocity	-1038 day tracer test: 0.091 m/day -476 day tracer test: 0.0933 to 0.0947 m/day -108 day tracer test: 0.081 m/day -emplaced source monitoring: 0.066 to 0.085 m/day	Mackay et al. (1986) Hubbard et al. (1994) Patrick (1986) King (1999a & b)
Apparent dispersivity	-tracer test with 11m plume displacement α_L = 0.08 m α_{TH} = 0.03 m $D_{TV} = 10^{-10}$ m^2/s -tracer test with approx. 60 m plume displacement α_L = 0.36 m α_{TH} = 0.039 m	Sudicky et al. (1983) Freyberg (1986)

Table 1.1: Characteristics of the Borden Aquifer

The creosote source was emplaced hydraulically upgradient of an existing network of approximately 250 multilevel samplers. Sand was mixed with creosote and emplaced in two adjacent excavations measuring approximately 1.5 m deep by 2 m wide by 0.5 m thick. The source configuration consisted of two identical sources emplaced side by side with 1 m between them. At the time of emplacement, it was thought that each source would develop a separate creosote plume, however as time progressed, the plumes emanating from each source were too close to one another and converged to form one single plume.

The samplers typically have 14 ports on 20 or 30 cm vertical intervals. Over 9000 groundwater samples were taken over a period of ten years on several snapshot days, with analysis for at least six or seven chemicals at each snapshot day. Concentrations of each chemical were recorded in a database listing the location of each sample and the sampling date. The progress of the six or seven chemicals of interest has been described in King [3] and Martin [8], along with mass balances for each plume. The mass balances calculated the mass flux from the source at a fence located approximately 3 m downgradient of the source; this fence was used in order to avoid data interpolation errors that would occur with the steep concentration gradients closer to the source. At each sampling day, samples were taken from wells along this 3 m fence and throughout the study area, and the concentrations entering the plume across this fence were well characterized at each snapshot day. By performing a three-dimensional integration of the sampling data, the total dissolved plume mass could be found; by integrating over the vertical plane of the 3 m fence, the mass flux into the plume at this fence could be calculated.

A funnel-and-gate treatment system was installed at approximately day 2100, and the behaviour of the naphthalene plume in the field after this time may have been affected, both physically and chemically, by this treatment system. The funnel-and-gate, located at approximately northing 4902570, was designed to funnel naphthalene contaminated water through the gate, and treat the naphthalene plume with nitrate briquettes. Treatment was ended before sampling day 3619. During the time when the funnel-and-gate was in use, no groundwater samples were taken downgradient of northing 4902570.

King [4] described a conceptual model of the creosote plume behaviour at this site with plume growth occurring by source dissolution, advection and dispersion, and plume mass decreasing by biodegradation. Oxygen was the primary electron acceptor at the edges of the plume, with nitrate, iron/manganese, sulfate and carbon dioxide acting as primary electron acceptors in the anaerobic core of the plume. The highest biodegradation potential was at the fringes of the plume where electron acceptor concentrations were highest, while the least biodegradation potential was

in the core of the plume where electron acceptors had been most depleted.

1.2 Previous Borden modeling work

Malcolmson [7] used an equilibrium solubility model in an attempt to predict the aqueous concentrations of creosote compounds at this field site. She did not attempt to model the transport of any of the creosote chemicals.

King performed some modeling of dibenzofuran using the code BIO3D [2]. In modeling this single chemical, he was unable to simulate the observed apparent steady state behaviour of this plume from sampling days 626 to 1357. Instead, the modeled plume migrated substantially further than the observed plume, with two possible explanations: 1) a significant portion of the biodegradation utilized electron acceptors other than oxygen, nitrate, iron, and sulfate, and 2) biodegradation did not proceed to complete mineralization so that the stoichiometric ratio used for dibenzofuran transformation was unrealistically large [2]. King performed a mass balance to evaluate the overall expected contribution of each electron acceptor to biodegradation of selected plume organics. He found that assuming complete mineralization, the change in electron acceptors accounted for much less than the observed organic mass transformed. Incomplete mineralization (fermentation) may have occurred in the field, as well as biodegradation utilizing other electron acceptors.

1.3 Purpose of this work

The purpose of this study is to better understand the processes governing biodegradation of the various components of the creosote plume by using groundwater models to simulate these processes, and attempting to calibrate reaction parameters in these models so that the model output matches field observations. As a first attempt, Visual MODFLOW with RT3D was used to produce a flow and transport model of the CFB Borden study site. This is a popular model used by many groundwater professionals; this part of the study examined how well an "off-the-shelf" model could simulate the transport and degradation of one component of the creosote plume. Only one contaminant could be simulated in the reaction module chosen, but multiple electron acceptors could be used. The contaminant source was represented as a fence of constant-concentration cells, with concentrations equal to observed aqueous phase concentrations at this same location. The concentrations

changed with time to reflect the changing flux values measured at the fence. This was the most convenient way to represent the mass entering the plume, as fixed concentration observations along the fence were available at each sampling day, and Visual MODFLOW did not have the capability to dissolve a complex NAPL source.

A more complex model was also used to simulate the transport and degradation of several plumes. This model, BIONAPL, is capable of representing the dissolving source DNAPL, resulting in a more comprehensive, physically realistic approach. The entire emplaced source mass was represented in the model; selected chemicals of interest were chosen to be simulated. Reaction parameters were varied to obtain a best fit to the observed data. In cases where the observed plume behaviour could not be simulated with this model, it was possible to conclude that the model was not representing all processes occurring in the field, i.e. chemical interaction and inhibition, and interference from degradation products. These factors could not be considered by King [4], but this study attempts to evaluate them with the use of the more sophisticated BIONAPL model.

A microcosm study was conducted to verify some of the proposed interactions of biodegrading chemicals. In the BIONAPL model, the chemicals that were simulated matched observations well for a time, but then the model degraded mass too quickly at later times for some chemicals, and degraded mass too slowly for other chemicals. The hypothesis was that in the field, interactions and inhibitions from chemicals not specifically modelled were slowing degradation of some of the chemicals of interest; interactions and cometabolism may have increased degradation in the field for other chemicals. This led to the model over-predicting the degradation rate of some chemicals, and under-predicting it for others. The microcosm study was designed to examine interactions between three chemicals, one of which was suspected of inhibiting degradation of the other two.

Chapter 2

Microcosms

2.1 Purpose

It was suspected that chemical interactions had occurred in the creosote plume at the CFB Borden field site. These interactions were believed to have affected the degradation of certain chemicals, such as naphthalene. In order to test this hypothesis, a microcosm study was initiated to study interactions, if any, between naphthalene and other plume chemicals. Naphthalene was the monitored plume chemical that travelled the farthest through the study site over the course of monitoring, and as this plume was at its largest, its behaviour at late times indicated that degradation was occurring more slowly than anticipated. The presence of any other chemicals in the area was investigated in order to see if these chemicals were likely to have interfered with the naphthalene plume. The only monitored plumes which overlapped significantly with the naphthalene plume at farther distances were 1-methylnaphthalene and acenaphthene.

This microcosm study compared the aerobic degradation of naphthalene in the presence of 1-methylnaphthalene and acenaphthene with the degradation of these three chemicals separately. The results will indicate if these three chemicals may be interacting to retard or enhance plume growth.

2.2 Method

The method for these microcosms was prepared by Marianne VanderGriendt, and a complete method is available in Appendix A. Five sets of static batch micro-

cosms were prepared: an inactive (sterile) mix of the three chemicals, a biologically active mix of the three chemicals, an active naphthalene only set, active 1-methylnaphthalene only, and active acenaphthene only. Each set was prepared in triplicate, with enough microcosms for ten sampling rounds.

Each microcosm contained 10 g of CFB Borden sand and 35 ml of CFB Borden groundwater in a 60 ml glass hypovial with a Teflon-faced septum and aluminum crimp top seal. The sand was taken from the study site in a creosote contaminated area where these three plumes had existed in the past, so that the microorganisms in the sand were already acclimated to the three chemicals. The groundwater was pristine, so that there was no existing concentration of any of the three chemicals or their degradation products in the water. Before use in the experiment, the groundwater was aerated with sterile air to a dissolved oxygen level of 8.2 mg / l. Further details of the sand and groundwater sampling procedures are provided in Appendix A.

Four types of groundwater were prepared for this experiment. Type 1 water contained all three chemicals, while types 2, 3 and 4 contained, respectively, added naphthalene, 1-methylnaphthalene and acenaphthene. The target concentrations in these waters was 2 mg / l of naphthalene, 2 mg / l of 1-methylnaphthalene and 1 mg / l of acenaphthene. All microcosms received the addition of 0.65 ml of Modified Bushnel Haas Medium to ensure that inorganic nutrients were available to the microorganisms. A headspace of approximately 20 ml was left in each microcosm to allow for aerobic conditions during biodegradation. Microcosms were sealed after groundwater addition, and incubated in the dark at room temperature.

Sampling times occurred after 1, 14, 23, 38, 48.5, 62, 135, 160, and 183 hours, and samples were analysed by gas chromatography as described in Appendix A.

2.3 Results

Results for the three chemicals used in the microcosms are shown in Figures 2.1, 2.2 and 2.3. As can be seen in each of these figures, the concentrations in the control microcosms (Con Mix) were stable through the experiment. In each of the other four sets, all three chemicals degraded to below method detection limits by the end of the 8 days of the experiment.

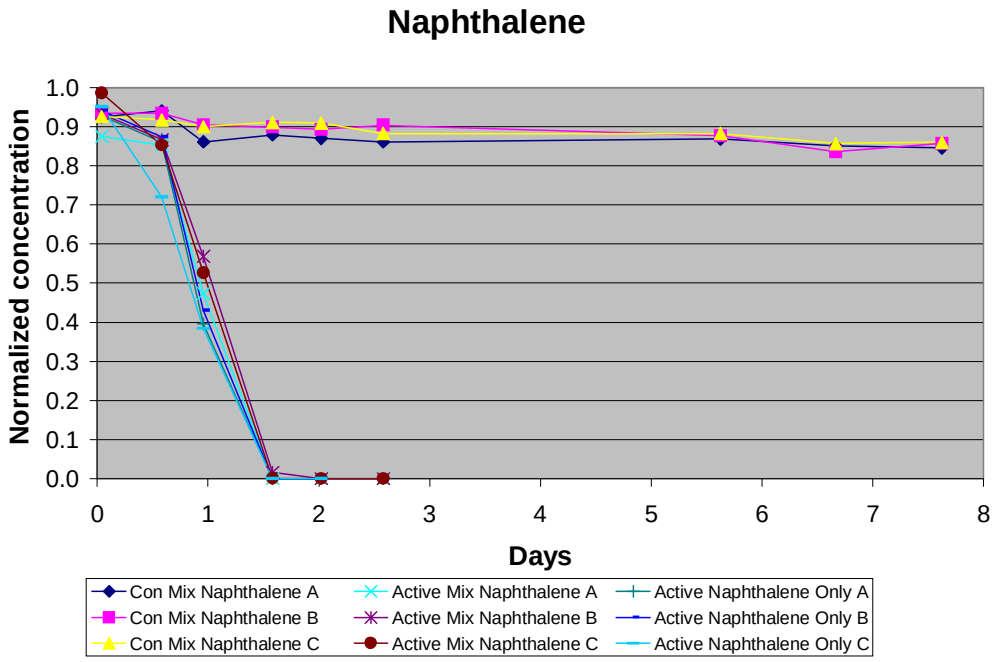

Figure 2.1: Microcosm results for naphthalene: "Con" = control set, "Active" indicates that soil was not sterilized, "Mix" indicates that all three chemicals were used

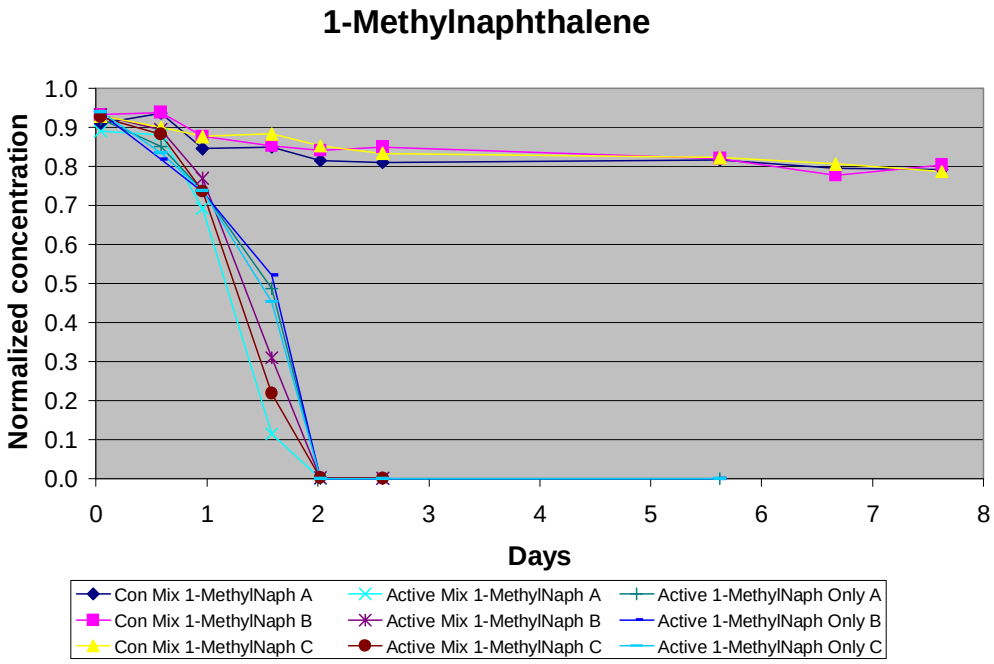

Figure 2.2: Microcosm results for 1-methylnaphthalene: "Con" = control set, "Active" indicates that soil was not sterilized, "Mix" indicates that all three chemicals were used

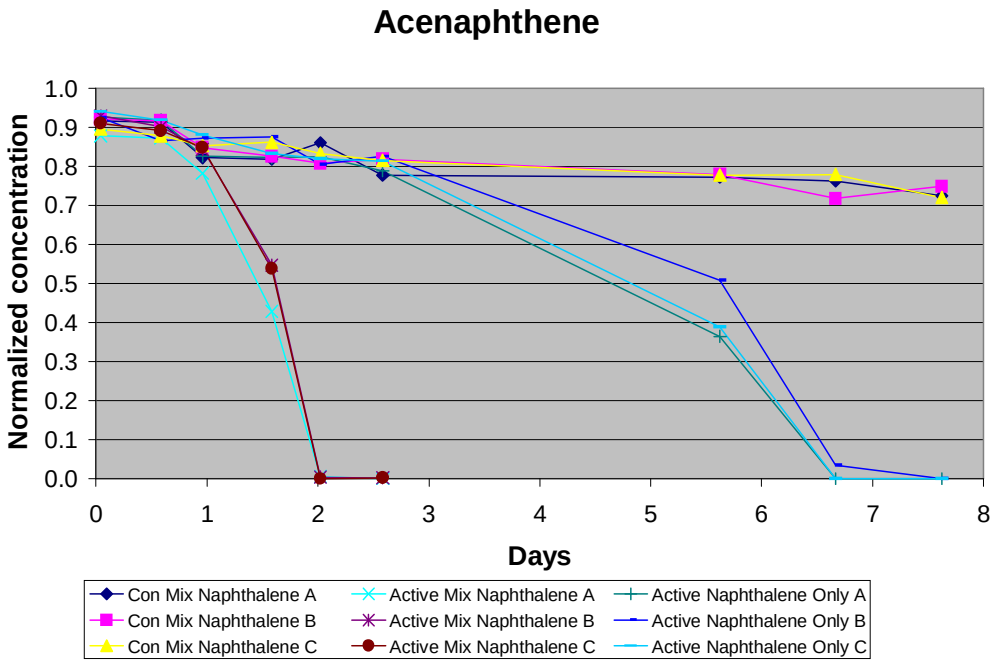

Figure 2.3: Microcosm results for acenaphthene: "Con" = control set, "Active" indicates that soil was not sterilized, "Mix" indicates that all three chemicals were used

2.3.1 Naphthalene

For the naphthalene sets, the initial concentrations were different for the "naphthalene only" set, as compared with the control mix set and the active mix set. This was due to breakage of the jar containing groundwater with dissolved naphthalene; this water was used in the setup of the "naphthalene only" microcosms. Unfortunately, when this water was remade, the naphthalene concentration was somewhat lower than in the active mix and control mix water. The initial concentrations for the naphthalene mix microcosms (active and control) ranged from 2.5 to 2.8 mg / l (Figure 2.1), while the "naphthalene only" set had initial concentrations closer to 2 mg / l.

In both active sets (mix and naphthalene only), naphthalene degraded completely in 38 hours. Both sets showed an initially slower degradation rate, with a dramatic increase in rate after 14 hours. After this point, both sets had approximately the same slope and degraded at approximately the same rate. The presence of 1-methylnaphthalene and acenaphthene did not appear to affect the degradation rate of naphthalene in this experiment.

2.3.2 One-methylnaphthalene

The 1-methylnaphthalene initial concentrations were all consistent at approximately 2 mg / l. The "1-methylnaphthalene only" set had an initial slower degradation rate which increased significantly after 14 hours, and the chemical was undetectable in the microcosms after 48.5 hours. The active mix showed an initial degradation rate that was slightly higher than in the "1-methylnaphthalene only" set, with a rate increase after 38 hours, but this set also had no detectable 1-methylnaphthalene after 48.5 hours. There is a slight difference in slope between the active mix set and the "1-methylnaphthalene only" set, but the difference is too small to be considered significant in this experiment. The presence of naphthalene and acenaphthene did not appear to affect the degradation rate of 1-methylnaphthalene.

2.3.3 Acenaphthene

The initial concentration of acenaphthene in the "acenaphthene only" set was at the target value of 1 mg / l. However, the initial concentration in the active mix and control mix sets was below the target concentration, at approximately $0.65 - 0.7$ mg / l. This was despite an additional amount of acenaphthene that was added to the water before the microcosms were assembled. In any case, the active mix

showed an initial degradation rate that was very slow, but increased after 23 hours had passed. Degradation continued until no acenaphthene was detected in this set after 48.5 hours. The "acenaphthene only" set also had a slow initial degradation rate, but this initial slow rate lasted for much longer - until 62 hours had passed, and possibly to some time before 135 hours. After this time, the "acenaphthene only" set degraded at a higher rate until the acenaphthene was completely consumed by 183 hours.

2.4 Conclusions and implications for future work

The naphthalene-containing microcosms showed no significant difference in degradation rates between sets containing only naphthalene, and sets containing the mix of three chemicals. Similar observations were made for the sets containing 1-methylnaphthalene. The degradation of naphthalene in this experiment was not affected by the presence of 1-methylnaphthalene or acenaphthene; similarly, the degradation of 1-methylnaphthalene was not affected by the presence of naphthalene or acenaphthene.

The acenaphthene sets showed some differences, which are made somewhat more difficult to interpret by the fact the active mix set and the "acenaphthene only" set had different initial concentrations of acenaphthene. However, the active mix set had an earlier onset of degradation than did the "acenaphthene only" set. Acenaphthene was observed to degrade more quickly in the presence of naphthalene and/or 1-methylnaphthalene. It may be argued that the microorganisms were hindered by the higher initial concentration in the "acenaphthene only" set and were not able to degrade mass as quickly as in the active mix set, however it is more likely that rapid degradation of the acenaphthene relied on the presence of enzymes that are involved in the initial oxidation of naphthalene. This is supported by a paper by Selifonov et al. [11] in which it was shown that acenaphthene could be cometabolized in an enrichment culture through the activity of enzymes such as naphthalene dioxygenase and phenanthrene dioxygenase. Selifonov et al. [11] also found a *Pseudomonas* species that could grow on acenaphthene as a primary substrate.

This experiment showed that the degradation of naphthalene and 1-methylnaphthalene was not affected by the presence of the compounds used in these microcosms. It was also shown that acenaphthene may degrade more easily in the presence of naphthalene and/or its degradation products. This experiment only compared a very small subset of the chemicals present in coal tar creosote, and

interactions between these and other chemicals in groundwater plumes emanating from creosote sources are more than likely. For modeling purposes, the behaviour of the acenaphthene plume may be considered dependant on other chemicals. In the CFB Borden field study, few other chemicals extended as far in the monitoring area as did naphthalene and 1-methylnaphthalene, so it is unlikely that chemicals interactions affected these plumes at far distances from the source, but in the cores of these plumes where there was more overlap with other plume chemicals, interactions may be more likely.

Chapter 3

Visual MODFLOW – simulation of the naphthalene plume

3.1 Purpose

Due to the spatial density of the sampling data and the length of the monitoring period, the CFB Borden emplaced creosote source dataset provided a unique opportunity to simulate the natural attenuation of an organic plume using RT3D. Sampling "snapshots" of the plume were taken at 55, 278, 439, 626, 1008, 1357, 2900, 3300 and 3619 days after source emplacement, so the concentration distributions and plume masses were well defined at each of these times. The size and extensive nature of this dataset offered an opportunity to test whether it was possible to calibrate such a model to observed naphthalene concentrations. Naphthalene was chosen to be simulated because it was the largest plume measured over the course of the monitoring. The purpose of the Visual MODFLOW portion of this study was to attempt to model the natural attenuation of naphthalene within the creosote plume, using two methods: a simple first order rate law model and a more complicated multiple electron acceptor model. The model was first calibrated to flow using chloride data collected from the field experiment of King [3], then the model degradation parameters were calibrated to observed naphthalene concentrations obtained from the field. The model was calibrated to early time data, allowing the model to be run forward to late time, in an attempt to see if the model could "predict" the late-time behaviour of the plume.

3.2 Visualization of observed data

The sheer volume of data made visualization of the three-dimensional extent of the naphthalene plume very difficult by two-dimensional contouring methods. Instead the program Visual Groundwater (Waterloo Hydrogeologic and SSESCO) was used to represent the complex three-dimensional sampling data in a format showing isosurfaces of various concentrations that could be animated through time. This program read in the sampling data at each well and interpolated these data to a three-dimensional grid. Once the grid was produced, it was possible to represent the observations as isosurfaces of constant concentration, and slices through the plume both vertically and horizontally were easily created. This made it possible to construct a slice through the approximate center of the naphthalene plume, at elevation 212.2 m above sea level. This slice has been used for comparing all plume images presented in this study, but during the calibration process, the entire plume was considered for the determination of goodness of fit. Goodness of fit was determined by eye; a good fit consisted of a plume contour which matched observations well in both length and width.

3.3 Method

In this study, the gradient was set using constant head boundaries at the ends of the study site, and the direction of groundwater flow was assumed to be constant in a northerly direction. Schirmer et al. (2001) showed that in the case of moderate changes of flow directions, such as at the Borden site, the use of a steady-state flow field can be justified, and the use of a higher transverse horizontal dispersivity under these conditions can adequately forecast plume development [10]. Recharge was applied to the top-most active layer. The flow model was constructed with a homogeneous hydraulic conductivity field in an attempt to see how well a very simple model could reproduce the field observations.

3.3.1 Choice of flow solution method

In Visual MODFLOW, there are many solution methods available with which to solve the flow portion of the model. Not every method will be applicable to every case, so extensive testing was performed to determine which solution method gave the most numerically accurate and mass-balanced solution. At the same time, the model grid was tested to determine the best grid discretization to suit the observed

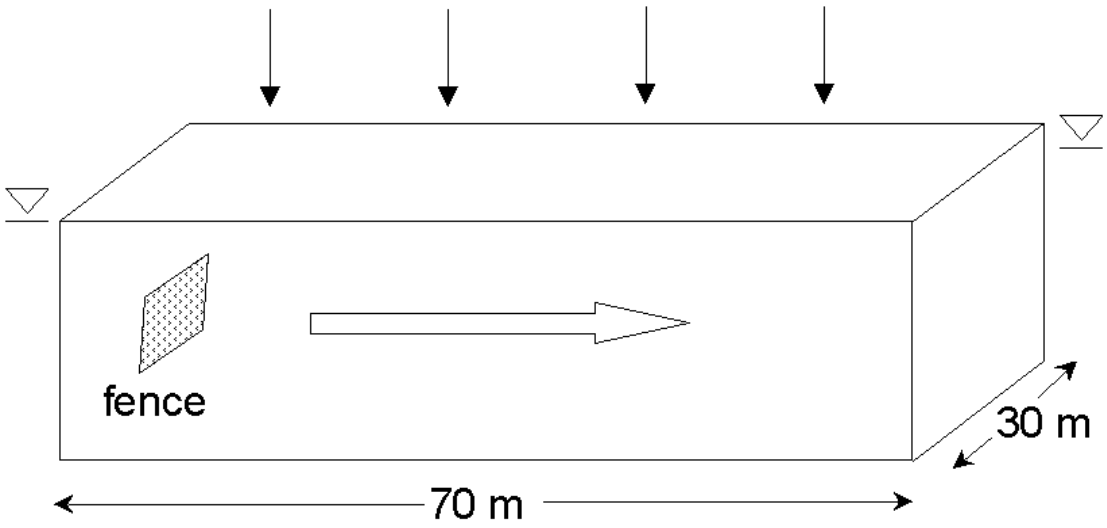

Figure 3.1: Conceptual figure of the CFB Borden model in Visual MODFLOW.

data, and to accommodate the model input. The model grid was initially defined as 30 m wide in the easterly direction, 70 m long in the northerly direction, and 7 m thick (Figure 3.1). The final grid had cells measuring 1 m $\times$1 m $\times$0.175 m, meaning that there were $30 \times 70 \times 40$ cells in the x-, y- and z-directions.

3.3.2 Calibration of the flow model

A quantity of sodium chloride was added to the source creosote at the time of emplacement as a non-reactive tracer [7]; the migration of this chloride was used to calibrate the flow model. This method was considered more accurate than relying on hydraulic head measurements, as there was less uncertainty in concentration measurements than in head measurements.

Chloride concentrations were measured twice before the chloride moved beyond the extent of the monitoring network, at days 55 and 439 after source emplacement. In the Visual MODFLOW simulation, the observed chloride concentrations at day 55 were input as a set of initial concentrations. These initial concentrations were modeled forward to day 439 using MT3D. Hydraulic conductivity and dispersion parameters were then manipulated within the range of literature values of these parameters (Table 3.1) to obtain the best fit of the calculated chloride concentrations to the field data. The best fit was determined by visual approximation of the

centre of mass, and by the location of various chloride contours.

3.3.3 First-order rate law model

Once the flow model was successfully calibrated it was used as a starting point for the first-order rate law model. Exactly the same flow conditions were used, but the migration and natural attenuation of the chemical naphthalene was simulated using the first order rate law.

The first-order rate law model uses the following governing equation:

$$R\frac{\partial C}{\partial t} = \frac{\partial}{\partial x_i}\left(D_{ij}\frac{\partial C}{\partial x_j}\right) - \frac{\partial}{\partial x_i}\left(v_i C\right) + \frac{q_s}{\theta}C_s - \lambda\left(C + \frac{\rho_b}{\theta}\bar{C}\right) \tag{3.1}$$

where

R is the retardation factor, defined as $R = 1 + \frac{\rho_b}{\theta}\frac{\partial \bar{C}}{\partial C}$, with ρ_b representing the bulk density of the porous medium

C is the dissolved contaminant concentration, ML^{-3}

t is time, T

x_i is the distance along the respective Cartesian coordinate axis, L

D_{ij} is the hydrodynamic dispersion coefficient, L^2T^{-1}

v_i is the seepage or linear pore water velocity, LT^{-1}

q_s is the volumetric flux of water per unit volume of aquifer representing sources and sinks, T^{-1}

C_s is the concentration of the sources or sinks, ML^{-3}

θ is the porosity of the porous medium, L^3L^{-3}

λ is the rate constant of the first-order rate reaction, T^{-1}

$\bar{C}$ is the concentration of contaminants sorbed on the porous medium, MM^{-1}.

A single rate reaction was used in this model to degrade the naphthalene plume. To simulate the creosote source, naphthalene was introduced to the model at a monitoring fence located approximately three metres from the source. This monitoring fence had been used extensively in past work characterizing the location of the chemical plumes. Since the distribution of chemicals in the near-source area was extremely complex, flux into each plume was measured at this three-metre-fence. In the model, the concentrations measured at each sampling port were assigned as constant concentration cells, with each concentration constant over a time interval that straddled each sampling day. Sorption of naphthalene was also simulated, using a solids partitioning coefficient (K_d) calculated by the batch test method described in [3]. The best fit of the naphthalene concentration contours to the observed data was found by manipulating only one parameter: the decay rate constant.

3.3.4 Multiple electron acceptor model

In the multi-electron acceptor model the same flow conditions, K_d, source concentrations and source configuration were used as in the first-order model, but multiple electron acceptor degradation reactions were used instead of the simple first-order reaction. The aerobic, denitrifying, and sulfate-reducing reactions were simulated since these were the most important electron acceptors with the potential to remove the most creosote mass from the plume [2]. The kinetic expressions used for modeling the naphthalene degradations are as follows:

$$r_{HC,O_2} = -k_{O_2}[HC]\left[\frac{[O_2]}{K_{O_2}+[O_2]}\right] \tag{3.2}$$

$$r_{HC,NO_3} = -k_{NO_3}[HC]\left[\frac{[NO_3]}{K_{NO_3}+[NO_3]}\right]\left[\frac{K_{i,O_2}}{K_{i,O_2}+[O_2]}\right] \tag{3.3}$$

$$r_{HC,SO_4} = -k_{SO_4}[HC]\left[\frac{[SO_4]}{K_{SO_4}+[SO_4]}\right]\left[\frac{K_{i,O_2}}{K_{i,O_2}+[O_2]}\right]\left[\frac{K_{i,NO_3}}{K_{i,NO_3}+[NO_3]}\right] \tag{3.4}$$

where

r_{HC,O_2} is the hydrocarbon destruction rate utilizing oxygen, $ML^{-3}T^{-1}$

r_{HC,NO_3} is the hydrocarbon destruction rate utilizing nitrate, $ML^{-3}T^{-1}$

r_{HC,SO_4} is the hydrocarbon destruction rate utilizing sulfate, $ML^{-3}T^{-1}$

$[HC]$ is the concentration of hydrocarbon, ML^{-3}

$[O_2]$ is the concentration of oxygen, ML^{-3}

$[NO_3]$ is the concentration of nitrate, ML^{-3}

$[SO_4]$ is the concentration of sulfate, $\_ML^{-3}$

k_{O_2} is the maximum degradation rate constant for hydrocarbon utilizing oxygen as the electron acceptor, T^{-1}

k_{NO_3} is the maximum degradation rate constant for hydrocarbon utilizing nitrate as the electron acceptor, T^{-1}

k_{SO_4} is the maximum degradation rate constant for hydrocarbon utilizing sulfate as the electron acceptor, T^{-1}

K_{O_2} is the Monod half-saturation constant for oxygen, ML^{-3}

K_{NO_3} is the Monod half-saturation constant for nitrate, ML^{-3}

K_{SO_4} is the Monod half-saturation constant for sulfate, ML^{-3}

K_{i,O_2} is the oxygen inhibition constant, ML^{-3}

K_{i,NO_3} is the nitrate inhibition constant, ML^{-3}.

The hydrocarbon (in this case naphthalene) degrades in the oxygen reaction at a rate dependant on the concentration of hydrocarbon, the concentration of oxygen, and the half-saturation constant. If the concentration of the hydrocarbon is high, then the degradation rate will be high. If the electron acceptor concentration is low, then the degradation rate will be low. If the half-saturation constant is high relative to the oxygen concentration, then the degradation rate will be low.

In the nitrate and sulfate reactions, the degradation rate is also dependant on inhibition constants. These constants control at what electron acceptor concentrations the naphthalene degradation will switch from a more energetic reaction to a less energetic reaction, e.g. from aerobic to denitrifying to sulfate-reducing. If the inhibition constants are low compared to the electron acceptor concentration, then the degradation reactions will tend to progress sequentially, using up each electron acceptor in sequence. If the inhibition constants are high relative to the electron

acceptor concentrations, then the various degradation reactions may occur more simultaneously.

Background electron acceptor concentrations measured at the site by King [4] were used as background concentrations in the model. Mass-based stoichiometric ratios for the consumption of naphthalene were calculated to be 3.0 for the oxidation reaction, 4.65 for denitrification, and 4.5 for sulfate reduction, as shown in the following reactions.

$$C_{10}H_8 + 12O_2 -> 10CO_2 + 4H_2O \tag{3.5}$$

$$C_{10}H_8 + 9.6NO_3^- + 9.6H^+ -> 10CO_2 + 4.8N_2 + 8.8H_2O \tag{3.6}$$

$$C_{10}H_8 + 6SO_4^{-2} + 12H^+ -> 10CO_2 + 6H_2S + 4H_2O \tag{3.7}$$

Three types of parameters were manipulated to obtain a best fit to the observed data: inhibition coefficients, half-saturation constants and decay rates.

3.4 Input problems

This experiment was initially designed so that the entire set of naphthalene concentration observations could be used in Visual MODFLOW to calibrate the reaction parameters. This involves plotting observed concentrations versus calculated concentrations at each sampling point. The better the match obtained between observed and calculated concentrations, the closer the plot would be to a $1:1$ slope. However, the total number of observations that Visual MODFLOW can import is limited to one thousand. The number of observations collected over the ten years of the study number more than nine thousand, often with more than one thousand samples taken in a single plume snapshot. This meant that it was impossible to use the calibration plot method provided in Visual MODFLOW. This method may have been quite useful in analysing the simulation results, however analysis of the goodness of fit was instead performed by comparing various longitudinal and transverse slices of the naphthalene plume.

Source of Dispersion Parameters	$\boldsymbol{\alpha_L}$(m)	$\boldsymbol{\alpha_H/\alpha_L}$	$\boldsymbol{\alpha_V/\alpha_L}$	**Hydraulic Conductivity** (m/s)
Best-fitting model	0.36	0.3	0.001	6.5×10^{-5}
Sudicky, 1983	0.08	0.38	0.0015	
Freyberg, 1986	0.36	0.11	n/a	

Table 3.1: Comparision of flow and transport parameters

3.5 Calibration

3.5.1 Flow model

After running the flow simulation and calibrating the flow parameters to observed data, the best fitting dispersion parameters were found to be $\alpha_L = 0.36$ m, $\alpha_H/\alpha_L = 0.3$, and $\alpha_V/\alpha_L = 0.001$ (Table 3.1), and the best fitting hydraulic conductivity was 6.5×10^{-5} m / s. These hydraulic conductivity and dispersion values are close to literature values, as found in [3]. In a tracer test with 11 m plume displacement, dispersion parameters were found to be $\alpha_L = 0.08$ m, $\alpha_H/\alpha_L = 0.38$, and $\alpha_V/\alpha_L = 0.0015$ [12], and in a tracer test with 60 m plume displacement, these parameters were found to be $\alpha_L = 0.36$ m and $\alpha_H/\alpha_L = 0.11$ [1]. This combination of parameters gives a normalized RMS value of 12.6%, slightly above the commonly accepted cosmetic target of 10%.

Upon examination of the observed chloride contours in Visual Groundwater (SSESCO Inc. and Waterloo Hydrogeologic Inc.), the calculated and observed chloride plumes at day 439 were similar in size, shape and location, as shown in Figure 3.2.

3.5.2 First-order rate law model results

The simple first-order rate model could not fit the naphthalene observations very well (Figure 3.3). The only variable that was altered in this model was the decay rate constant, but manipulation of the decay rate was not sufficient to duplicate the observed character of the plume. If the modeled rate constant was increased, then observed areas of high concentration near the source would become too depleted in the model; if the rate constant was decreased, then the low-concentration contours would extend too far in the model domain. Since the degradation rate was proportional to the rate constant and concentration, areas of high mass (near the source) would have been degraded at a higher rate than areas with low mass (away

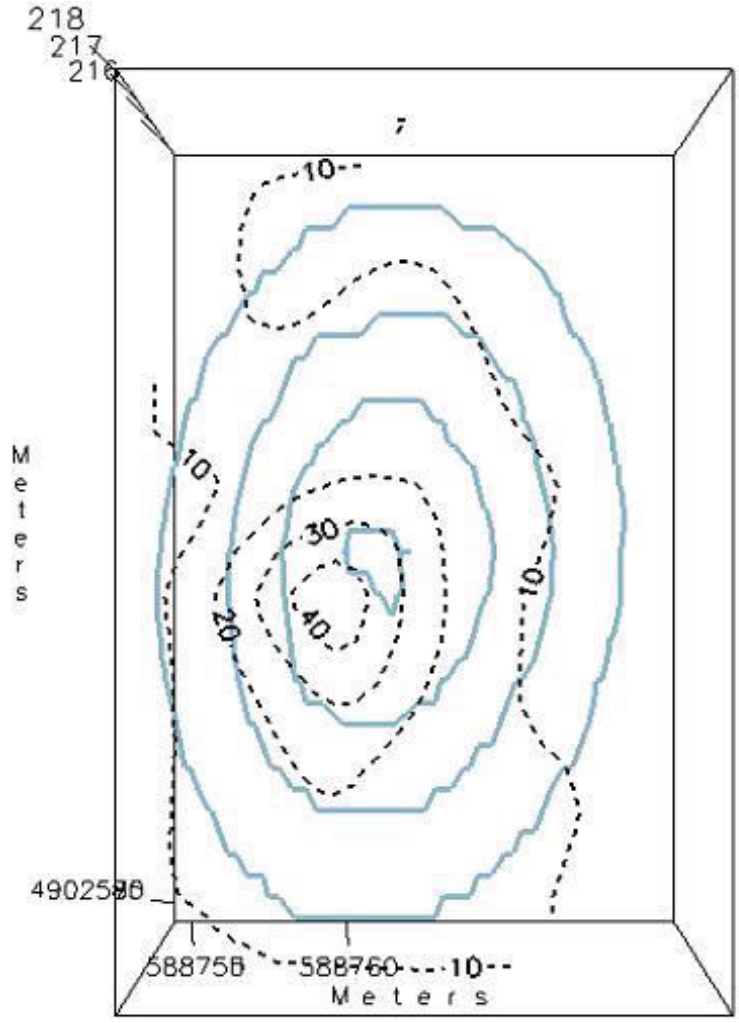

Figure 3.2: Day 439 calculated chloride contours (solid) overlaid on labeled observations (dash), layer elevation 218.2m. Contour interval is 10 mg/L.

	Cumulative Mass Degraded (kg)			**Plume Mass** (kg)		
Day	Observed	First-Order	Multi-e	Observed	First-Order	Multi-e
626	n/a	0.399	0.415	0.733	0.379	0.384
1357	0.277	1.138	1.169	1.243	0.240	0.253
3619	2.656	2.266	2.401	0.202	0.113	0.066

Table 3.2: Tabulation of naphthalene mass calculations for: observed mass change, best match first-order model and best match multi-electron acceptor model. n/a=figure not available. Observed figures taken from [1]

from the source). However, in the conceptual model as outlined in [4], the highest degradation potential should have occurred at the edges of the plume where more electron acceptors would be present.

As a result, the modeled plume concentrations were lower than observed near the source, and higher than observed away from the source (Figure 3.3). This was the case for each decay constant that was simulated. The best-fitting solution, matched to the observed $10\,\mu g\,/\,l$ contour, had a decay constant of $0.007\,d^{-1}$. The extent of the $10\,\mu g\,/\,l$ contour matched the observed results fairly well for most snapshots throughout the simulation, but in later snapshots the higher concentration contours (200 and $2000\,\mu g\,/\,l$) did not extend as far from the source as was observed. Too much degradation of naphthalene was occurring near the source. This reaction was not complex enough to simulate the naphthalene degradation very well, or perhaps other reaction parameters were not adequately represented in this model.

Mass balance results from the simulations are shown in Table 3.2. By day 3619, the first-order model degraded 2.27 kg of naphthalene, less than the 2.66 kg that was observed, and the modeled plume mass was smaller than observed at each of the sampling days.

3.5.3 Multiple electron acceptor model results

The best match had the reaction parameters shown in Table 3.3. Using the multi-electron acceptor model, the results were quite similar to the first-order model (Figure 3.4). The modeled plume concentration contours are still too spread out; throughout the simulation, higher concentrations still did not migrate as far from the source as was observed, although at day 1357, the $200\,\mu g\,/\,l$ contour showed some improvement over the first order model. However, too much degradation of naphthalene was still occurring near the source, and there was no significant improvement in the highest concentration contours. The mass degraded by the

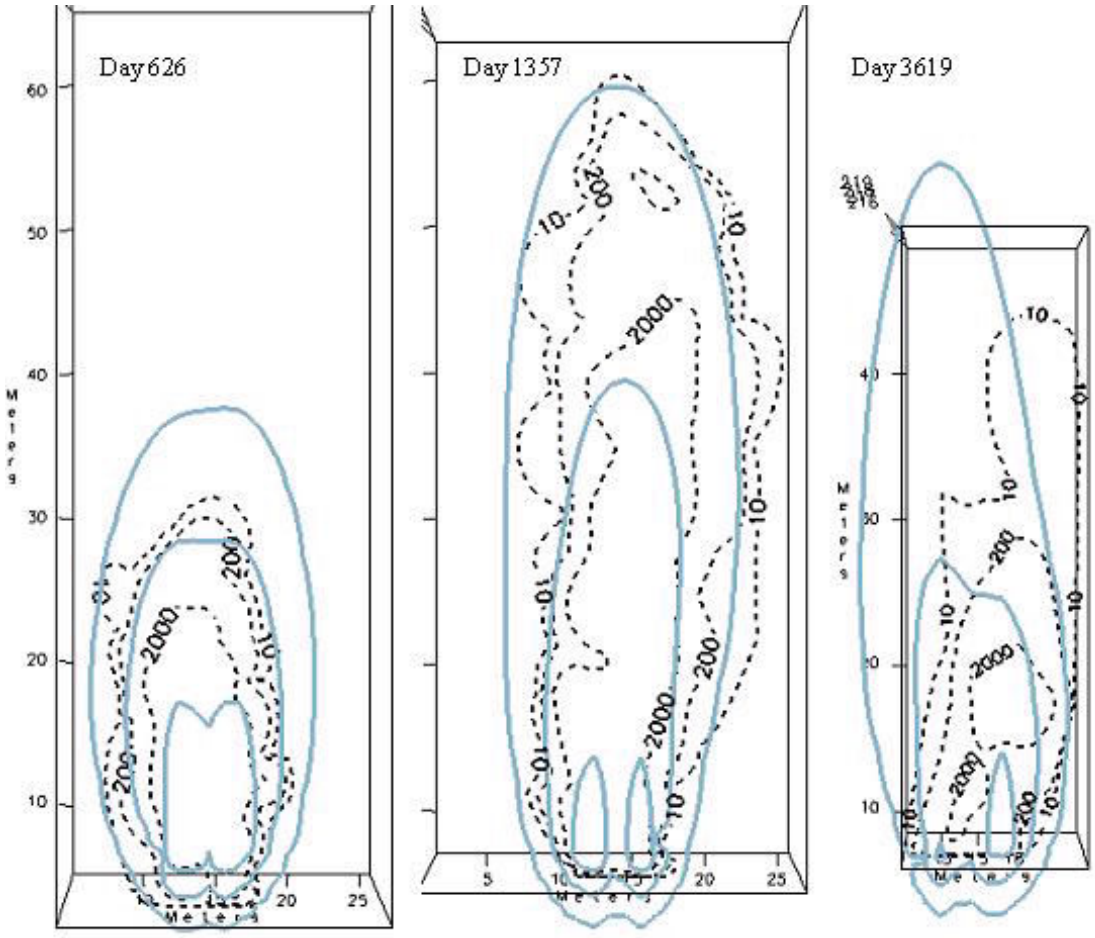

Figure 3.3: Best first-order model results (solid) for naphthalene, overlaid on observations (dash), layer elevation 218.2m. Contours are 10, 200 and 2000 ug/l.

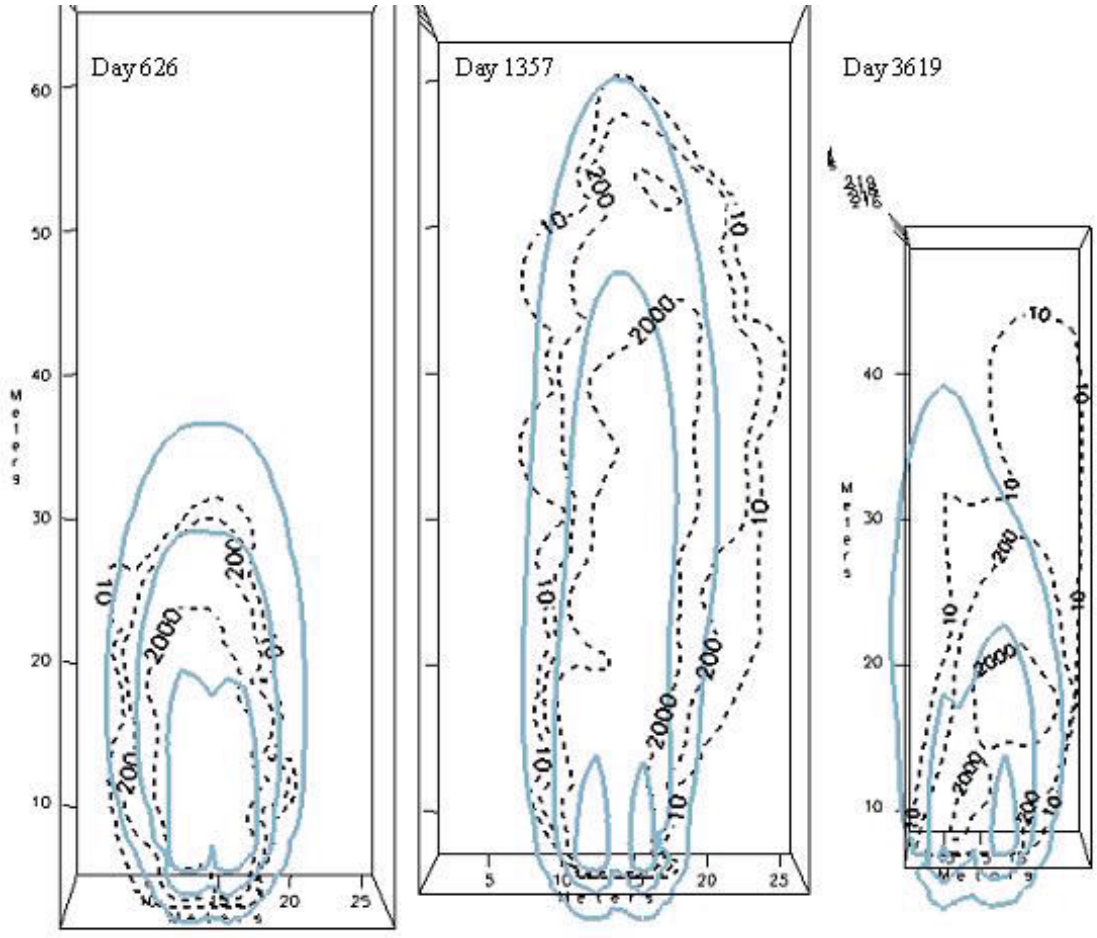

Figure 3.4: Best multi-electron acceptor model results (solid) for naphthalene, overlaid on observations (dash), layer elevation 218.2m. Contours are 10, 200 and 2000 ug/l.

Parameter	Value	Units
k_{O_2}	0.02	d^{-1}
k_{NO_3}	0.01	d^{-1}
k_{SO_4}	0.005	d^{-1}
K_{O_2}	2000	$\mu\mathrm{g}\,/\,\mathrm{l}$
K_{NO_3}	2000	$\mu\mathrm{g}\,/\,\mathrm{l}$
K_{SO_4}	2000	$\mu\mathrm{g}\,/\,\mathrm{l}$
K_{i,O_2}	24000	$\mu\mathrm{g}\,/\,\mathrm{l}$
K_{i,NO_3}	23000	$\mu\mathrm{g}\,/\,\mathrm{l}$
K_{i,SO_4}	144000	$\mu\mathrm{g}\,/\,\mathrm{l}$

Table 3.3: Reaction parameters for the best match multi-e model

multi-electron acceptor model was calculated to be 2.40 kg, a slight improvement on the first-order model results (Table 3.2). Due to the increased mass degraded, the plume mass at day 3619 was smaller than the first-order results, and much smaller than observed.

Electron acceptor concentrations in the plume were also determined in this model, and were found to be within the range of observed values. At day 1357, observed concentrations of dissolved oxygen were less than 0.6 mg / l within the plume, and sulfate was approximately 11.5 mg / l in the plume. From the multiple electron acceptor model, dissolved oxygen in similar locations was lower than approximately 1.0 mg / l in the plume, and sulfate concentrations were approximately 12 mg / l or lower in the plume. These results match well with observations found by King [4].

3.5.4 Addition of zone of zero electron acceptors

It became clear from the modeling results that Visual MODFLOW and RT3D were not adequately representing the chemical and biological processes occurring in the field. Given the solution parameters, it was impossible to match the model to the observations at all times. The most likely condition that was ignored was the naphthalene degradation that occurred between the emplaced source and the three-metre fence. The model represented the naphthalene entering the source as aqueous concentrations at the fence, thus any depletion of electron acceptors by biodegradation occurring in the near-source zone was not represented in the model. Therefore it was decided to artificially impose this depletion of electron acceptors in the near-source zone. This concept was supported by electron acceptor data from

the plume; King measured background dissolved oxygen levels on the periphery of row 3 of $1.4 - 4.4\,\mathrm{mg}\,/\,\mathrm{l}$, and in the centre of row 3 (in the plume) the dissolved oxygen concentrations were all below $0.6\,\mathrm{mg}\,/\,\mathrm{l}$ [2].

The simulation of the depletion of electron acceptors was accomplished by delineating a three-dimensional area, in the zone between the three–metre fence and the source, where electron acceptors were forced to equal zero. No electron acceptors were allowed to enter the near-source core of the plume, allowing the higher naphthalene concentrations to persist longer in this zone, and to travel farther through the model. These results can be seen in Figure 3.5. At the same time, the "constant concentration" cells representing the source were replaced with "point source" cells. The naphthalene mass entering the model did not change as a result of this modification, however using the point source cells gave a better mass balance than did the constant concentration cells. The constant concentration cells maintained a constant chemical concentration in each cell over a time period; they were prone to mass loss errors due to the high concentration gradients present between the source and the background cells. This did not happen with the point source cells, which instead "inject" a constant mass of chemical into a cell over a time period, with a very small volume of water. The injected concentrations become more smoothed over adjacent cells, reducing mass loss errors.

As can be seen in Figure 3.5, with the zero electron acceptor zone, the high concentration contours now extend farther in the domain and match quite well to the observed contours. The decay rates used were $0.02\,\mathrm{d}^{-1}$ for the oxygen reaction, $0.01\,\mathrm{d}^{-1}$ for the nitrate reaction, and $0.005\,\mathrm{d}^{-1}$ for the sulfate reaction. The improvement is most visible at days 626 and 1357. At these snapshot days, the observed and calculated contours are very close and the model does very well in matching the plume shape and extent. At day 3619 the $10\,\mu\mathrm{g}\,/\,\mathrm{l}$ contour extends farther than in the simulation with no electron acceptor limitations, however the mass enclosed by this contour is quite small when compared to the total plume mass. Additionally, the $200\,\mu\mathrm{g}\,/\,\mathrm{l}$ contour is too long and the $2000\,\mu\mathrm{g}\,/\,\mathrm{l}$ contour is too short. Thus the model simulates the naphthalene plume very well for the first few years of the experiment, but did not represent the plume processes as well at late times. There may be more degradation or interaction processes affecting the naphthalene plume at later time which are not simulated with this model.

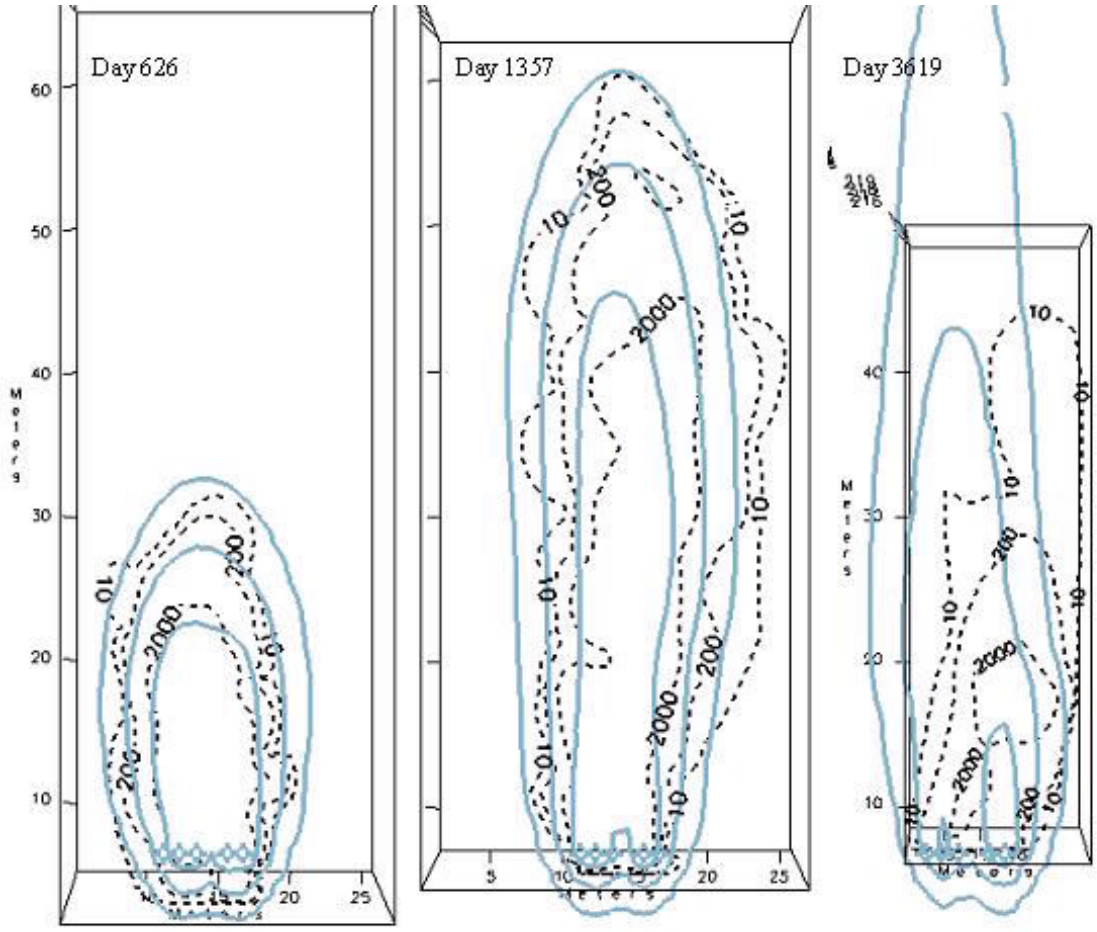

Figure 3.5: Source represented as point sources, zero electron acceptors passing through the source zone, same reaction parameters as constant concentration source model. Multi-electron acceptor model results (solid) for naphthalene, overlaid on observations (dash), layer elevation 218.2m. Contours are 10, 200 and 2000 ug/l.

3.6 Conclusions and implications for future work

From this modeling exercise, it was determined that the first order model and the multi-electron acceptor model produced very similar results in simulating the naphthalene plume. The higher-concentration contours were slightly improved by using the multi-electron acceptor model, however the mass distribution and mass balances are very similar in both models. Both models degraded too much mass in the core of the plume, and the high-concentration contours did not extend far enough in either model. The mass degraded in each model was slightly less than was observed to degrade.

There are several possible reasons why neither the first-order rate reaction model nor the multi-electron acceptor model reflected the field observations very well. These models still showed degradation in the core of the plume when the dissolved oxygen concentrations were lower than $0.6\,\mathrm{mg}/\mathrm{l}$. Realistically, degradation rates should be very low at such a low oxygen concentration. In the first-order model, too much mass was degraded too quickly in the core of the plume. In the multi-electron acceptor model, the high concentrations of naphthalene in these areas diminish the effect of the Monod-type term, allowing high rates of degradation to occur in the core of the plume. If the value of the Monod-type term is decreased by increasing the half-saturation constants, then the decay rate constants must be increased to compensate for the lower degradation rate. This in turn will increase the amount of mass degraded and decrease the size of higher-concentration areas near the source.

Another possible reason that the results did not reflect observations is that the models do not account for any acclimation of the bacteria to the organic contaminant. The field results seem to show that this may be the case (Figure 3.6), as shown by the small mass degradation rate up to day 1357, and sudden increase in this rate after day 1357. Another explanation may be that at early time, other plume chemicals or their degradation products were inhibiting the degradation of naphthalene. This would only occur where naphthalene was present with other creosote chemicals, and this hypothesis will be examined in subsequent chapters.

This study found that by simulating the complete consumption of electron acceptors in the near-source zone, the multi-electron acceptor model was able to better simulate the naphthalene concentrations. The resulting concentration distributions were much improved by the addition of a zero-electron acceptor zone behind the simulated source, and by simulating the depletion of electron acceptors, insight into the plume behaviour was gained.

A better understanding of the plume would be gained by simulating the dissolution of the source, and the plume's transport and degradation in the near-source

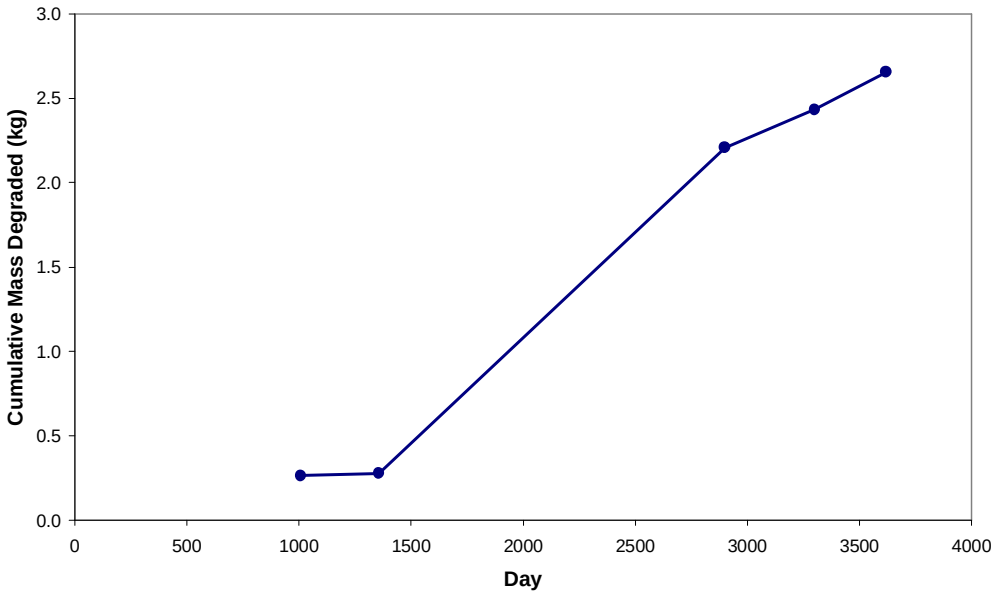

Figure 3.6: Field observations showing cumulative naphthalene mass degraded to day 3619; data from [1].

zone. This would be a more physically-based simulation of the plume's behaviour. As well, the simulation of interactions between several chemicals would give more insight into the behaviour of the various plumes at later times.

Chapter 4

BIONAPL - single chemical

4.1 Purpose

Visual MODFLOW was able to simulate the naphthalene plume well during the early- to mid-times of the simulation, but it was not able to simulate the naphthalene plume well at late times. The program BIONAPL/3D was used to determine if a different model could better simulate the transport and degradation of naphthalene at late times. The same mass input method was used (using measured aqueous concentrations at the three-metre fence), and it was also assumed that all electron acceptors were consumed between the emplaced source and the three-metre fence.

4.2 Method

The program BIONAPL is a three-dimensional numerical model capable of simulating multi-component non-aqueous phase liquid (NAPL) dissolution and biodegradation in a porous aquifer. It couples a transient, groundwater flow model with an advective-dispersive multi-component transport model [9]. In this chapter, BIONAPL was used to simulate only one chemical.

BIONAPL solves a reactive transport equation for each of the source components and electron acceptors. Immobile microbe populations are also simulated [9]. The following equations and definitions are all taken from the BIONAPL/3D User's Guide [9]. The governing equation for mass transport of component C^α is given as:

$$\frac{\partial C^\alpha}{\partial t} R = \frac{\partial}{\partial x_i}\left(D_{ij}\frac{\partial C^\alpha}{\partial x_j}\right) - v_i \frac{\partial C^\alpha}{\partial x_i} + \lambda^\alpha_{dis}\left(C_s - C^\alpha\right) - \lambda^\alpha_{bio} C^\alpha \qquad (4.1)$$

where the dissolution rate term is:

$$\lambda_{dis}^{\alpha} = \frac{ShD^{\alpha}}{(d_{50})^2} \left(\frac{f^{\alpha} S_{ni}}{S_{no}} \right)^{\beta} \tag{4.2}$$

and the effective solubility is:

$$C_s = C_o^{\alpha} \chi^{\alpha} \tag{4.3}$$

The biodegradation term is:

$$\lambda_{bio}^{\alpha} = \sum_{n=1}^{N_A} \left[k^{\alpha,n} M^n \left(\frac{1}{K_C^{\alpha,n} + C^{\alpha}} \right) \cdot \left(\frac{A^n}{K_A^{\alpha,n} + A^n} \right) \cdot I^n \right] \tag{4.4}$$

where

C^{α} is the contaminant concentration for organic component α, $\mathrm{kg} / \mathrm{m}^3$

A^n is the electron acceptor concentration, $\mathrm{kg} / \mathrm{m}^3$

M^n is the microbe concentration, $\mathrm{kg} / \mathrm{m}^3$

$k^{\alpha,n}$ is the maximum organic utilization rate, d^{-1}

$K_C^{\alpha,n}$ is the organic half-utilization-rate concentration, $\mathrm{kg} / \mathrm{m}^3$

$K_A^{\alpha,n}$ is the oxygen half-utilization-rate concentration, $\mathrm{kg} / \mathrm{m}^3$

C_o^{α} is the pure phase solubility of the organic, $\mathrm{kg} / \mathrm{m}^3$

χ^{α} is the mole fraction of organic component

v is the groundwater velocity, m / d

D is the hydrodynamic dispersion coefficient, $\mathrm{m}^2 / \mathrm{d}$

R is the linear retardation coefficient; $R = 1 + \rho_b K_d^{\alpha} / \theta$

K_d^{α} is the linear sorption distribution coefficient, $\mathrm{m}^3 / \mathrm{kg}$

ρ_b is the bulk density of the porous medium, $\mathrm{kg} / \mathrm{m}^3$

θ is the porosity

λ^{α} is the dissolution rate coefficient, d^{-1}

t is time, d

x_i is the spatial dimension, m ($x_i = x, y, z$)

Sh is the Sherwood number, an empirical parameter used to account for unresolved geometry (such as thickness of diffusion layer, surface area of blobs) controlling the dissolution

d_{50} is the median grain diameter

S_{ni} is the NAPL degree of saturation at point i

S_{no} is the initial NAPL degree of saturation

f^{α} is the local volume fraction of NAPL component α

N_A is the number of electron acceptors

The governing equation for the electron acceptor can be written in a form similar to 4.1 and expressing the decay term as

$$\lambda_{bio}^{n} = \sum_{\alpha} \left[k^{\alpha,n} M^{n} X^{\alpha,n} \left(\frac{C^{\alpha}}{K_C^{\alpha,n} + C^{\alpha}} \right) \cdot \left(\frac{1}{K_A^{\alpha,n} + A^{n}} \right) \cdot I^{n} \right] \tag{4.5}$$

where $X_{\alpha,n}$ is the stoichiometric mass ratio of the electron acceptor to organic consumed. It is assumed that the microbial population is stagnant and grows according to:

$$\frac{\partial M^{\alpha}}{\partial t} = \sum_{\alpha} \left[Y^{\alpha,n} M^{n} k^{\alpha,n} \left(\frac{C^{\alpha}}{K_C^{\alpha,n} + C^{\alpha}} \right) \cdot \left(\frac{A^{n}}{K_A^{\alpha,n} + A^{n}} \right) \cdot I^{n} \right] - b M^{n} \tag{4.6}$$

where Y is the microbial yield coefficient and b is a linear decay rate (d^{-1}). In the case of multiple electron acceptors, the inhibition function (I^n) allows either a gradual or abrupt change between preferred electron acceptors. The function takes the form

$$I^{n=1} = 1; I^{n>1} = \prod_{i=2}^{n} \left[\frac{1}{1 + \frac{A^{i-1}}{K_i^{i-1}}} \right] \tag{4.7}$$

Where K_I is the inhibition coefficient for electron acceptor n. BIONAPL uses Monod kinetics in calculating biodegradation.

To use this model, first a grid had to be defined. Flow parameters (dispersion, hydraulic conductivity, etc.) were taken from the Visual MODFLOW calibration described in Chapter 3, and from literature values. Sorption parameters were taken from literature values [2].

At each snapshot day, aqueous concentrations of naphthalene were sampled in seven wells which formed a "fence" three metres from the source. Samples were taken vertically every 20 cm at these wells, and the resulting data was used to measure mass flux into the plume at the fence. This data could also be used in a model to simulate the mass input of naphthalene, as was the case here. The mass input was in the form of a changing boundary conditions, with measured concentrations applied along the left (upgradient, fence) side of the model. The boundary concentrations changed at each sampling day.

The primary reaction parameter that was modified was the "utils" parameter for naphthalene, defining the maximum utilization rate of this compound, in $\mathrm{kg}_{organic} / \mathrm{kg}_{microbe} / \mathrm{d}$. By modifying this parameter, the model output could be calibrated to observed concentrations at the field site.

4.3 Grid setup

The grid cell size in this model had to be small enough to satisfy the Peclet and Courant criteria, while large enough to keep computational time reasonable. The Peclet criterion simplifies to $\Delta x \leq 2\alpha_L$. Using the dispersion parameters determined in Chapter 3, $\Delta x \leq 2(0.36\,\mathrm{m}) = 0.72\,\mathrm{m}$. Thus the grid cell size in the x-direction should be less than 0.72 m. For flow which is dominantly one-dimensional (i.e. in the x-direction, as found here), there is no Peclet constraint in the y- and z-directions. The discretization should still be fine enough that the transverse concentration gradients are well reproduced. The extent of grid discretization is also restricted by the amount of computer memory available and by the need for a reasonable simulation time. The resulting final grid setup is shown in Table 4.1 and in Figure 4.1.

This grid is somewhat different from the Visual MODFLOW grid, which had a cell size of 1 m $\times$1 m $\times$0.175 m.

Dimension	**Range**	**Grid size** (m)	**Number of cells**
x	$0 - 20\,\mathrm{m}$	0.5	40
	$20 - 60\,\mathrm{m}$	1.0	40
y	$0 - 3\,\mathrm{m}$	1.0	3
	$3 - 4.5\,\mathrm{m}$	0.5	3
	$4.5 - 10.5\,\mathrm{m}$	0.333	18
	$10.5 - 12\,\mathrm{m}$	0.5	3
	$12 - 15\,\mathrm{m}$	1.0	3
z	$0 - 6.8\,\mathrm{m}$	0.4	17

Table 4.1: Final grid discretization in BIONAPL, representing entire source

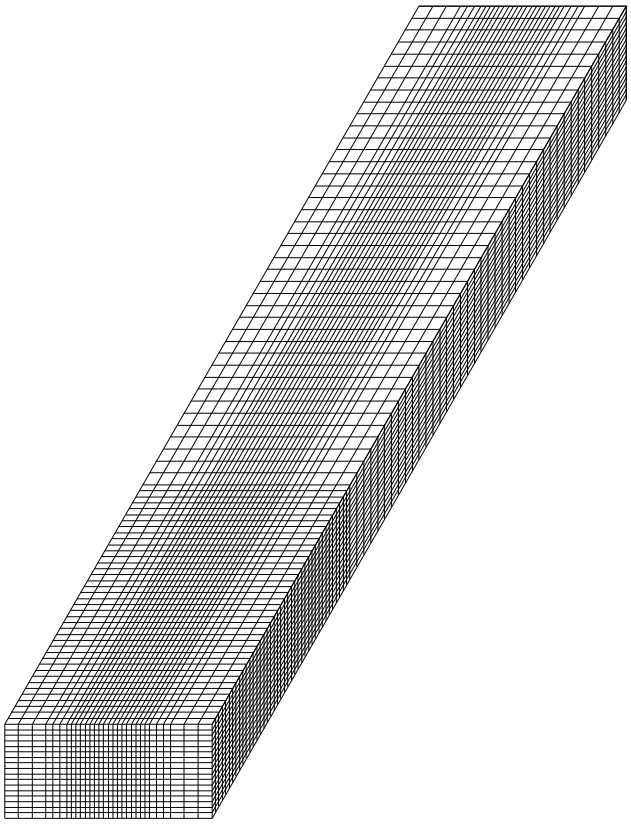

Figure 4.1: Layout of BIONAPL grid

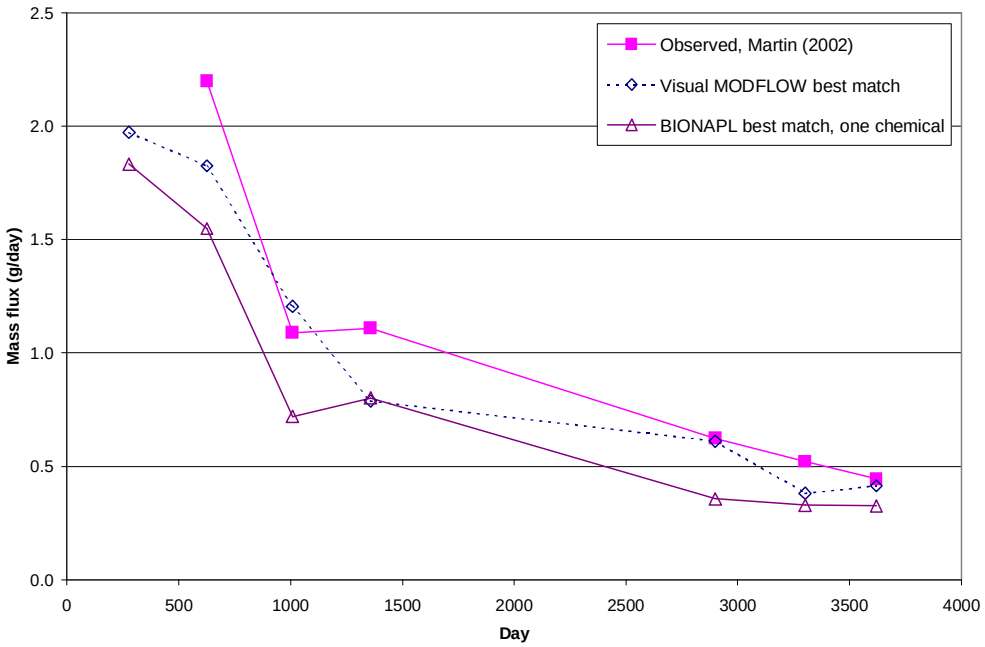

Figure 4.2: Mass flux across the fence over time for observations (solid squares), Visual MODFLOW (open diamonds, see Chapter 3) and BIONAPL with naphthalene (open triangles). Observations taken from Martin, 2002

4.4 Results

The naphthalene mass flux out of the three-metre fence was below the mass flux calculated in [8] for all of the snapshot days (Figure 4.2), however the mass flux was close to the mass flux used in the Visual MODFLOW simulation on most days. Any differences between these two simulations may be attributed to interpolation differences in the input concentrations. As the BIONAPL grid has a larger z-dimension, it was more difficult to interpolate as closely to the concentrations observed at the three-metre fence, as compared to the Visual MODFLOW grid. The overall trend of the BIONAPL model's mass flux follows the trend shown by observed values.

The best match to observations was found when the maximum utilization ("utils") for each of the three electron acceptors was 0.01 $\mathrm{kg}_{organic} / \mathrm{kg}_{microbe} / \mathrm{d}$ for oxygen, 0.005 for nitrate, and 0.01 for sulfate. Mass profile plots are found in Figure 4.3. These plots compare the observed chemical mass in slices of the plume with the

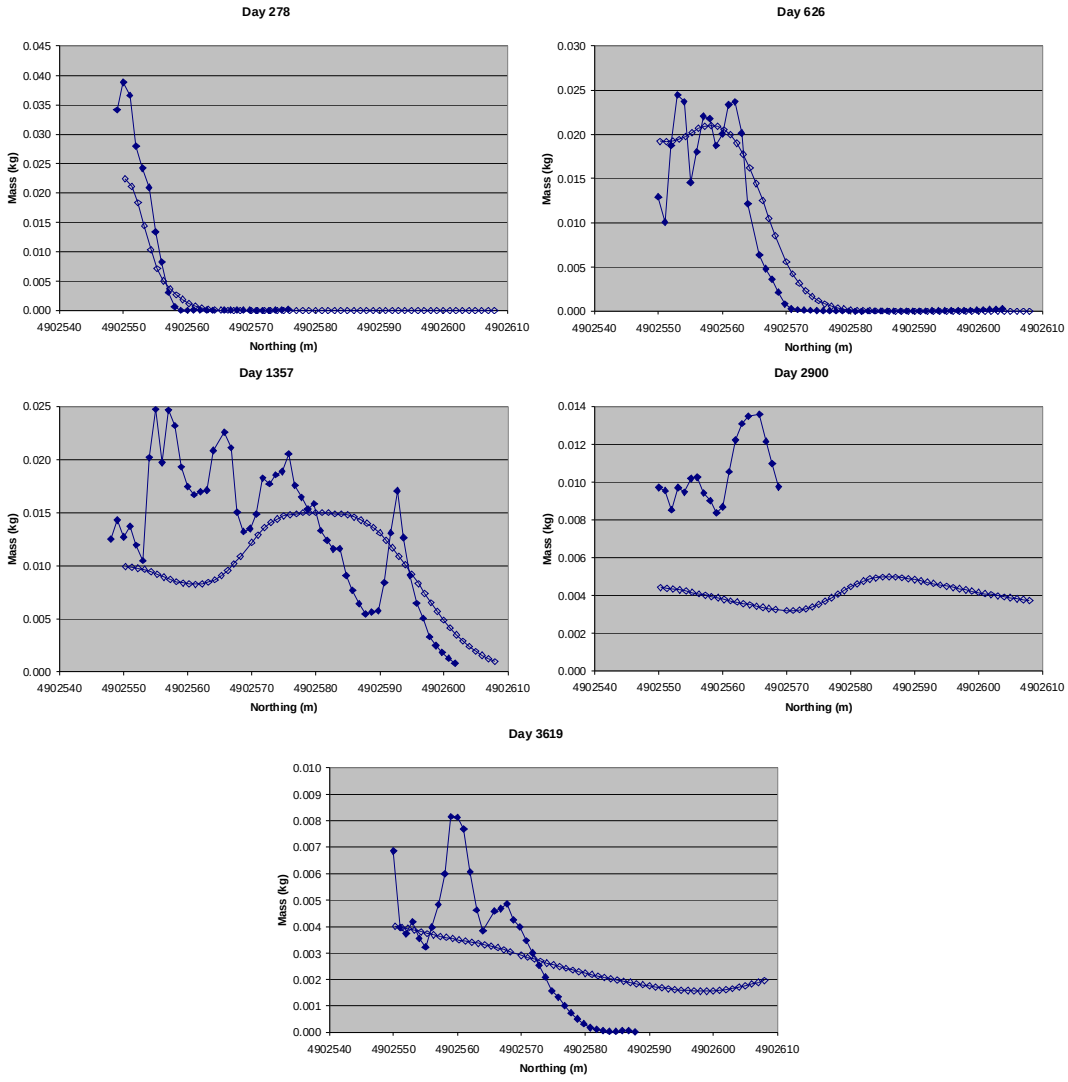

Figure 4.3: BIONAPL model simulating naphthalene transport from the three-metre fence (open symbols) - best match to observations (solid symbols)

mass calculated with BIONAPL. If one imagines each chemical plume as a loaf of bread with the long axis of the loaf aligned in the direction of flow, then these plots compare the mass of each "slice of bread," in slices of 1 m constant width. The purpose of these plots was to compare the three-dimensional model output in an easy-to-read way that demonstrated how closely the model matched the observed plume mass.

At day 278, the naphthalene mass is below observed for the entire profile, however the character of the modeled profile is very similar to observations. The lower mass flux in this model is the likely reason for the smaller overall modeled mass. At day 626, the modeled profile follows observations very well, however the front of the modeled plume traveled approximately 8 m farther than the observed plume. The match at this day is quite good. At day 1357, there is far too little mass near the source, and a good match halfway down the plume. It appeared that a lump of naphthalene mass was travelling through the model, and this was most likely due to the averaging of mass flux over long time periods. Since the plume was sampled at approximately yearly intervals by this point, it is highly likely that mass flux would fluctuate between sampling periods. There must have been too little mass entering the model prior to sampling day 1357, leading to the mismatch seen in Figure 4.3. At day 2900, the mass in the model was too low throughout the plume. This may have been due to a mass flux which was below observations entering the model, or to a naphthalene degradation rate which was too high. At day 3619, the near-source concentrations matched very well to observations, however slightly downgradient of the source, the model failed to represent the peak in mass at northing 4902560. Too much mass was present in the far end of the model at this snapshot. The model likely did not reproduce the peak because there was a mass input in the field not recorded at the snapshot days. A funnel-and-gate was present in the field after day 2900 at northing 4902570, so the excess mass seen in the model after this time and past this gate may be a result of the model not being able to simulate this treatment structure.

4.5 Conclusions

The mass flux into the BIONAPL single chemical model is below observations at all snapshot days, however the general trend of mass flux is representative of field trends. The model was able to produce good matches to observations at days 278 and 626, but after this point there tends to be too little naphthalene mass entering the model. There were also several times where it appeared that mass flux was

changing more rapidly than observations were recorded, and the model was unable to represent observations well as a result.

This model performed slightly less well than the Visual MODFLOW model at matching observations, however this is most likely due to the differences in mass flux. The mass flux into BIONAPL was interpolated to a coarser grid, and may have led to less mass entering this model. Since BIONAPL has the capability to represent a dissolving NAPL source, this more comprehensive and physically realistic approach may have more success in simulating the flux of chemicals into the model.

Chapter 5

BIONAPL - multiple chemicals

5.1 Purpose

Once results for one chemical had been simulated in both Visual MODFLOW and BIONAPL, the simulation of multiple chemicals from the creosote plume was desired. Since Visual MODFLOW was unable to do this with the included reaction packages, it was decided that the software BIONAPL/3D would be used to simulate the transport, degradation and interaction of several plume chemicals. This program allowed for simultaneous treatment of numerous organic chemicals and electron acceptors.

5.2 Method

The program BIONAPL is a three-dimensional numerical model capable of simulating multi-component non-aqueous phase liquid (NAPL) dissolution and biodegradation in a porous aquifer. It couples a transient, groundwater flow model with an advective-dispersive multi-component transport model [9]. As such, it was an ideal choice for simulating the multi-component complex plume observed at CFB Borden.

To use this model, first a grid had to be defined. Since the original source actually consisted of two identical sources emplaced side-by-side with approximately 1 m between them, to save computational time only one side of the whole two-part source was modeled. By taking advantage of the plane of symmetry at this site, computational time was significantly reduced. Flow parameters (dispersion,

Dimension	Range	Grid size (m)	Number of cells
x	$0 - 20\,\mathrm{m}$	0.5	40
	$20 - 60\,\mathrm{m}$	1.0	40
y	$0 - 3\,\mathrm{m}$	0.33	9
	$3 - 4.5\,\mathrm{m}$	0.5	3
	$4.5 - 7.5\,\mathrm{m}$	1.0	3
z	$0 - 6.8\,\mathrm{m}$	0.4	17

Table 5.1: Original grid discretization in BIONAPL, using plane of symmetry

hydraulic conductivity, etc.) were taken from the Visual MODFLOW calibration described in Chapter 3, and from literature values.

Once the grid was designed, several chemicals were chosen to be simulated. The choice of chemicals was refined through the course of the study. As model runs were completed, model output consisting of concentration contours and mass profiles was compared to observations, and reaction parameters were increased or decreased as necessary to better match the modeled contours to the observed contours.

The reaction parameters that were modified were primarily the "utils" parameter for each compound, defining the maximum utilization rate of each compound, in $\mathrm{kg}_{organic} / \mathrm{kg}_{microbe} / \mathrm{d}$. By modifying these parameters, the model output could be calibrated to observed concentrations at the field site.

5.3 Grid setup

The grid was originally set up to represent half of the two-part creosote source, taking advantage of the plane of symmetry through the site. The grid cell size in this model had to be small enough to satisfy the Peclet and Courant criteria, while large enough to keep computational time reasonable. The Peclet criterion simplifies to $\Delta x \leq 2\alpha_L$. Using the dispersion parameters determined in Chapter 3, $\Delta x \leq 2(0.36\,\mathrm{m}) = 0.72\,\mathrm{m}$. Thus the grid cell size in the x-direction should be less than 0.72 m. For flow which is dominantly one-dimensional (i.e. in the x-direction, as found here), there is no Peclet constraint in the y- and z-directions. The discretization should still be fine enough to ensure that the transverse concentration gradients are well reproduced. The extent of grid discretization is also restricted by the amount of computer memory available and by the need for a reasonable simulation time. The original grid setup is shown in Table 5.1.

As trials with this grid setup progressed, it became apparent that using this

Dimension	Range	Grid size (m)	Number of cells
x	$0 - 20\,\mathrm{m}$	0.5	40
	$20 - 60\,\mathrm{m}$	1.0	40
y	$0 - 3\,\mathrm{m}$	1.0	3
	$3 - 4.5\,\mathrm{m}$	0.5	3
	$4.5 - 10.5\,\mathrm{m}$	0.333	18
	$10.5 - 12\,\mathrm{m}$	0.5	3
	$12 - 15\,\mathrm{m}$	1.0	3
z	$0 - 6.8\,\mathrm{m}$	0.4	17

Table 5.2: Final grid discretization in BIONAPL, representing entire source

plane of symmetry was not working well. Low concentration contours were being pulled towards the no-flow boundary on the east side of the domain. This "plume warping" distorted the true progress of the plume. As well, by only simulating one half of the source, any of the interactions between the two sources were not being represented, i.e. any real mass that travelled over the apparent line of symmetry towards the other half of the source would not be accounted for in the biodegradation reactions. The grid setup was therefore changed to include both sides of the source, ignoring symmetry, and simulating the total source in an attempt to prevent erroneous mass loss, as well as better simulating interactions between the plumes emanating from either side of the source. The resulting final grid setup is shown in Table 5.2.

5.4 NAPL dissolving source

The source in this model was designed as an internal NAPL source of components, dissolving according to a kinetic model. This dissolving source was more physically comprehensive than the point source fence used in the Visual MODFLOW model and the BIONAPL concentration fence. For each modeled component of the NAPL, the density, molecular weight, aqueous solubility, and number of moles in the source was specified. Each chemical of interest was assigned to one of six available component slots in the program, while a "remainder" component had to use up one of the six slots. The purpose of this remainder component was to account for the total mass of the source. If the remainder component was not used, the more soluble components would have higher effective mole fractions, and would dissolve much more quickly than was inferred from observations. The remainder component also contained the unquantified fraction of the creosote source as emplaced; not all

compounds in the source were analysed in the initial source characterization, but it was known that the total creosote mass was approximately 74 kg [3]. By assuming a reasonable molecular weight and density of the "remainder", the number of moles in the source could be estimated, and a reasonable aqueous solubility was assumed as well. Since most of the compounds in the remainder group had low aqueous solubilities and higher molecular weights and densities, the remainder component was predicted to dissolve very little.

Additionally, there was a group of well-quantified chemicals that travelled relatively slowly through the field site, but more quickly than the "remainder" component". These chemicals were generally less soluble, leading to their slower travel time. Although these compounds had been well-quantified through the term of the field observations, these chemicals were of less interest in the simulation. Chemicals which travelled through the study area more quickly and interacted more with the available electron acceptors were of more interest. As a result, a second group of "slow" chemicals was used in the model, whose components were separately well characterized, but grouped together for the sake of leaving more component slots open to chemicals of interest.

The Sherwood number is an empirical parameter which is used to account for unresolved pore scale geometry that controls the dissolution. The unresolved geometry includes such parameters as the thickness of the diffusion layer and surface area of the creosote blobs. During the setup of this BIONAPL model, it was found that a Sherwood number of 0.002 allowed the creosote chemicals to reach aqueous concentrations in the source which were at, or just below, their effective solubilities. If the Sherwood number was any higher, the source may have dissolved too quickly, and oscillations in the source could have been produced. These oscillations would cause all or most of the NAPL to dissolve in the first time step; in the next time step, the concentration gradient would be negative and much of the dissolved chemicals would re-form as NAPL. The Sherwood number must be chosen carefully so that this oscillation is avoided, and the source chemicals dissolve at their effective solubilities.

5.5 Choice of chemicals

The chemicals first chosen to be simulated were: 1) naphthalene, 2) a group composed of phenol, p-cresol and m-xylene, and 3) a group composed of biphenyl and acenaphthylene. The remainder of the quantified chemicals were in a fourth group, and the "remainder" less soluble components of the source occupied a fifth group.

Naphthalene was a main chemical of interest; it was the largest plume of the monitored chemicals in the field study and would have had a large impact on the electron acceptors in the study area. The phenols travelled more quickly than naphthalene; these were of interest to see if they consumed significant quantities of electron acceptors ahead of the naphthalene plume, causing a "shadow" of depleted electron acceptors which could affect naphthalene's degradation rate. Biphenyl and acenaphthylene had similar degradation patterns: they both had small plumes which grew, then retreated, within the time frame of the plume monitoring, and so they made a coherent group.

One electron acceptor, oxygen, was originally chosen for this model. In King's modeling [2], oxygen was the main electron acceptor used in degrading the chemicals investigated. Given oxygen's importance to the field situation, it was treated as the main electron acceptor, and given an initial concentration of $2.4\,\mathrm{mg}/\mathrm{l}$, equal to the average of measured background concentrations [4]. However, early into this study, the quantity of electron acceptors available was questioned; it appeared that insufficient electron acceptor concentrations were available to degrade the simulated chemicals, allowing the chemicals to travel much too far in the model domain. As a result, sulfate was added as a second electron acceptor, at an initial concentration of $14\,\mathrm{mg}/\mathrm{l}$.

This solution was more complex to model as there were now two electron acceptors, and the results were similar to a simulation which had a single electron acceptor at a high concentration, equal to the combined concentrations of the two electron acceptors. It was decided to go back to a single electron acceptor, with an initial concentration of $20\,\mathrm{mg}/\mathrm{l}$. This was justified since the stoichiometric mass ratio for the sulfate-reducing reactions was larger than the ratio for the aerobic reactions, as shown in the following equations.

$$C_{10}H_8 + 12O_2 -> 10CO_2 + 4H_2O \tag{5.1}$$

$$C_{10}H_8 + 6SO_4^{-2} + 12H^+ -> 10CO_2 + 6H_2S + 4H_2O \tag{5.2}$$

For example, for naphthalene, the aerobic and sulfate-reducing stoichiometric mass ratios were 3.24 and 4.50 respectively. Using the calculation $4.50/3.24 = 1.39$, the mass of sulfate needed to mineralize a mass of naphthalene is 1.39 times greater than the mass of dissolved oxygen needed to mineralize this same mass of naphthalene. Therefore the background sulfate concentration of $14\,\mathrm{mg}/\mathrm{l}$ is equivalent to $(14\,\mathrm{mg}/\mathrm{l})(1.39) = 19.4\,\mathrm{mg}/\mathrm{l}$ of oxygen. Summing the oxygen background concentration and the equivalent sulfate concentration, the total background concentration of electron acceptors was rounded to a total of $20\,\mathrm{mg}/\mathrm{l}$.

5.5.1 Refinement of choices

After a simulation had been completed and analysed, it was sometimes necessary to re-examine why certain chemicals were being represented in the model. For example, the influence of phenol on the amount of electron acceptors encountered by naphthalene was important. If there was no electron acceptor shadow behind the phenol plume, then perhaps the phenol plume had little effect on the naphthalene plume, and phenol did not have to be simulated, freeing up another component slot for another chemical of interest. A simulation was run, showing that the phenol shadow passed out of the model domain approximately 20 m ahead of the next fastest chemical, m-xylene. There was some residual effect of the phenol shadow, however it was felt that this shadow would only affect the fastest chemicals (naphthalene and m-xylene) during the early parts of the simulation, and after this time oxygen would be replenished by diffusion and advection. It was also felt that the presence of m-xylene ahead of the naphthalene plume would deplete oxygen as well, and would determine the amount of oxygen that the naphthalene plume encountered. As a result, phenol was not included as a separate chemical in further simulations.

The influence of biphenyl and acenaphthylene was found to be minor, as these two chemicals comprised a very small portion of the original source mass. Early on these chemicals were added to the fourth component, grouped with the rest of the quantified chemicals of lesser interest.

5.5.2 Adding acenaphthene

Acenaphthene became a chemical of interest after it was realized that it had been observed to migrate quite far in the domain, and may have interacted with naphthalene and 1-methyl-naphthalene. The behaviour of acenaphthene was not examined in previous plume studies at this site, so in early simulations it was not considered a chemical of interest. However, in an attempt to explain why the model was unable to successfully simulate the behaviour of the naphthalene plume, interactions between naphthalene and other chemicals were sought. Acenaphthene was observed to travel almost as far as naphthalene in the field, and was one of very few chemicals to do so, leaving it as one of the only known possibilities for chemical interaction or competition. Zamfirescu and Grathwohl [13] observed that acenaphthene was degraded only within 50 m downstream of a creosote source, then its concentration remained constant further downgradient. This was explained by acenaphthene's dependence on the presence of naphthalene dioxygenase or phenanthrene dioxygenase, without which it will not degrade. A similar interaction or dependence was

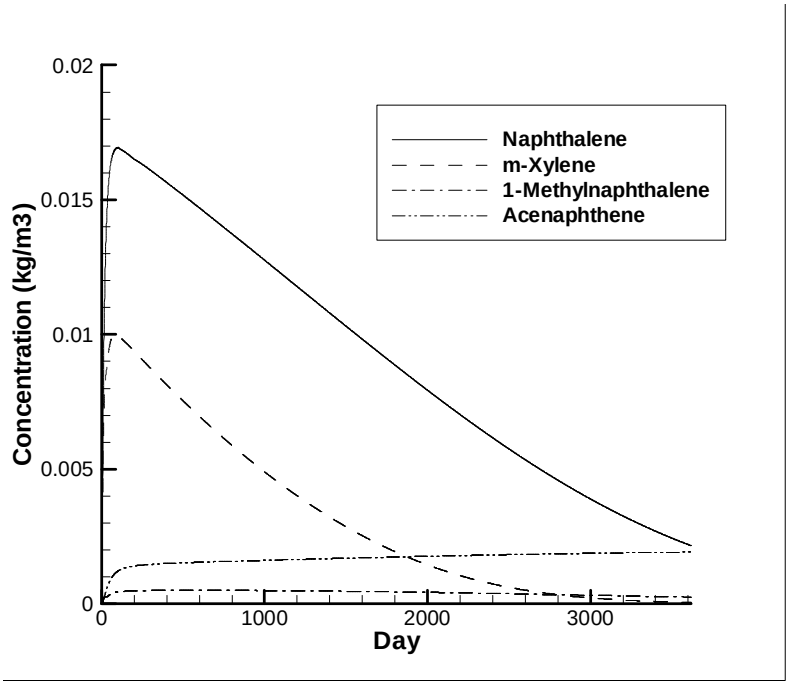

Figure 5.1: Concentrations (in kg / m^3) of chemicals dissolving just downgradient of the NAPL source

possible for the CFB Borden creosote site, and was supported by the lab experiment described in Chapter 2, so acenaphthene was added to the BIONAPL simulation.

5.6 Mass flux from source

Chemical concentrations dissolving from the source are shown in Figure 5.1. This plot shows the dissolved chemical concentrations over time at a node just downgradient of the source.

In order to be able to justify comparing the modeled plume with observations made at the field site, the mass flux dissolving from the source in the model should be similar to the mass flux dissolving from the source in the field. If a vastly different mass of chemicals was dissolving from the modeled source, it would not be valid to compare the resulting plume with observations. Since the observational dataset measured mass flux at the three-metre fence, the mass flux in the model was also compared to the three-metre fence mass flux, with results shown in Table

Naphthalene

Day	observed mass flux at 3m fence	BIONAPL best match, mass flux at 3m fence
278	2.70	2.64
626	2.53	2.31
1008	n/a	1.94
1357	0.97	1.61
2900	0.54	0.49
3300	n/a	0.31
3619	0.35	0.21

1-methylnaphthalene

Day	observed mass flux at three-metre	BIONAPL best match, mass flux at 3m fence
278	0.14	0.050
626	0.150	0.054
1008	n/a	0.052
1357	0.070	0.048
2900	0.084	0.022
3300	n/a	0.017
3619	0.074	0.013

M-xylene

Day	observed mass flux at three-metre	BIONAPL best match, mass flux at 3m fence
278	2.22	1.21
626	1.19	0.90
1008	n/a	0.60
1357	0.27	0.38
2900	0.039	0.019
3300	n/a	0.007
3619	0.005	0.003

Acenaphthene

Day	observed mass flux at three-metre	BIONAPL best match, mass flux at 3m fence
278	0.25	0.11
626	0.26	0.27
1008	n/a	0.29
1357	0.14	0.30
2900	0.21	0.34
3300	n/a	0.34
3619	0.15	0.34

Table 5.3: Mass flux at the fence for observations and best BIONAPL simulation. All figures in g/day, and n/a indicates that data were not available

5.3.

The modeled naphthalene mass flux was similar to observations, falling somewhat below observations at most days, but overall representing this chemical well. The m-xylene modeled mass flux followed the same general pattern of observations, starting with a higher mass flux and gradually decreasing, followed by a large drop in mass flux at day 2900. However for many of the snapshot days, the modeled m-xylene mass flux is lower than observations. Modeled mass flux for 1-methylnaphthalene is too low at all days, by a factor ranging from 1.5 to 6. This chemical should have dissolved more mass at the beginning of the simulation, decreasing slightly for the rest of the simulation. The mass flux of acenaphthene in the model started at a lower value, then gradually increased, however observations showed an opposite pattern of an initially higher mass flux which then decreased, in general.

The modeled mass fluxes do not match well to the mass fluxes measured in the

field. The chemicals naphthalene and m-xylene showed mass fluxes very close to observed values, but the chemicals 1-methylnaphthalene and acenaphthene did not match observations well. Since these latter two chemicals were not dissolving as fast as was observed, a simulation was run in which the Sherwood number was increased for all chemicals, in an attempt to cause 1-methylnaphthalene and acenaphthene to dissolve more quickly from the NAPL source. All chemicals dissolved faster as a result, however 1-methylnaphthalene and acenaphthene were not improved significantly, and naphthalene and m-xylene dissolved too quickly, resulting in a much lower mass flux at the end of the simulation. The Sherwood number did not appear to be the parameter that was limiting mass flux for 1-methylnaphthalene and acenaphthene at early time.

It is acknowledged that the chemicals which do not match well to observed mass fluxes cannot be analysed as critically as those that do match well to observations. However, it seems that BIONAPL does not incorporate all dissolution processes that may be occurring in this complex source. The distribution of NAPL in the emplaced source may be non-uniform, causing water flowing through the source to encounter varying concentrations of NAPL. However, this would affect all chemicals in the source, and it would slow dissolution in the field; simulating this process would not improve the mass flux simulated in the model. When mass flux was measured in the field, it would have represented the mass flux at only one snapshot day, and this mass flux may vary to a significant extent from month to month. It is possible that the density of measurements of mass flux is insufficient for comparison with the model. Despite these issues, a comparison of model output with field observations was conducted, while keeping in mind that the mass flux in the model may or may not be correct.

5.7 Best match results

The final simulation had six chemical groups: naphthalene, m-xylene, 1-methylnaphthalene, acenaphthene, a lumped component representing the remainder of the quantified chemicals (Remainder - known), and a lumped component representing the remainder of the source mass, whose mass was known but individual components were not identified (Remainder - unknown). The simulation which showed the best results had reaction parameters as described in Table 5.4.

Several plots of the plume mass have been assembled; these plots compare the observed chemical mass in slices of the plume with the mass calculated with BIONAPL. If one imagines each chemical plume as a loaf of bread with the long axis

Chemical Group	Maximum utilization rate
Naphthalene	0.05
m-Xylene	0.12
1-Methylnaphthalene	0.15
Acenaphthene	0.001
Remainder - known	0.10
Remainder - unknown	0.05
*All chemicals had substrate half-utilization constants of 0.002 kg / m^3, and oxygen half-utilization constants of 0.005 kg / m^3	

Table 5.4: Reaction parameters for the BIONAPL simulation which best matched observations

of the loaf aligned in the direction of flow, then these plots compare the mass of each "slice of bread," in slices of 1 m constant width. The purpose of these plots was to compare the three-dimensional model output in an easy-to-read way that demonstrated how closely the model output fit to observed plume mass. Close to the simulated source, chemical mass is high as each chemical dissolves into the groundwater; farther away from the source, less mass is present due to degradation and dispersion. These plots are presented in Figures 5.3 through 5.6, with observed values represented as solid symbols, and model results as open symbols. Plan-view cross-sections through the middle of the naphthalene plume are included in Figure 5.2.

5.7.1 Naphthalene

The naphthalene results are shown in Figures 5.2 and 5.3. Figure 5.2 shows slices through the naphthalene plume at a similar elevation as in Figure 3.5, and the observed contours may be compared from this figure. At sampling day 278, the calculated mass near the source is slightly lower than was observed. However, for the rest of this profile, the mass matches well to observations, only falling slightly short of the observed mass. At day 626, the mass near the source was too high, and remained too high along the rest of the profile, however the general character and shape of the plume was reproduced. At day 1357, the calculated naphthalene plume seems to follow closely to an average of the observed mass values. The observations fluctuate widely, but tend to follow a typical plume profile on the average. The simulation seemed to fall a bit below this average plume, but represented the character of the observed plume well. At day 2900, however, the calculated naphthalene plume fell far below observations in the near-source area.

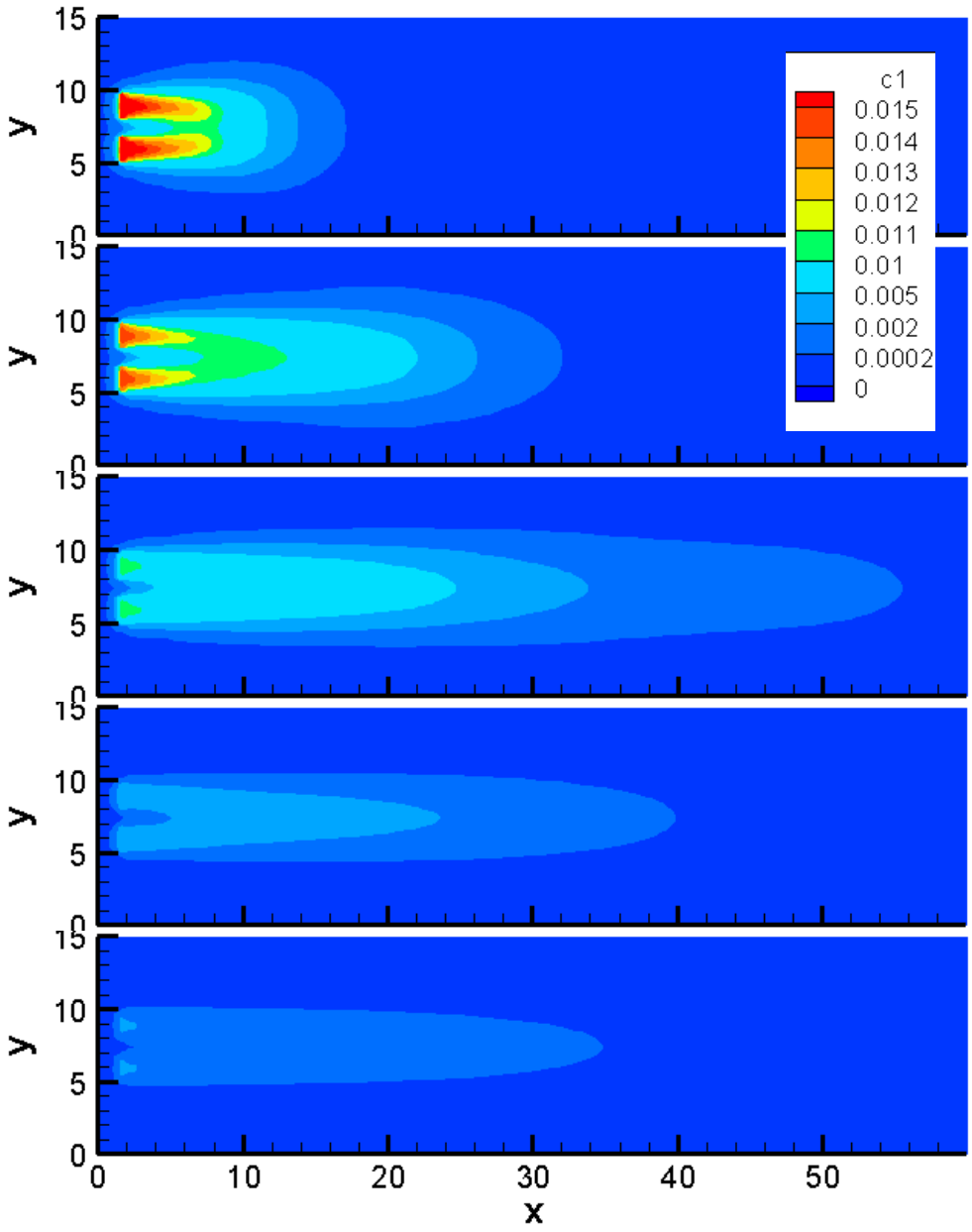

Figure 5.2: BIONAPL best match simulation, as described in text. Shown are horizontal (xy) slices through the centre of the naphthalene plume, at days 278, 626, 1357, 2900, 3619 (top to bottom). Concentrations shown are in kg / m^3, or g / l

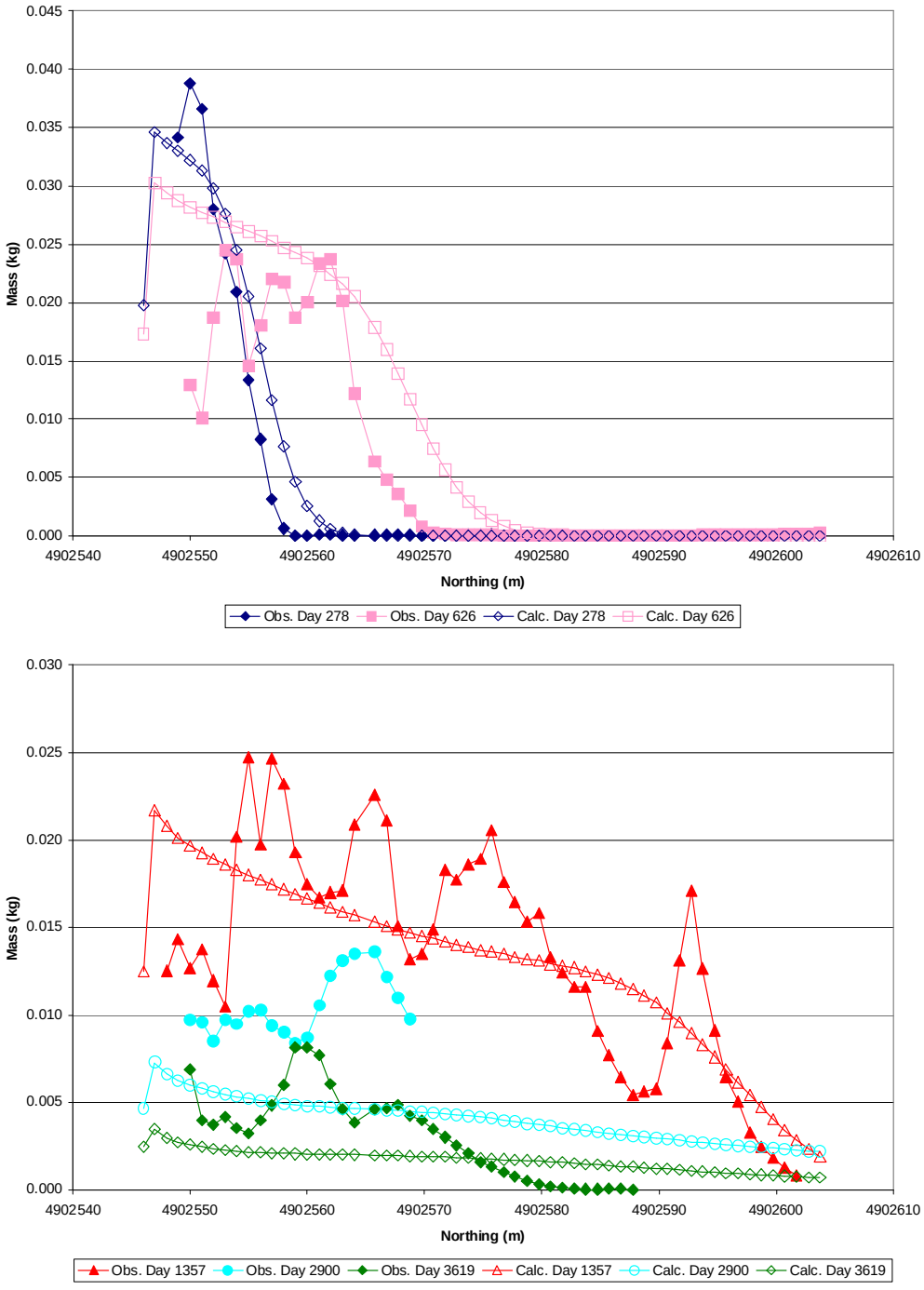

Figure 5.3: Best BIONAPL match results for naphthalene showing mass in transverse slices along the flow direction

Too much degradation was occurring near the source. Due to the presence of the funnel-and-gate, approximately at northing 4902570, no samples were taken in the far half of the plume, however due to a trend of decreasing plume size shown by this day, it was expected that very little naphthalene mass would exist far from the source. However, the model predicted that the plume would continue to tail off in the far half of the plume, and too much mass was shown in the simulation. At day 3619, this pattern of underpredicting mass near the source and overpredicting mass far from the source was repeated.

BIONAPL was able to represent the character of the naphthalene plume well until day 1357, but at days 2900 and 3619, too little naphthalene mass was present near the source, and too much mass was present far from the source. The model was degrading too much mass in the near-source area and too little mass in the more distant areas of the plume. Some process must have been occurring at the field site at late time to slow the naphthalene degradation in the near-source area.

5.7.2 m-Xylene

The m-xylene results are found in Figure 5.4. At sampling day 278, the model calculated far less m-xylene mass than was observed. However, at day 626, the agreement between model and observations was very good near-source. Farther from the source, the model showed too much mass, and the modeled plume tended to tail off for a much larger distance than the observed plume did. At day 1357, the model did not reproduce the large peak in observed mass found at northing 4902555, but it did match well to the near-source values around this peak. Again, the calculated plume persisted much farther downgradient than was observed. At days 2900 and 3619, the observed mass dropped to a very low value. The model also showed a drop to very low masses on these days, but unlike the observed plume, a tailing-off character of the modeled plume was also observed on these days. Due to the very low total m-xylene mass present at these late times, the absolute difference in mass between observed and modeled plumes is very small.

The model tended to show the same pattern for m-xylene at most sampling days: underestimating mass near the source, and overestimating mass far from the source, often tailing off for long distances past the observed plume. Mass was underestimated at the first sampling day for the entire length of the plume. This pattern of mismatch is similar to the pattern shown in the naphthalene plume, but there is no snapshot day for which the character of the modeled m-xylene plume matched well with the observed plume. Perhaps the dissolution of m-xylene from

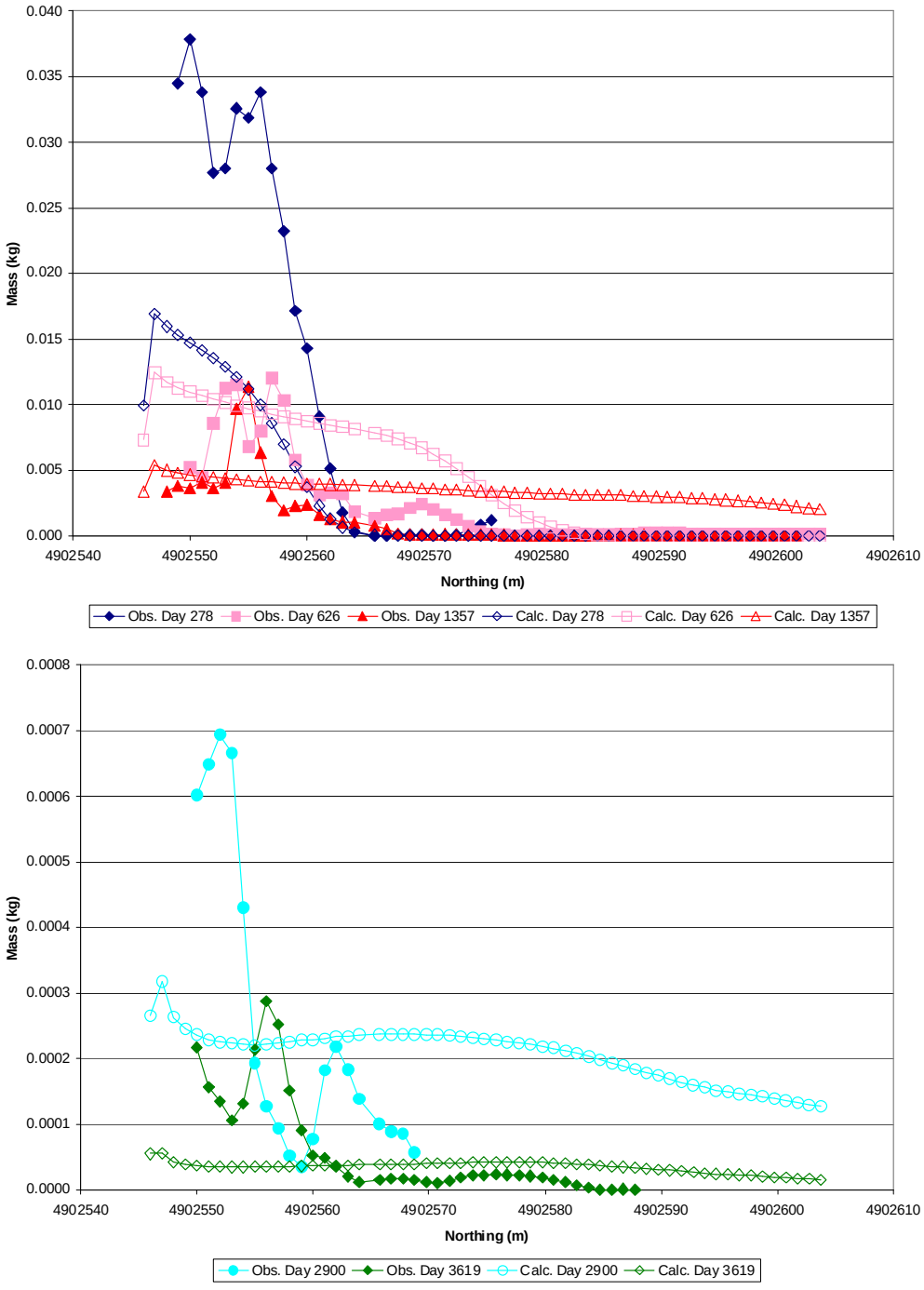

Figure 5.4: Best BIONAPL results for m-xylene showing mass in transverse slices along the flow direction

the NAPL source was not being properly represented, and mass was travelling too quickly through the model.

5.7.3 1-methylnaphthalene

The 1-methylnaphthalene results are found in Figure 5.5. At sampling days 278 and 626, the modeled and observed masses of this plume were very low. At day 278, the model calculated less mass than was observed, but the plume shape was good, and it ended at the same northing as was observed. At day 626, the modeled plume mass was too low through the near-source zone, and some tailing-off was present farther from the source. For days 1357, 2900 and 3619, the model consistently showed far too little 1-methylnaphthalene mass, compared to the mass that was observed. The observed plume persisted for much longer than the modeled plume. The mismatch between the model and observations is likely due to an different modeled mass flux, or perhaps to some unidentified process in the field that slowed 1-methylnaphthalene degradation at mid- to late-times.

5.7.4 Acenaphthene

The acenaphthene results are found in Figure 5.6. At sampling day 278, the modeled plume matched well to observations. At day 626, the model calculated too much mass, but both the plume character and shape were good. At day 1357, again the plume shape was good, but the model calculated more mass than was observed, and the plume profile extended too far away from the source. At day 2900, the model did not capture the peak seen at northing 4902566, and acenaphthene may have extended too far in the model. However, the concentrations calculated through the near-source area were close to the range observed in this area. At day 3619, the modeled mass was too great throughout the domain. The plume tailed off for much too far a distance, and concentrations near the source were calculated to be too high.

The model tended to predict more acenaphthene mass than was observed. The maximum utilization rate was quite low for acenaphthene, but if it was set any higher, then the results at day 278 would have not matched well to observations, since too much mass would have degraded by this time. The approach to matching the model to observations involved calibrating the model to early times, then seeing how well the model performed at late time. In this case, matching the plume to early time with a low rate resulted in too much mass being present in the model at

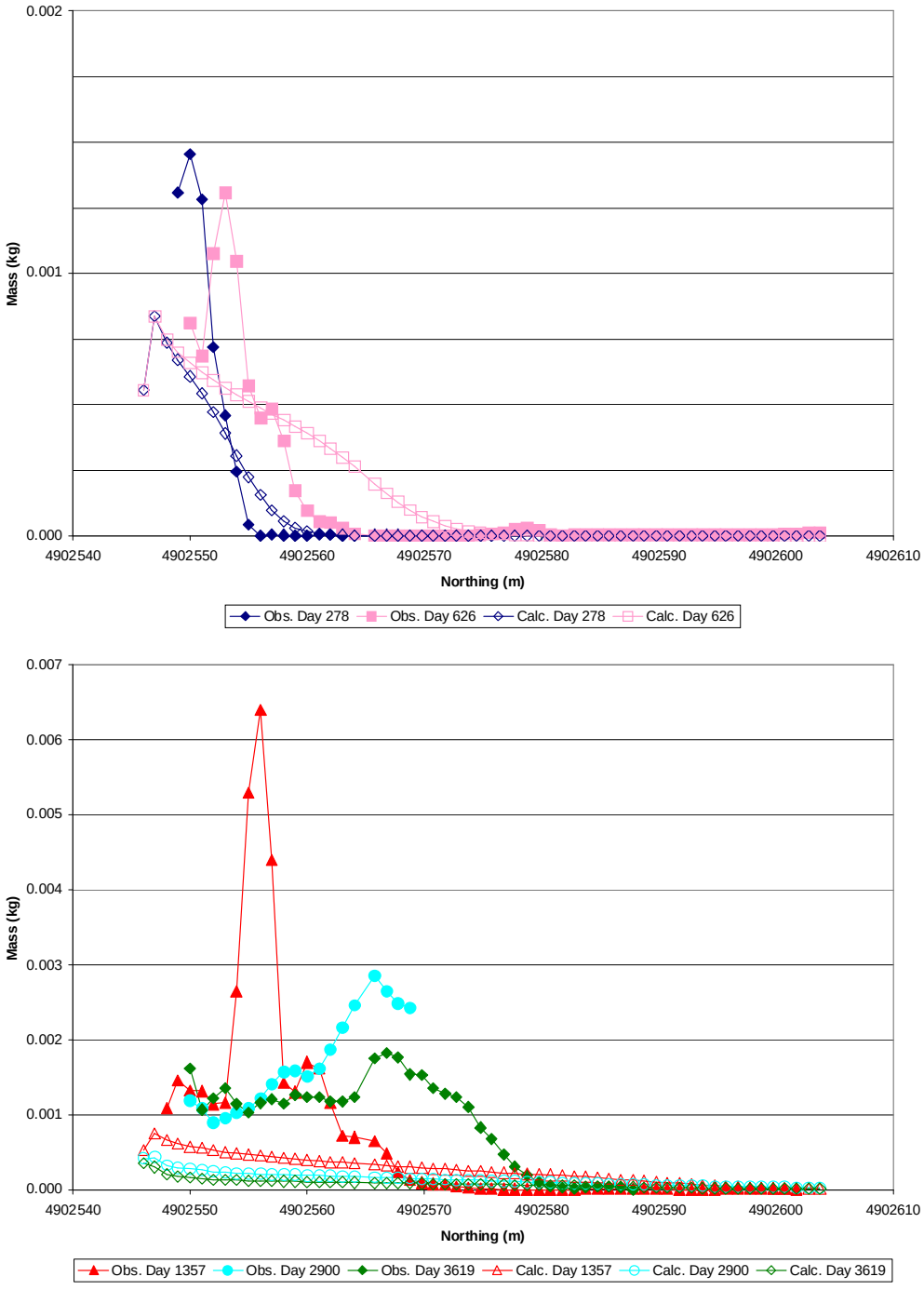

Figure 5.5: Best BIONAPL results for 1-methylnaphthalene showing mass in transverse slices along the flow direction

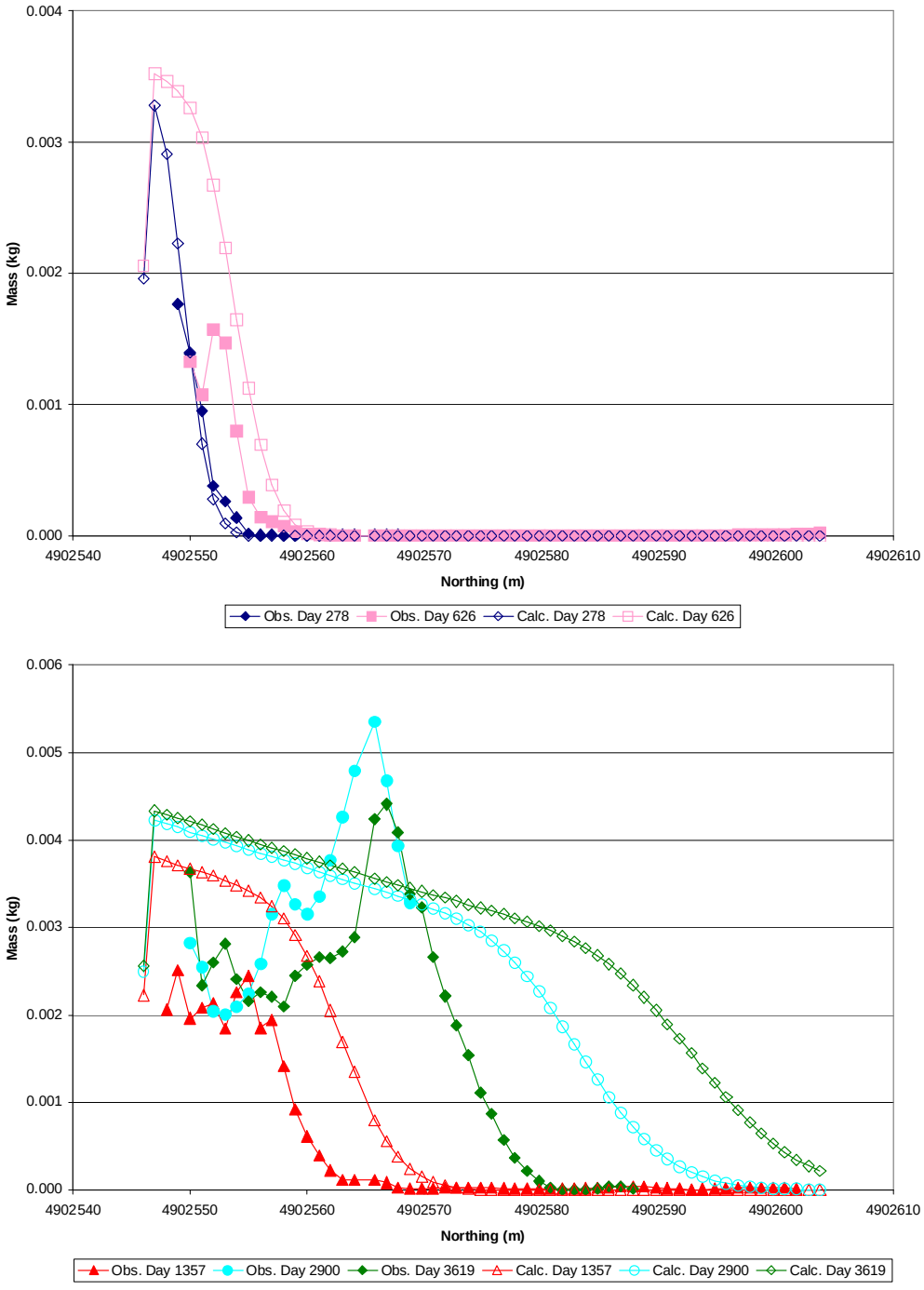

Figure 5.6: Best BIONAPL results for acenaphthene showing mass in transverse slices along the flow direction

late times. Some other process not represented by the model may be acting in the field to reduce the acenaphthene mass at late times. As suggested by the microcosm study (Chapter 2) and by Selifonov [11], cometabolism of acenaphthene supported by naphthalene dioxygenase may be occurring in the field. This would remove the excess mass seen in the model. Perhaps the acenaphthene should dissolve more quickly from the source, thereby allowing for an increase in maximum utilization rate as more mass enters the model earlier, and also reducing the acenaphthene mass present at late times.

5.8 Testing of alternate model parameters

In the above results, several different suggestions were made as to why a certain chemical in the model did not match well to its observed values. Often, the results showed a good match at early times, but a poor match at late times. This was partly a result of the calibration method used here, which attempted to first match early times to the observed values, then seeing if late times were modeled well with these model parameters. Other processes must be occurring in the field that are not represented in the model, and if these processes were incorporated into the model, then presumably the model would be capable of producing good matches at all times for all chemicals. These processes may include faster or slower NAPL dissolution, varying degradation rates, chemical interaction and inhibition, fermentation, and increased or decreased electron acceptor availability. Many of these processes were tested using a simplified model that consisted only of naphthalene, a group of the rest of the identified chemicals, and a remainder group of the rest of the creosote mass. Total creosote mass and the initial naphthalene mole fraction were kept the same as in Section 5.7. As a baseline, reaction parameters were kept the same as the best BIONAPL match; in subsequent simulations, parameters were varied one by one and even combined to see what effect this had on the match of the modeled naphthalene plume and the observed plume. Baseline plots are shown in Figure 5.7.

5.8.1 Decreasing electron acceptor availability by half

In this simulation, the background electron acceptor concentration was reduced from $20\,\mathrm{mg}/\mathrm{l}$ to $10\,\mathrm{mg}/\mathrm{l}$. The hypothesis was that if the electron availability was lower, then degradation would be lower in the core of the plume, and higher concentrations of naphthalene could persist in the plume core. The results from

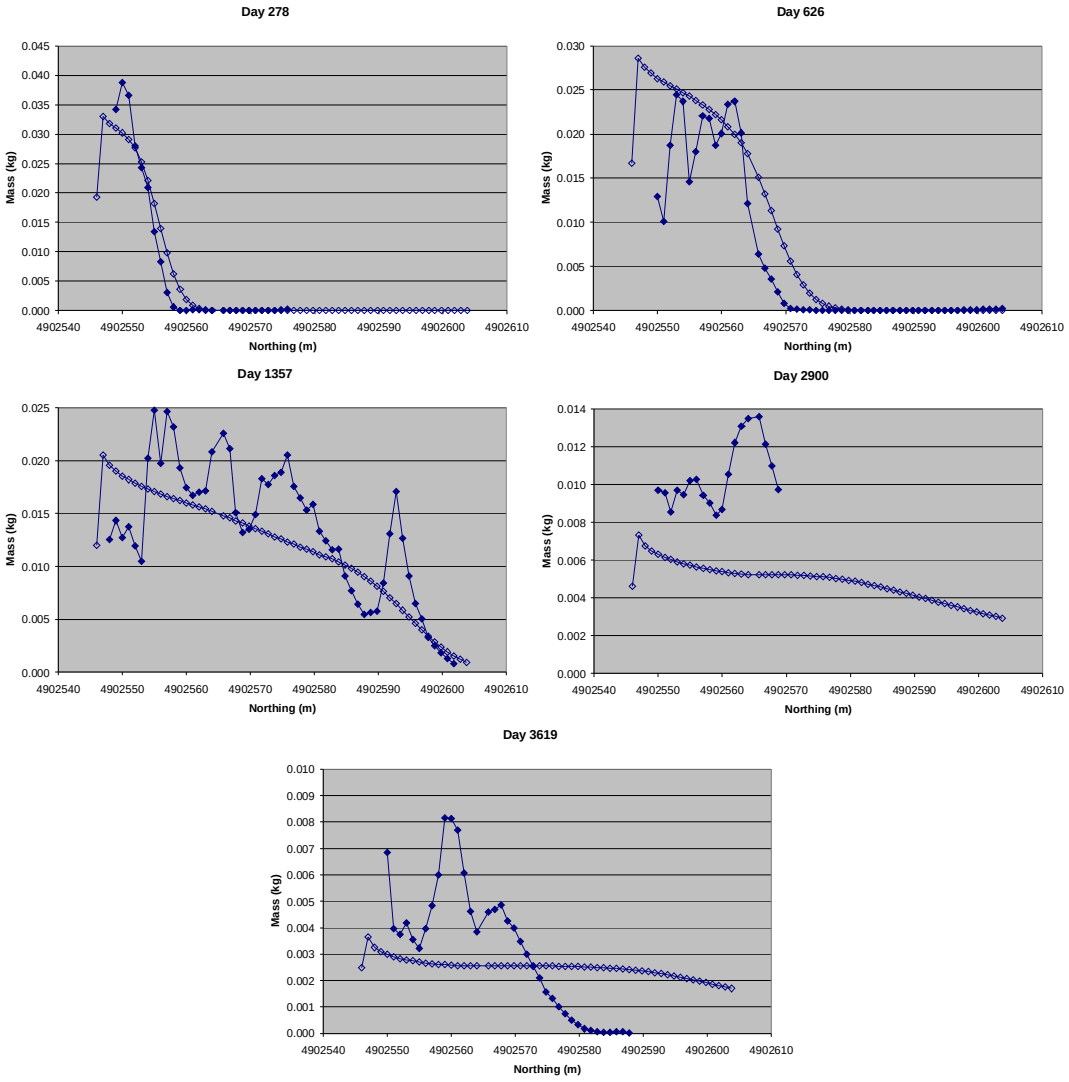

Figure 5.7: Naphthalene mass profiles comparing field observations (closed symbols) with model observations (open symbols). This simulation was run with reaction parameters the same as the best BIONAPL match described above.

this simulation are shown in Figure 5.8. Little to no change was found between the baseline and this simulation at day 278. At day 626, this new simulation was a much worse match to observations, and too much naphthalene mass was present in the model. At day 1357, this simulation was closer to the high peaks of the observed curve, but may have had too much mass. At day 2900, this simulation was a better match than the baseline simulation at near-source areas, but the plume did not decrease in mass farther from the source. Since the funnel-and-gate was in operation, no observations were available beyond northing 4902570. It was expected that field observations should decrease in mass beyond this point due to a decreasing mass flux, however the simulation did not show any such decrease in mass. There was too much naphthalene mass in that simulation. At day 3619, again the match was better in the near-source areas, but worse in the more distant areas of the plume.

Decreasing oxygen availability did not help to improve the match between the observed plume and the simulation. Instead, too much naphthalene mass tended to persist in the more distant areas of the model. In combination with lower oxygen availability, increasing the maximum utilization rate would likely not have helped improve the match, since more mass would be removed from the near-source zone as well as the areas farther from the source, and the overall match would be worse.

5.8.2 Increasing oxygen availability by a factor of two

In this simulation, the background oxygen concentration was increased from 20 mg / l to 40 mg / l. The hypothesis was that if the electron availability was higher, then degradation could be higher at the fringes of the plume, and the tailing-off behaviour found in the areas farther from the source would be eliminated. Another possibility was that incomplete mineralization was occurring in the field, and by adding more electron acceptors to the model, this process might be simulated. The results from this simulation are shown in Figure 5.9. At day 278, the new simulation had a worse match than did the baseline case, as more mass was removed from this simulation. At day 626, and at all subsequent sampling days, the mass removed from this simulation was far too much. Not only was mass removed from the distant parts of the naphthalene plume, but large amounts were also removed from the core of the plume.

Increasing the oxygen availability was not successful in improving the match to observed data. Too much mass was removed from the model with the increased oxygen concentration, in both the near-source and far parts of the plume. This might be improved by decreasing the maximum utilization rate for naphthalene,

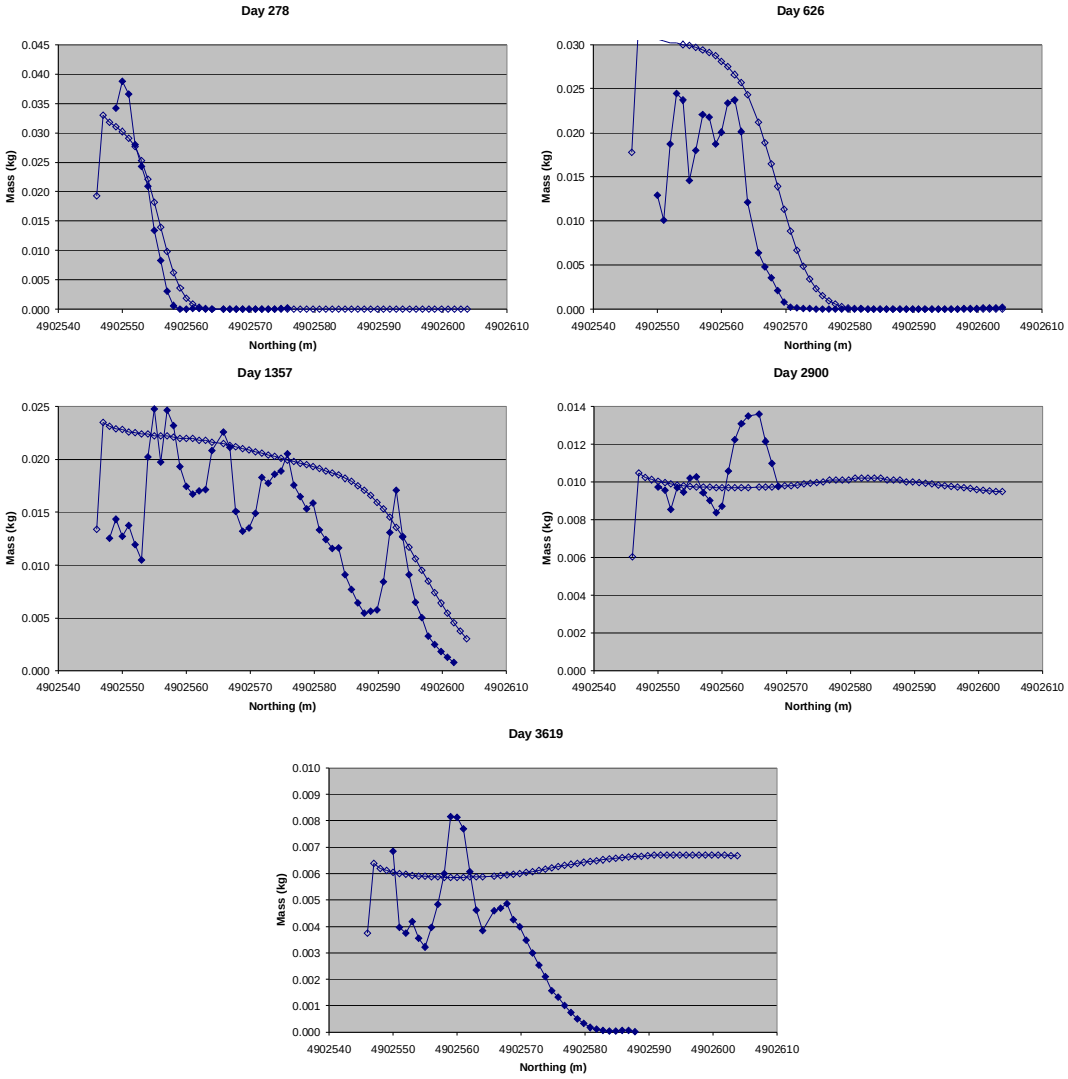

Figure 5.8: Naphthalene mass profiles comparing field observations (closed symbols) with model observations (open symbols). This simulation was run with naphthalene only and lower initial electron acceptor concentrations (see text).

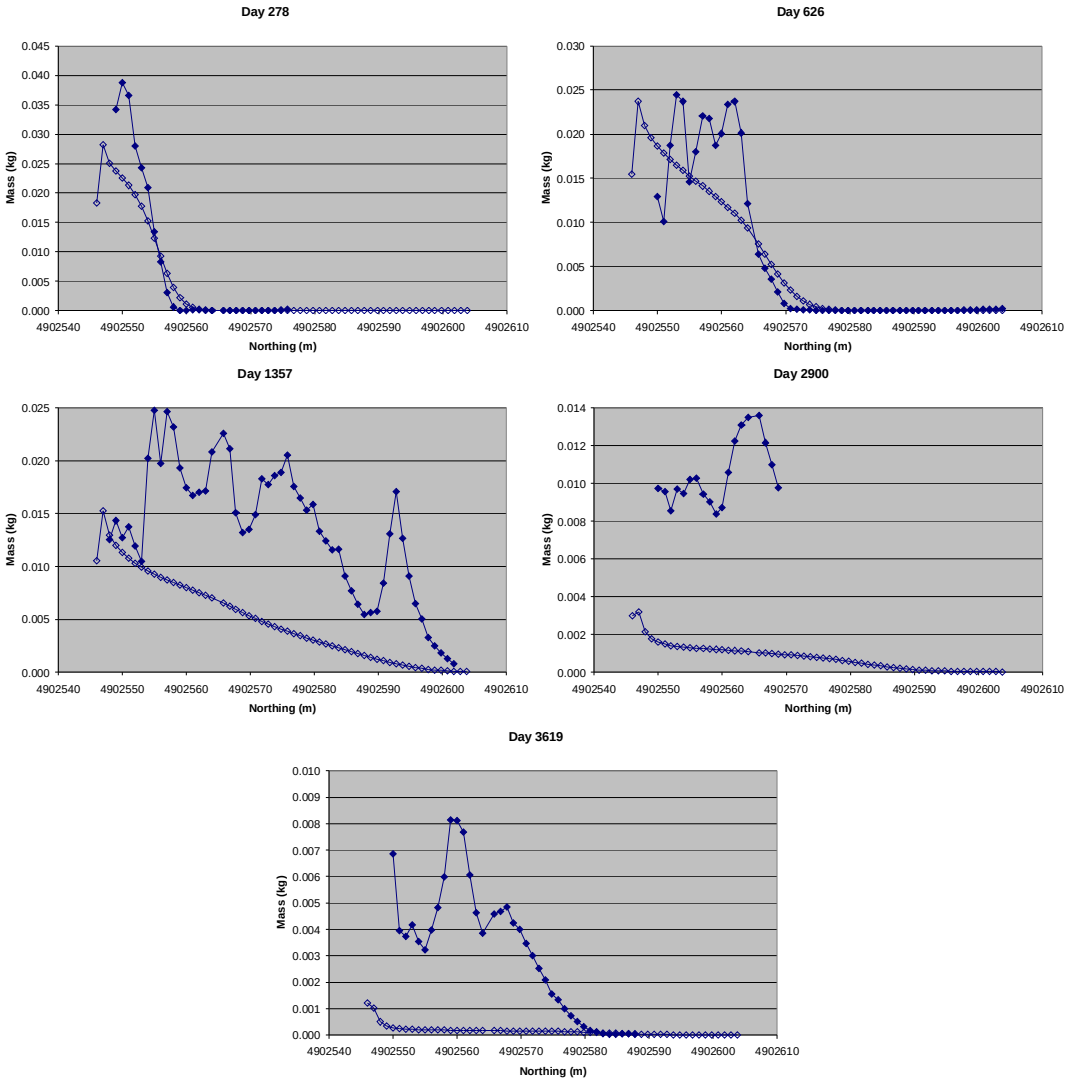

Figure 5.9: Naphthalene mass profiles comparing field observations (closed symbols) with model observations (open symbols). This simulation was run with naphthalene only and higher initial electron acceptor concentrations (see text).

but even then it is likely that the tailing-off behaviour seen far from the source would return.

5.8.3 Simulating two electron acceptors

In this simulation, the background values for oxygen and sulfate concentrations were used, instead of combining them into one electron acceptor as was done in the baseline simulation. The background concentrations used were 2.4 mg / l for oxygen, and 14 mg / l for sulfate. The purpose of this simulation was to test whether or not there was a significant difference in concentration profiles when simulating the electron acceptors separately or combined. The results from this simulation are shown in Figure 5.10. At day 278, this simulation consumed more naphthalene than in the baseline simulation. At day 626, this simulation matched more closely to observations, with mass reduced along the entire profile. At day 1357, mass was reduced again, and the new simulation had too little naphthalene mass along the entire plume. At days 2900 and 3619, again mass was reduced across the whole plume, and the match to observed values became worse.

Since this simulation tended not to match observations since mass was too low in the plumes, it was decided to try decreasing the sulfate-naphthalene maximum utilization rate. The sulfate-naphthalene maximum utilization rate was reduced from 0.05 to 0.02. However, once this simulation was run, the naphthalene mass decreased at day 278, and in the later snapshot days, along the entire plume (Figure 5.11). This may be explained due to less sulfate being consumed early in the simulation and therefore more available at later times, leading to more naphthalene mass consumed. In any case, this did not help to improve the match between the model and observations.

5.8.4 Slower NAPL dissolution

In this simulation, the NAPL source was made to dissolve more slowly than equilibrium by reducing the Sherwood number of all chemicals from 0.002 to 0.001.

By reducing the Sherwood number, it was expected that the creosote source would dissolve more slowly, decreasing the mass dissolved and degraded in the early times, and allowing more mass to exist in the model at late times. This would help increase the naphthalene and 1-methylnaphthalene concentrations at late times in the model, as more mass would be available to dissolve from the source at these times. The results from this simulation are shown in Figure 5.12.

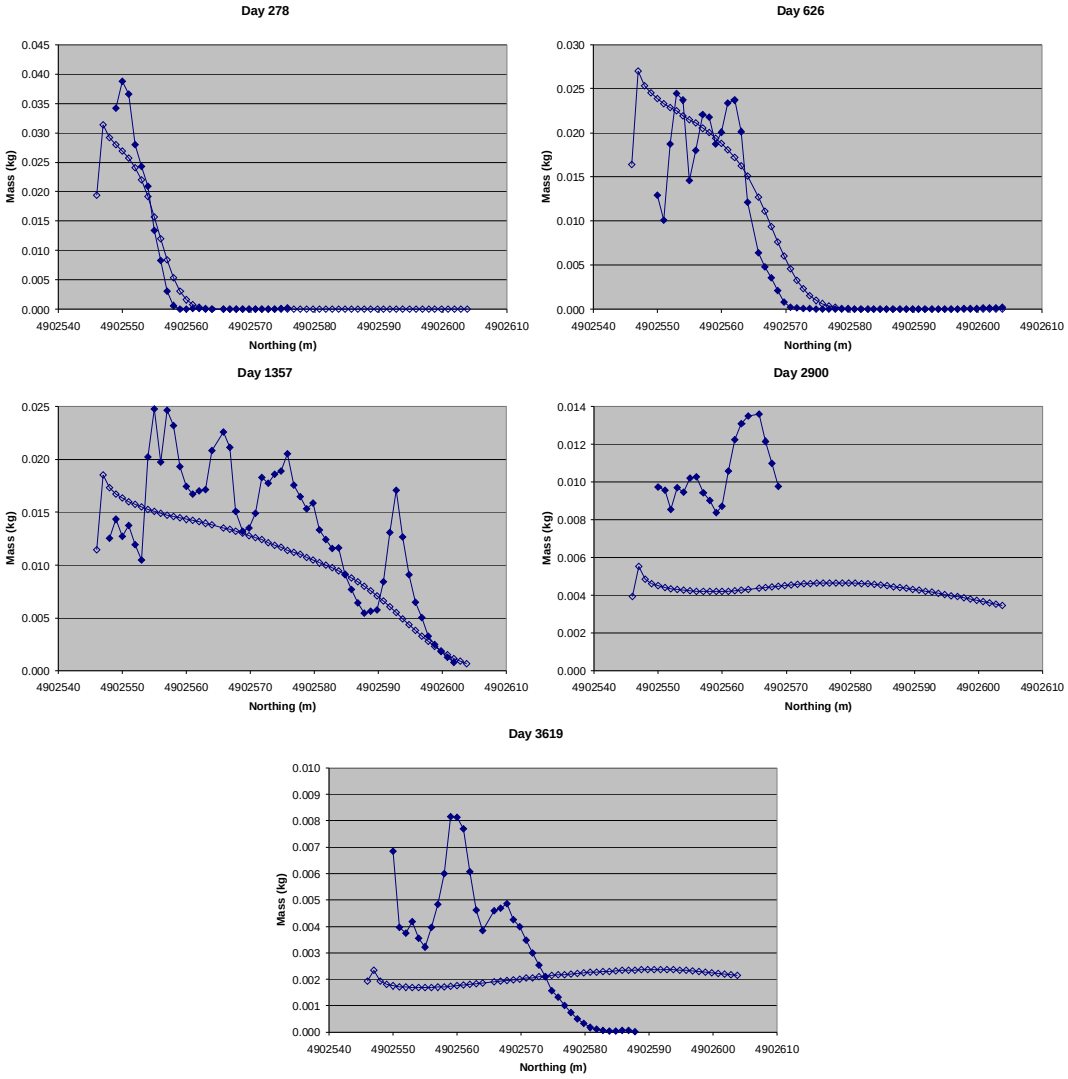

Figure 5.10: Naphthalene mass profiles comparing field observations (closed symbols) with model observations (open symbols). This simulation was run with two separate electron acceptors (see text).

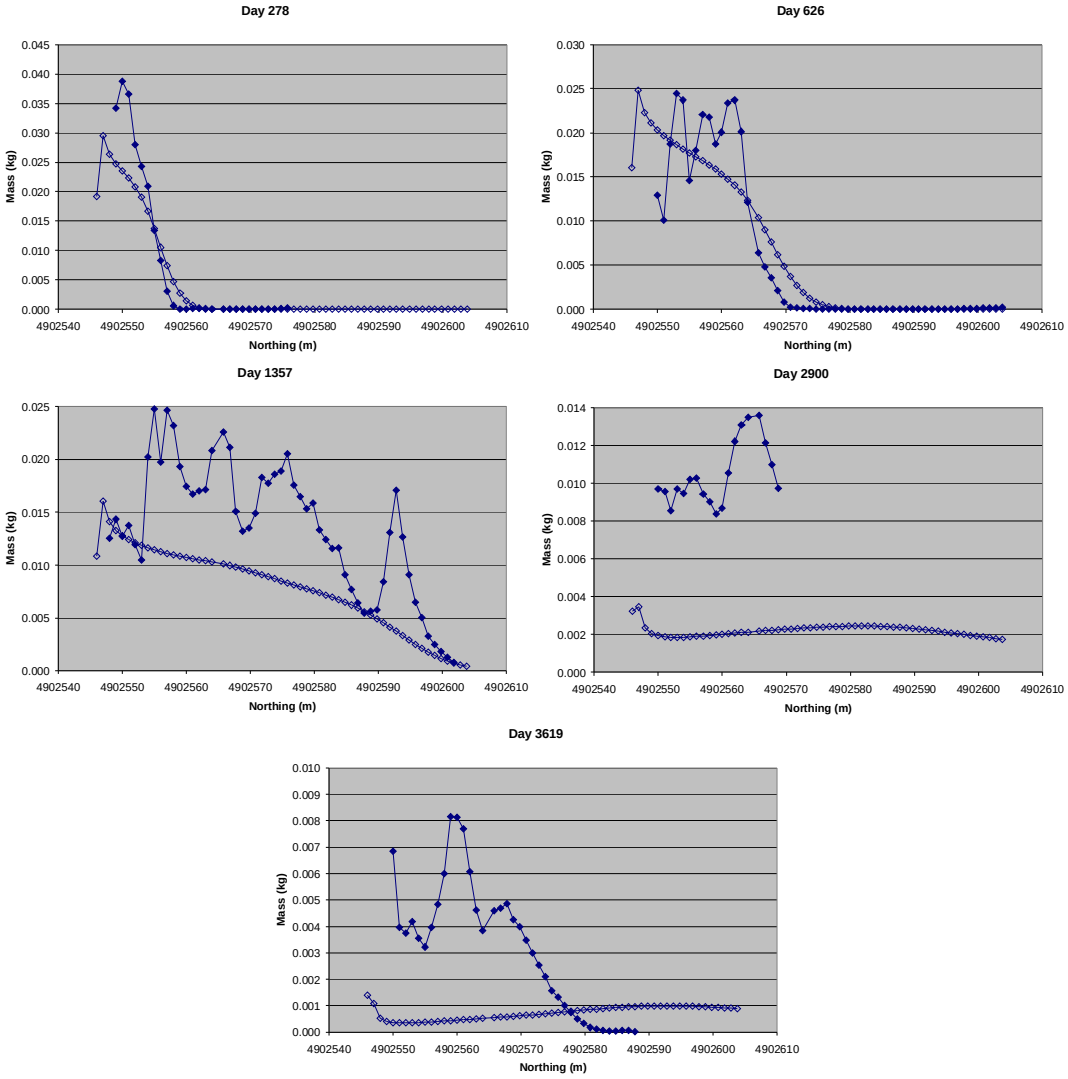

Figure 5.11: Naphthalene mass profiles comparing field observations (closed symbols) with model observations (open symbols). This simulation was run with two electron acceptors and a lower sulfate utilization rate (see text).

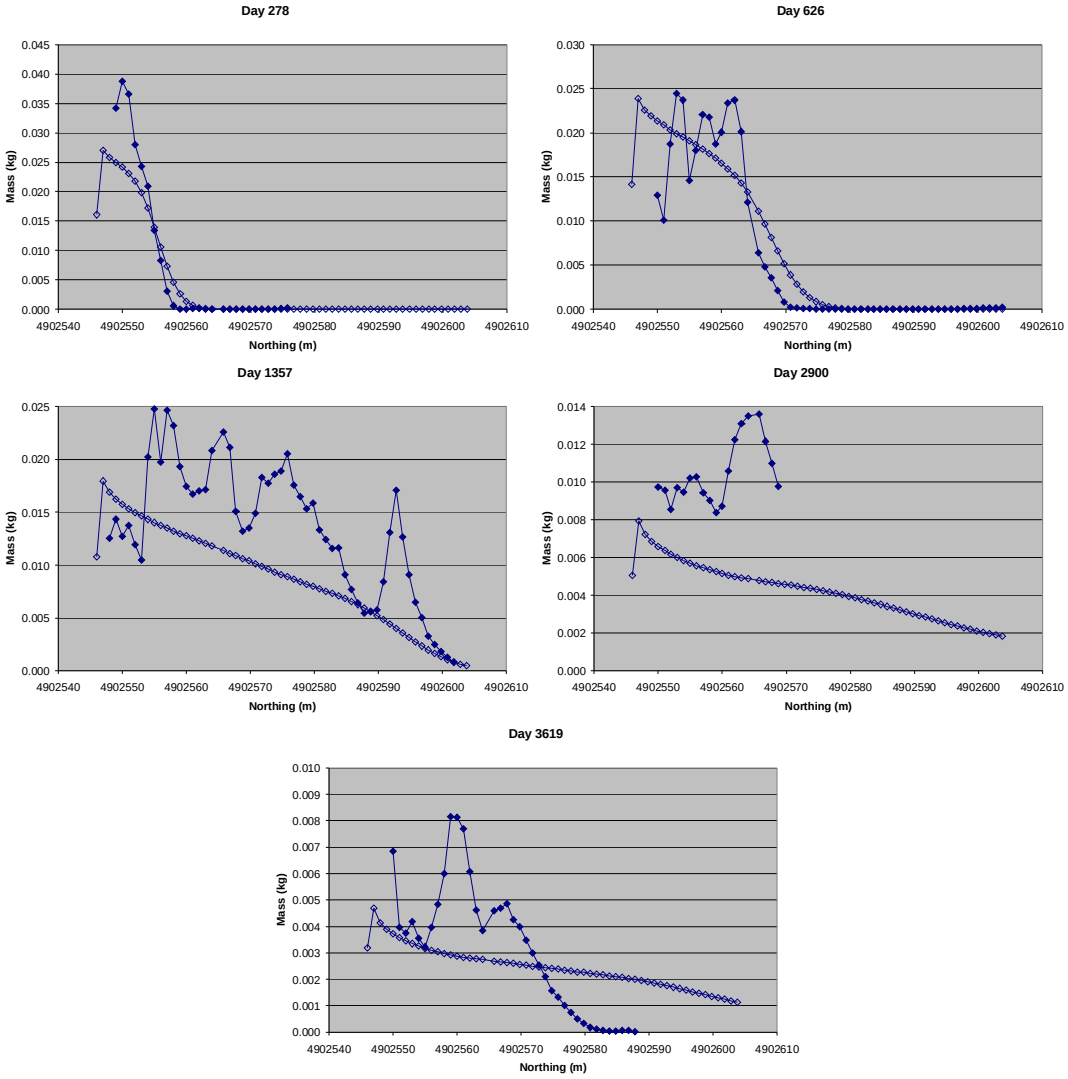

Figure 5.12: Naphthalene mass profiles comparing field observations (closed symbols) with model observations (open symbols). This simulation was run with a lower Sherwood number (see text).

At day 278, too little mass was present in this simulation as compared to observations, and less mass was present in this simulation than in the baseline case. Since less mass was dissolving, less mass was available by this time. At day 626, again less mass was present in this simulation, but the mass profile fit the observations better than the baseline case did. The near-source peak matched better, and a similar profile shape was found than in the baseline. At day 1357, however, the slower-dissolving source caused this simulation to calculate too little mass present. The day 2900 and 3619 snapshots had slight improvements over the baseline case, and some of the tailing-off behaviour was minimized. Nevertheless, the mass present at these two days was still far below what was observed near the source, and too high in the areas far from the source.

Decreasing the rate of source dissolution in this simulation did have some helpful effects on the model output. The mass profile matched better at days 626, 2900 and 3619, but became worse at days 1357 and 278. The improvement at days 2900 and 3619 was only slight, and at all snapshot days but day 626, too little mass was present in the simulation. Too much degradation may have been occurring, decreasing the dissolved mass at these days.

To test this hypothesis, a simulation was run exactly as above, with the low Sherwood number, but also with a lower maximum naphthalene utilization rate. This rate was decreased from 0.05 to 0.02. Results are shown in Figure 5.13. By reducing the maximum utilization rate, the mass present at day 278 improved from the above simulation, but it was still below observations. At day 626, the mass in the simulation also increased, to a profile more similar to the baseline case. This simulation also showed slightly more mass present at the front of the plume. At day 1357, the mass in this simulation increased, and matched better to observations than the baseline case did. However, a slightly higher mass in the simulation would match more closely to the average of the observations. At day 2900, the mass present just downgradient of the source matched very well to observations. Still, in this simulation, the mass far from the source was too high, and naphthalene travelled too far in the study area. A very similar pattern was seen at day 3619, matching well near the source, but with too much mass in the simulation at distances farther from the source.

The presence of the funnel and gate from day 2100 onward may explain the mismatch at late time. In the field, the funnel and gate may have treated the naphthalene plume, decreasing its size and mass. However, the model did not simulate the effect of the funnel and gate, possibly resulting in the mismatch in mass profiles seen at late time.

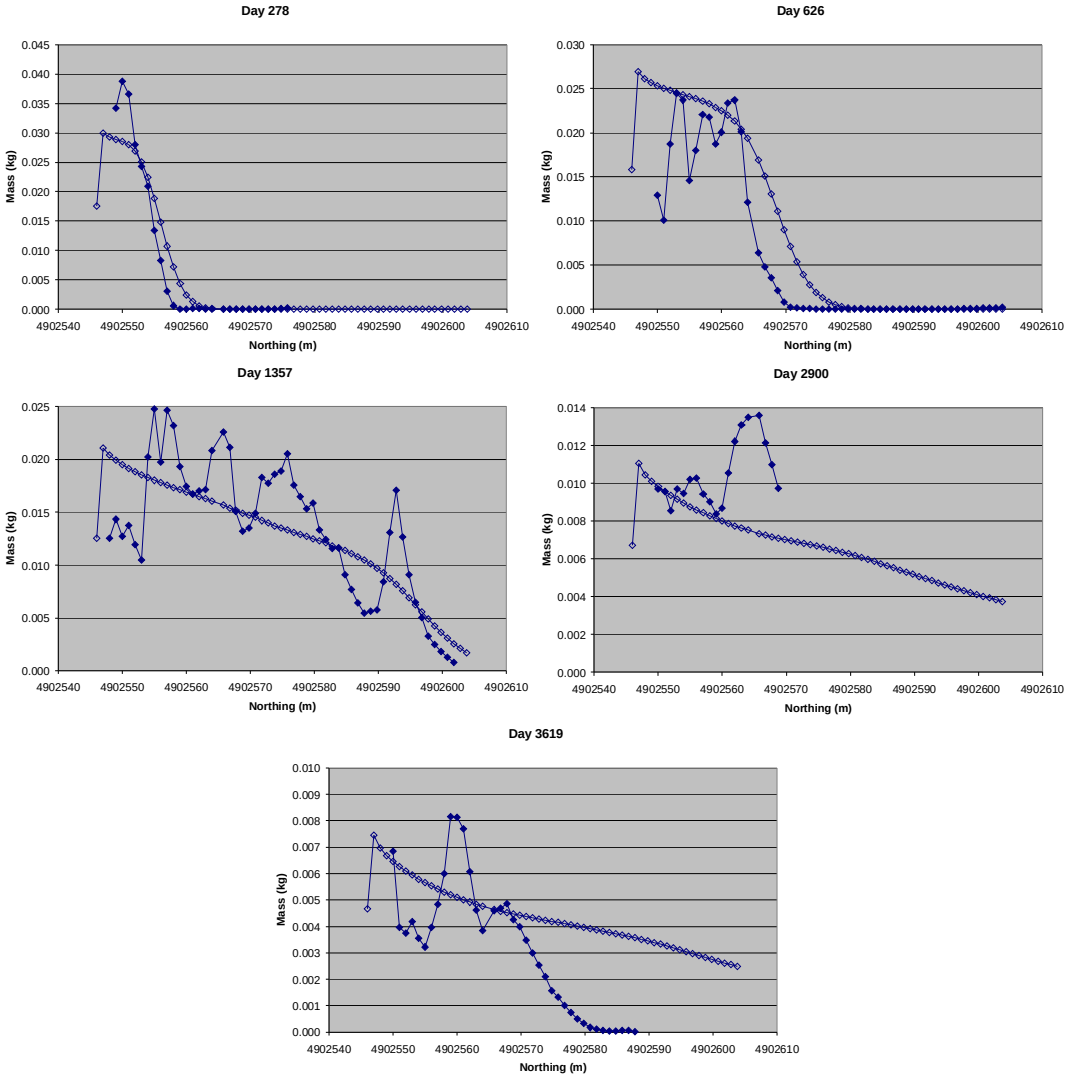

Figure 5.13: Naphthalene mass profiles comparing field observations (closed symbols) with model observations (open symbols). This simulation was run with a lower Sherwood number and lower oxygen utlization rate (see text).

5.8.5 Conclusions - Testing of alternate model parameters

Several model parameters were tested in a simplified model of the CFB Borden coal tar creosote emplaced source study site. This simplified model presented detailed results for naphthalene only, and was used to examine if adjusting a certain model parameter or combination of parameters would improve the model results for the more complex model which simulated several chemicals. The model parameters that were tested included electron acceptor concentrations, simulating the electron acceptors separately, slower NAPL source dissolution, and combining any of these with a lower naphthalene maximum utilization rate.

From this testing, it was found that increasing or decreasing the electron acceptor concentration did not improve the match of the simulated naphthalene mass profiles to the observed naphthalene mass profiles. Decreasing the oxygen concentration allowed mass to persist in the more distant areas of the model, while increasing oxygen concentrations decreased naphthalene mass too much in the near-source areas. Changing the naphthalene maximum utilization rate would likely not have helped improve the match in either case, since more mass would be removed from or allowed to persist throughout the model, not just in the areas where too much or too little mass was present.

No improvement was found by simulating sulfate and oxygen as separate electron acceptors, versus the lumped electron acceptor concentrations used through the remainder of the simulations.

By allowing the NAPL source to dissolve more slowly, there was some improvement seen in the naphthalene mass profiles as compared to the baseline case. However, the improvement was not seen in all snapshot days, and the mass in the model was still too low throughout the simulation. When the naphthalene maximum utilization rate was decreased, the model results again improved, matching more closely to the observed mass profile. This combination of a slower dissolution and lower naphthalene maximum utilization rate was not a solution to the problem of naphthalene mass travelling too far in the domain, and naphthalene masses were too high at late times, in the area far from the source.

The presence of the funnel and gate in the field after day 2100 may explain the poor match of the model to observations at days 2900 and 3619. The funnel and gate may have decreased the naphthalene mass present in the field, but the model did not simulate this process.

None of the tested parameters was able to provide a solution to the problem of mass persisting in the model area far from the source, however by using a slower NAPL dissolution, some improvement was seen. Improvement for the other plume

chemicals in the more complex model is also possible with a slower NAPL dissolution.

5.9 Application of new model parameters to multi-component source case

In light of the improvement seen in the simplified model results when NAPL dissolution was slower, it was decided to apply this lower NAPL dissolution to the more complex BIONAPL model. The simplified model only simulated naphthalene and a remainder group, and there was interest to see if applying this new model parameter to the more complex model would cause the model to match more closely to observations. In the complete model which simulated several chemicals of interest, a slower dissolution rate may have improved the modeled results for some chemicals, and may have worsened the match for other chemicals. In the model, naphthalene and m-xylene may have benefited from dissolving more slowly from the NAPL source, while 1-methylnaphthalene and acenaphthene may have benefited from dissolving more rapidly.

Based on the "best match" BIONAPL simulation described previously, the Sherwood numbers of all chemicals in this new simulation were decreased from 0.002 to 0.001; mass profiles of the output are presented in Figures 5.14 through 5.17. At day 278, the naphthalene and m-xylene simulation results became worse than the "best match" results. The higher mass peaks near the source dropped in mass, and the chemicals spread farther downgradient. As expected, less mass of these two chemicals had dissolved, and chemical masses were lower close to the source. Similarly, the 1-methylnaphthalene results became somewhat worse, with less dissolved mass present. The acenaphthene mass profile improved somewhat, with slightly more mass present farther downgradient, matching more closely to the observed profile.

At day 626, the naphthalene and m-xylene masses became lower throughout the profile, and matched more closely to their observed mass profiles. The mass peaks near the source were quite close to observations, and these two profiles simulated the observed character of each profile quite well. The 1-methylnaphthalene profile dropped in mass as compared to the "best match" and became a worse match to observations. The acenaphthene profile dropped slightly in mass as well, but this was an improvement on the "best match" results.

At day 1357, both the naphthalene and 1-methylnaphthalene profiles dropped too low in mass. These two chemicals were too far below the observed profiles, and

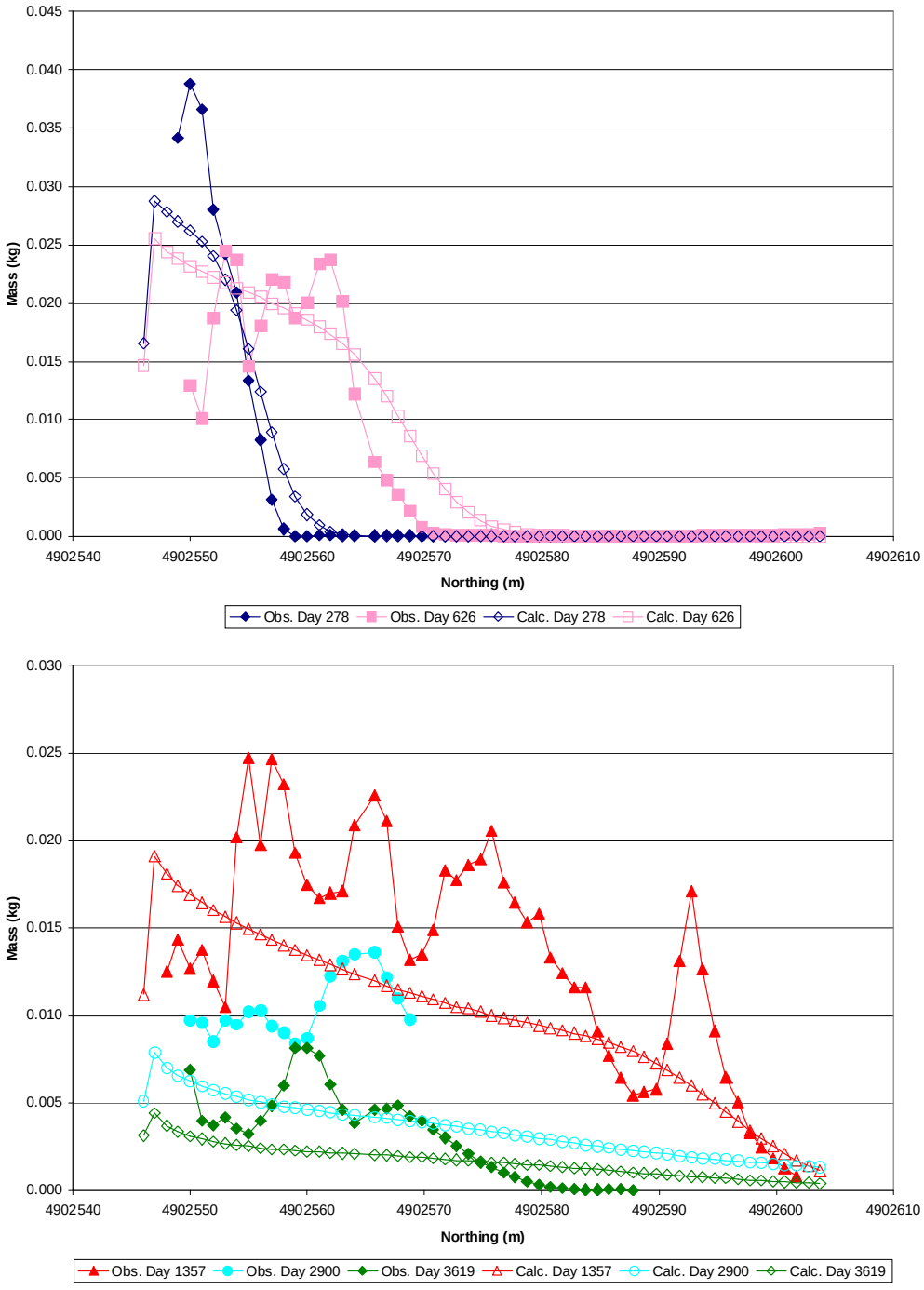

Figure 5.14: BIONAPL results for naphthalene, with a decreased Sherwood number

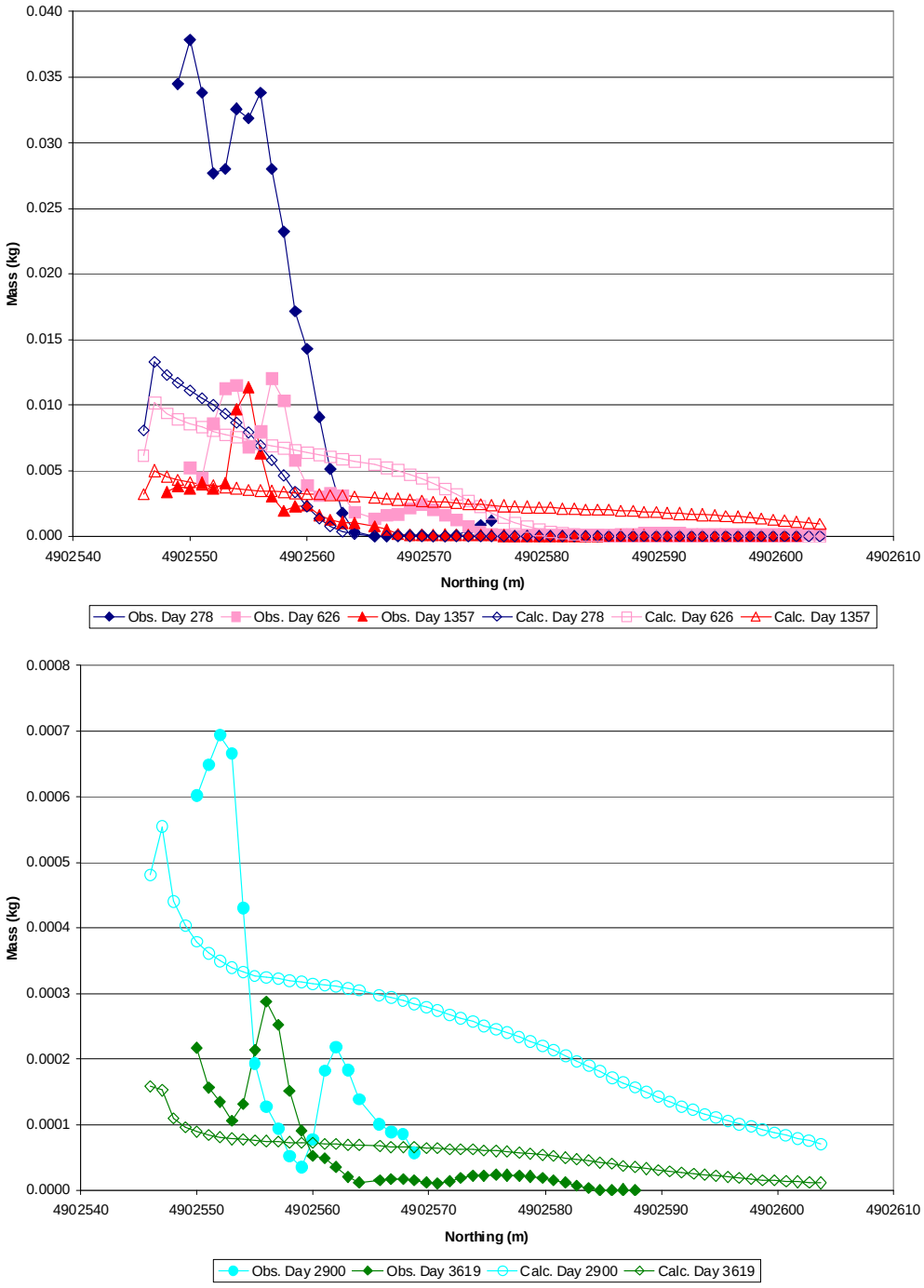

Figure 5.15: BIONAPL results for m-xylene, with a decreased Sherwood number

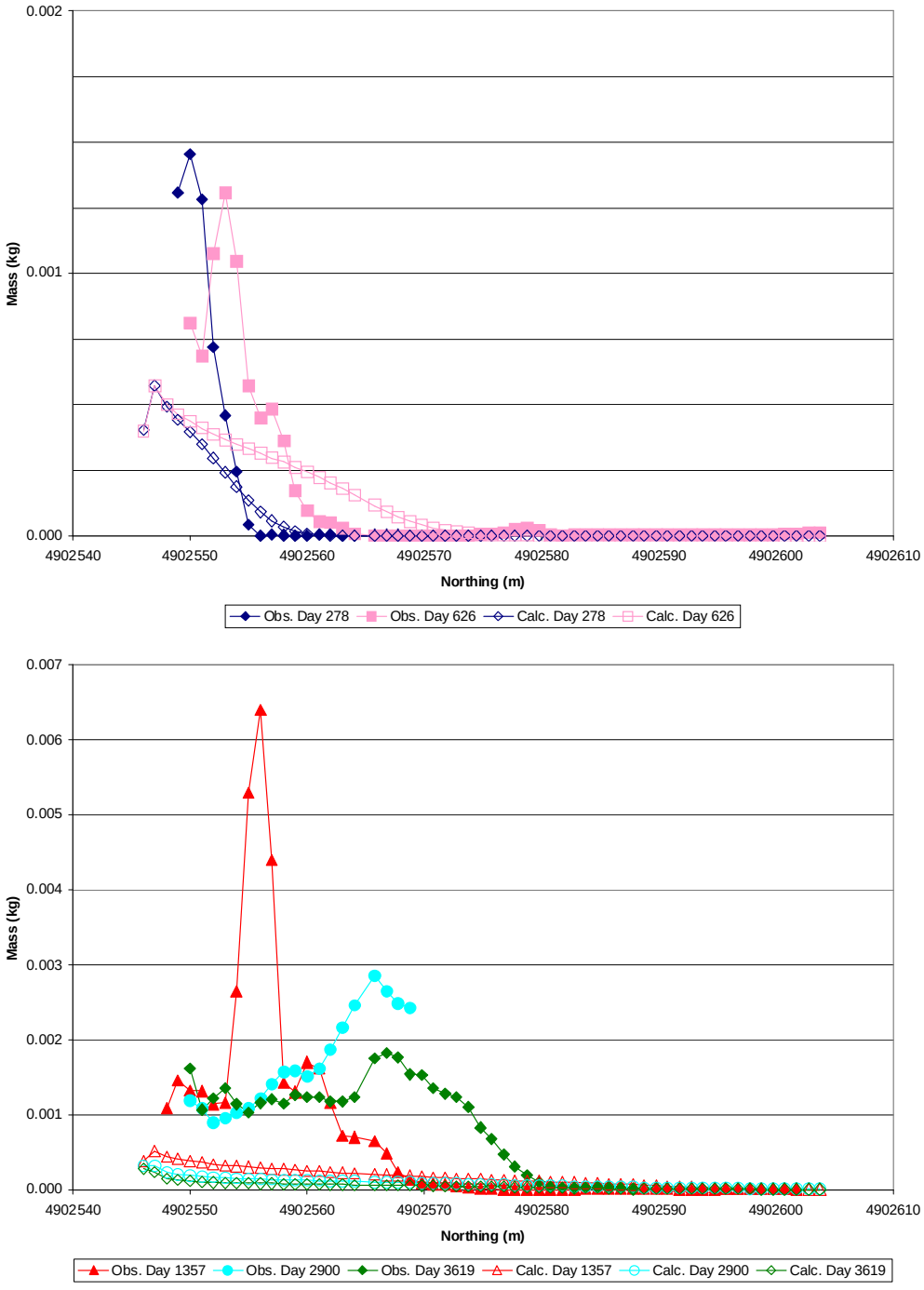

Figure 5.16: BIONAPL results for 1-methylnaphthalene, with a decreased Sherwood number

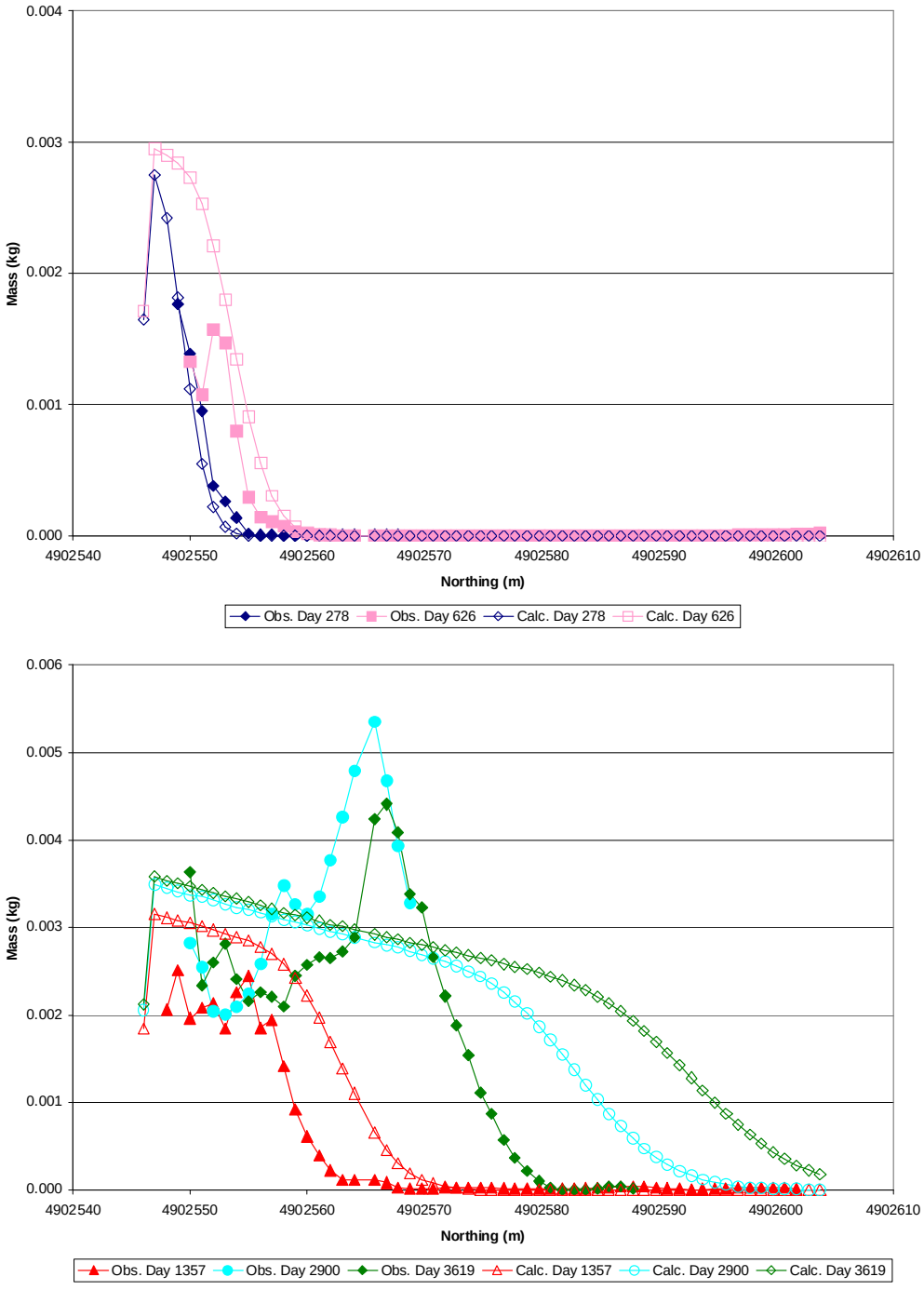

Figure 5.17: BIONAPL results for acenaphthene, with a decreased Sherwood number

far too little mass was present at this snapshot day. The m-xylene plume dropped in mass as well, and the profile did not reflect the observed character well at all. The simulation missed the peak present at northing 4902555, and too much mass was present in the area far from the source. The acenaphthene plume was the only chemical to improve at this snapshot day, relative to the "best match", with the mass profile dropping much closer to observations. The character of this plume is represented well, but a bit too much mass was found in the areas far from the source.

At day 2900, the naphthalene plume had a higher peak close to the source, with a value closer to observations, but the overall mass decreased, especially at the far end of the plume. However, the character of the profile is very similar to the "best match" simulation, and too much mass is present in the areas far from the plume. The m-xylene profile increased in mass throughout, matching better to observations near the source, but allowing too much mass to exist far from the source. The 1-methylnaphthalene profile decreased in mass along the entire profile, and its mass is close to zero, much too far below observations. The acenaphthene plume decreased in mass along the entire profile, matching more closely to the mass close to the source, but matching more poorly in the middle section of the profile.

At day 3619, the naphthalene profile increased in mass near the source, and decreased in mass far from the source, leading to a better match overall to observations. However, there is still far too little mass present in the model at this snapshot day. The m-xylene profile was somewhat higher at this snapshot day, leading to a better match. The 1-methylnaphthalene plume became lower in mass, very close to zero, and far below observations. The acenaphthene plume also dropped in mass, matching very well to observations in the near-source to middle areas of the plume, but too much mass was persisting in the far sections of the plume.

By decreasing the Sherwood number and slowing NAPL dissolution, there was no significant and global improvement seen. Some chemicals had better profiles at some days, and were worse at other days. Some chemicals had better matches to observations when other chemicals matched more poorly. Decreasing the Sherwood number did not improve the match to observations well, and was not a solution to the mismatches described earlier.

5.10 Conclusions and implications for future work

Mass flux into this multi-chemical BIONAPL model matched fairly well to observations of naphthalene and m-xylene, and poorly for 1-methylnaphthalene and

acenaphthene. There are processes that may be occurring in the field which BIONAPL does not model, resulting in this mismatch of mass fluxes. Additionally, the mass fluxes measured in the field may not be representative of the actual mass flux that occurred. There may have been a variability to the mass emanating from the source, and BIONAPL may be modeling the mass flux more accurately than is currently believed. The chemicals which do not match well to observed mass fluxes cannot be analysed as critically as those that do match well to observations. Nonetheless, a comparison of all four chemicals to observations was performed, with the mismatch in mass flux kept in mind.

BIONAPL 3/D was able to model naphthalene fairly well at most times. The poorest matches occurred at days 2900 and 3619, in the part of the plume that existed downgradient of the funnel-and-gate. The funnel-and-gate was installed at about day 2100, and the behaviour of the naphthalene plume in the field after this time may have been affected, both physically and chemically, by this treatment system. There may have been a greater degree of plume mixing downgradient of the funnel-and-gate, and the nitrate briquettes present in the gate may have decreased the naphthalene concentrations passing through the gate. The effect of these processes has not been considered here. As a result, at days 2900 and 3619, results from downgradient of the funnel-and-gate were not considered as relevant to this analysis as those from upgradient. Overall, the naphthalene plume was modeled fairly well.

m-Xylene was modeled better at some days than at others. The pattern of decreasing plume mass for this component is represented well by the model. The mass flux modeled for m-xylene was lower than that observed at most snapshot days, and this may be the most important factor for the mismatch between observations and the model. m-Xylene was not observed to travel as far from the source as naphthalene, and was not affected by the funnel-and-gate to as great a degree.

1-Methylnaphthalene was modeled fairly well at the first two snapshot days, but quite poorly afterwards. The modeled mass flux of 1-methylnaphthalene was much lower than observations, and if this was improved, it would be possible to make more comprehensive conclusions about this plume's behaviour.

Acenaphthene matched well at the first two snapshot days, then after this point, far too much mass was present in the model. This is due to the modeled mass flux at the fence behaving differently from the measured mass flux. The observed mass flux decreased with time, while in the model it increased, leading to a poor match to observations at late time. Again, if the modeled mass flux was improved, more conclusions could be made about this plume's behaviour.

Chapter 6

Summary and Conclusions

A microcosm study, using CFB Borden sand acclimated to creosote and CFB Borden pristine groundwater, showed that the degradation of both naphthalene and 1-methylnaphthalene was unaffected by the presence of the other compounds in a mixture of acenaphthene, naphthalene and 1-methylnaphthalene. The degradation of acenaphthene was found to be more rapid when naphthalene and/or 1-methylnaphthalene was present in the microcosm. In a separate study by Selifonov et al. [11], naphthalene dioxygenase and phenanthrene dioxygenase were found to allow cometabolism of acenaphthene. In the CFB Borden microcosms, the same interaction between naphthalene and acenaphthene may be occurring, as supported by this microcosm study.

Using the programs Visual MODFLOW and RT3D, the transport and degradation of naphthalene at CFB Borden was simulated with three electron acceptors: oxygen, nitrate and sulfate. At early times, this model was able to reproduce observed field naphthalene concentrations well, but not at late times. At the end of the simulation, at 3619 days, the lower-concentration naphthalene contours were too large, and the higher-concentration contours were too small. Too much naphthalene was degraded in the core of the naphthalene plume, and too little was degraded on the plume fringes. The model was unable to reproduce late time observed concentrations, likely because the model was not able to simulate degradation and inhibition processes that were occurring in the field. These processes may include chemical interactions, chemical and biological inhibition, cometabolism, and any effect of the funnel and gate installation.

The program BIONAPL/3D was also used to model the naphthalene plume, in an attempt to improve the naphthalene match at late time. Early time results were

good, however, difficulties in simulating the mass flux into the plume led to poor results at late time.

In an effort to learn more about these processes that may be occurring in the plume, the program BIONAPL/3D was used to simulate the transport and degradation of several of the creosote chemicals simultaneously. As with the Visual MODFLOW model, the BIONAPL model which best matched observations generally worked well at early times, but did not at late times. Too little mass was simulated in the near-source areas of several plumes, and too much mass was found in the parts of the plumes farther from the source.

An attempt was made to determine if there was a single process or a combination of processes that would have improved the match of the BIONAPL model to observations. A simpler model was used, with only the chemical naphthalene simulated. The parameters tested were: increase or decrease in electron acceptor concentrations, simulation of two separate electron acceptors, and slower NAPL dissolution through a lower Sherwood number. None of these were successful in making any significant improvements to the match to observations. There was a limited improvement seen when the Sherwood number was decreased.

The Sherwood number of the more complex model was then also decreased to see if slower NAPL dissolution improved the match for all of the chemicals of interest. However, improvements were seen for some chemicals but not others, and at some times but not others. This was not the process that needed to be changed to allow the model to better match observed concentrations.

The mismatch between the model and observations was in great part due to modeled mass fluxes at the three-metre fence which did not match observations. Since different amounts of mass were entering the model, different amounts of mass were present to be degraded, and the mass profiles plots did not match well for all chemicals. The chemicals which matched best throughout the timeframe of the model were naphthalene and m-xylene, and these two chemicals matched observed mass fluxes most closely. Acenaphthene and 1-methylnaphthalene had poor matches to mass flux, and as a result did not match observed mass profiles well.

Overall, there are many processes occurring in this complex source that are not represented by Visual MODFLOW or BIONAPL. Dissolution from the NAPL source was not modeled well for all chemicals, but some success was seen with other chemicals. Chemical and biological interactions may be occurring, such as bacterial inhibition by the presence of certain chemicals, cometabolism of various chemicals, and fermentation. An attempt was made to simulate these processes, with little success. It may be that our understanding of these processes is insufficient, and so we are unable to model them.

Chapter 7

Recommendations

The mass flux into the BIONAPL model at the three-metre fence must be improved for all chemicals, but most importantly for 1-methylnaphthalene and acenaphthene. If a more accurate mass flux were used in the model, then it is likely that much better results would be obtained, especially for these two chemicals.

By incorporating a transient flow field, these models would represent field conditions in a more realistic manner, and more success may be had in matching model output to observations. Heterogeneous distribution of the creosote in the source would also result in a more realistic model.

If the match to observations is improved in this manner, then a better analysis of the effect of various plume processes may then be performed.

Bibliography

[1] Freyberg, D.L., 1986. A natural gradient experiment on solute transport in a sand aquifer: 2. spatial moments and the advection and dispersion of nonreactive tracers, Water Resources Research, 22(13), 2031-2046.

[2] King, M.W.G., 1997. Migration and natural fate of a coal tar creosote plume, Ph.D. Thesis, University of Waterloo, Waterloo, Ontario.

[3] King, M.W.G., Barker, J.F., 1999. Migration and natural fate of a coal tar creosote plume: 1. Overview and plume development. Journal of Contaminant Hydrology, 39, 249-279.

[4] King, M.W.G., Barker, J.F., Devlin, J.F., Butler, B.J., 1999. Migration and natural fate of a coal tar creosote plume: 2. Mass balance and biodegradation indicators, Journal of Contaminant Hydrology, 39, 281-307.

[5] MacFarlane, D.S., Cherry, J.A., Gillham, R.W., Sudicky, E.A., 1983. Migration of contaminants in groundwater at a landfill: a case study: 1. groundwater flow and plume delineation, Journal of Hydrology, 63, 1-29.

[6] Mackay, D.M., Freyberg, D.L., Roberts, P.V., Cherry, J.A., 1986. A natural gradient experiment on solute transport in a sand aquifer: 1. approach and overview of plume movement, Water Resources Research, 22(13), 2017-2029.

[7] Malcolmson, H, 1992. Dissolution of an emplaced creosote source, CFB Borden, Ontario, M.Sc. Thesis, University of Waterloo, Ontario.

[8] Martin, C.A., 2002. The long-term fate of a coal tar creosote plume, B.Sc. Thesis, University of Waterloo, Waterloo, Ontario.

[9] Molson, J., 2002. BIONAPL/3D: A 3D model for groundwater flow, multicomponent NAPL dissolution and biodegradation, User Guide

[10] Schirmer, M., Durrant, G.C., Molson, J.W., Frind, E.O., 2001. Influence of transient flow on contaminant biodegradation, Ground Water 39(2), 276-282.

[11] Selifonov, S.A., Chapman, P.J., Akkerman, S.B., Gurst, J.E., Bortiatynski, J.M., Nanny, M.A., Hatcher, P.G., 1998. Use of 13C nuclear magnetic resonance to assess fossil fuel biodegradation: Fate of [13-C]Acenaphthene in creosote polycyclic aromatic compound mixtures degraded by bacteria. Applied and Environmental Microbiology 64, 1447–1453.

[12] Sudicky, E.A., Cherry, J.A., Frind, E.O., 1983. Migration of contaminants in groundwater at a landfill: a case study: 4. a natural gradient dispersion test, Journal of Hydrology, 63, 81-108.

[13] Zamfirescu, D and Grathwohl, P., 2001. Occurrence and attenuation of specific organic compounds in the groundwater plume at a former gasworks site, Journal of Contaminant Hydrology 53, 407-427.

Appendix A

Microcosm experiment methods

LABORATORY MICROCOSMS: AEROBIC BIODEGRADATION- INTERACTIONS OF NAPHTHALENE, 1-METHYL-NAPHTHALENE AND ACENAPHTHENE (CREOSOTE COMPOUNDS)

FOR CAITLIN MARTIN AND MICHELLE FRASER

by Marianne VanderGriendt

START DATE: MARCH 30, 2004

A.1 INTRODUCTION:

A series of static batch microcosm experiments was designed to follow the aerobic biodegradation of naphthalene, 1-methylnaphthalene, and acenaphthene (possibly co-metabolic), both singularly, and in combination (to determine if biodegradation rates would differ). The microcosms contained CFB Borden aquifer material from a creosote contaminated area, and pristine CFB Borden groundwater supplemented with inorganic nutrients. Concentrations of each creosote compound were monitored at nine sampling times over the course of 8 days.

A.2 MATERIALS AND METHODS:

Aquifer soil material ($4-5$ ft aluminum cores) was collected from around row 15-2 from a depth of 10 to 15 ft (in front of the funnel and gate) at the CFB Borden

Microcosm Identification	Soil (g)	Groundwater (ml)	Naphthalene	1-Methyl-Naphthalene	Acenaphthene	Sodium Azide
Control Mix (Sterile) A,B,C	10	35	Yes	Yes	Yes	Yes
Active Mix A,B,C	10	35	Yes	Yes	Yes	No
Active Naphthalene A,B,C	10	35	Yes			No
Active 1-Methyl Naphthalene A,B,C	10	35		Yes		No
Active Acenaphthene A,B,C	10	35			Yes	No

Table A.1: Design of 5 types of microcosms

Creosote contaminated field site, March 2004. In the laboratory, soil was pared out of the cores (excluding the first few centimeters at the ends of the core, and the $1-2$centimeters contacting the core wall) and mixed together in a sterile air flow cabinet in preparation for use in the experiment.

Pristine groundwater was collected at CFB Borden from a background well located in front of the Barker Barn in March of 2004. Before use in the experiment, the groundwater was aerated with sterile air to a dissolved oxygen level of $8.2\,\mathrm{mg}/\mathrm{l}$.

All equipment used during the microcosm set-up was sterilized prior to use and aseptic technique was employed throughout the experiment. Microcosms were assembled in the sterile air flow cabinet.

A.3 EXPERIMENTAL DESIGN AND PROCEDURE:

A.3.1 DESIGN (TableA.1):

5 types of microcosms * 3 (triplicate) * 10 sampling times = 150 microcosms

A.3.2 PROCEDURE:

Thirty control microcosms (60 ml glass hypovials with Teflon crimp top seals) received 10 g of soil and were autoclaved for 1 hour on three successive days to sterilize the soil. This was followed by the addition of 0.35 ml of Sodium Azide solution (Appendix A) to poison added groundwater over the course of the experiment to ensure inactivation of microbial activity. One hundred and twenty active microcosms received 10 g of soil. All microcosms received the addition of 0.65 ml of Modified Bushnell Haas Medium (Appendix B). Four types of groundwater were prepared for the experiment. Type 1 groundwater contained added naphthalene, 1-methylnaphthalene, and acenaphthene and was used for Control mix and Active mix microcosms (Table 1)(Appendix C). Type 2, type 3 and type 4 groundwater contained, respectively, added naphthalene, 1-methyl naphthalene, and acenaphthene and were used to prepare, respectively, Active Naphthalene, Active 1-methyl naphthalene and Active Acenaphthene microcosms (Table 1)(Appendix C). A repipet® syringe was used to dispense thirty-five ml of the appropriate groundwater to all microcosms. This left a headspace within the microcosms of approximately 20 ml, which was determined to be enough to allow for aerobic conditions during biodegradation (Appendix D). Microcosms were sealed immediately after groundwater addition and incubated in the dark at room temperature.

Sampling times occurred after 1, 14, 23, 38, 48.5, 62, 135, 160, and 183 hours.

During sampling, microcosm hypovials were opened and 16 ml of sample was removed with a 20 ml glass syringe. The 16 ml was placed in an 18 ml vial and 1 ml of methylene chloride was added. The vial was sealed immediately and shaken for 20 min on a rotary shaker. This sample was used for analysis of the creosote compounds (Appendix E).

A.4 APPENDICES:

A.4.1 Appendix A:

Sodium Azide Addition: 0.35 ml of a 10% solution (w/v) of sodium azide was added to the Control Mix microcosms.

A.4.2 Appendix B:

Modified Bushnell Haas Medium consisted of per L: K_2HPO_4, 1.0 g; KH_2PO_4, 1.0 g; NH_4NO_3, 1.0 g; $MgSO_4$*$7H_2O$, 0.2 g; $CaCl_2$*$2H_2O$, 0.02 g; $FeCl_3$, 0.005 g; distilled H_2O, 1000 ml and pH to 7.0 (Mueller et al. 1991. ES and T, 25:1045-1055)

Added 0.65 ml per microcosm (35 ml and 10 g of soil)

A.4.3 Appendix C:

Calculate mass required to add to each microcosm to obtain a water concentration of 2 mg / l

Mass total = Mass (air) + Mass (water) + Mass (soil)

H dimensionless Henry's constant

C concentration

V volume

M mass

$\mathbf{K}_d$ soil partitioning coefficient-values obtained from Mark King's thesis (for naphthalene and 1-methyl naphthalene or calculated using the formula from Mark King's thesis (acenaphthene – $F_{oc}0.002$ and $log(K_{ow}) = 3.92$ (from Sangster, 1989), $K_d = 0.4106$ (from Caitlin Martin))

For Naphthalene:

$$\begin{aligned} M_t &= (H \times C_w) \times V_a + C_w \times V_w + K_d \times C_w \times M_s \\ M_t &= (0.0199 \times 2\,\text{mg / l}) \times 0.020\,\text{l} + 2\,\text{mg / l} \times 0.035\,\text{l} \\ &\quad + (0.16\,\text{ml / g})(0.002\,\text{mg / ml})(10\,\text{g}) \\ M_t &= 0.000796\,\text{mg} + 0.07\,\text{mg} + 0.0032\,\text{mg} \\ M_t &= 0.073996\,\text{mg} / 35\,\text{ml} \end{aligned}$$

Concentration required= 2.114 mg / l

For 1-Methyl-naphthalene:

$$\begin{aligned} M_t &= (H \times C_w) \times V_a + C_w \times V_w + K_d \times C_w \times M_s \\ M_t &= (0.0186 \times 2\,\text{mg}\,/\,\text{l}) \times 0.02\,\text{l} + 2\,\text{mg}\,/\,\text{l} \times 0.035\,\text{l} \\ &\quad + (0.37\,\text{ml}\,/\,\text{g})(0.002\,\text{mg}\,/\,\text{ml})(10\,\text{g}) \\ M_t &= 0.00744\,\text{mg} + 0.07\,\text{mg} + 0074\,\text{mg} \\ M_t &= 0.078144\,\text{mg}\,/35\,\text{ml} \end{aligned}$$

Concentration required $= 2.23\,\text{mg}\,/\,\text{l}$

For Acenaphthene:

$$\begin{aligned} M_t &= (H \times C_w) \times V_a + C_w \times V_w + K_d \times C_w \times M_s \\ M_t &= (0.00997)(1\,\text{mg}\,/\,\text{l}) \times 0.02\,\text{l} + 1\,\text{mg}\,/\,\text{l} \times 0.035\,\text{l} \\ &\quad + 0.4106\,\text{ml}\,/\,\text{g}(0.001\,\text{mg}\,/\,\text{ml})(10\,\text{g}) \\ M_t &= 0.0001994\,\text{mg} + 0.035\,\text{mg} + 0.004106\,\text{mg} \\ M_t &= 0.393054\,\text{mg}\,/35\,\text{ml} \end{aligned}$$

Concentration required $= 1.123\,\text{mg}\,/\,\text{l}$

Type 1 groundwater (mix) (see Table A.2):

- Use $4.32\,\text{l}$ Bottle
- Use a pestle and mortar to grind chemicals before use
- Incubate groundwater at $37\,^{\circ}\text{C}$ for 24 hours while dissolving chemicals into water
- Note: With this larger $4.3\,\text{l}$ bottle chemicals did not dissolve in as well as smaller volume bottles ($2.3\,\text{l}$) (used for types 2 to 4)
- Concentrations after 24 hours of stirring were not what we wanted ... they were low... so had to add more chemical, added additional $0.004\,\text{g}$ of naphthalene, added $0.004\,\text{g}$ of acenaphthene and $1\mu\,\text{l}$ of 1-Methyl-naphthalene

Type 2, 3, and 4 Groundwater (Naphthalene only, 1-Methylnaphthalene only and Acenaphthene Only):

- Use $2.5\,\text{l}$ Bottle

Type 1 Groundwater	**Concentration from mass calculation**	**Dilution from MBH * 1.018**	**4.32 L bottle**	**Actual Addition**
Naphthalene (solubility = 31.7 mg/L	2.114 mg/L	2.15 mg/L	4.32L*2.15 mg/L = 9.2976mg	Fudge Factor: (from preliminary experiment) 1.13*9.2976 mg = 10.05 or **0.0105 g**
1-Methyl naphthalene (solubility = 28.5 mg/L) (density=1.001)	2.2327 mg/L	2.2728 mg/L	4.32L*2.2728 mg/L = 9.8188mg	Fudge Factor: none Add 0.01 g or **10µl (liquid)**
Acenaphthene (solubility = 3.9 mg/L)	1.123 mg/L	1.143214 mg/L	4.32L*1.143214mg/L = 4.938685 mg	Fudge factor: 1.217*4.938685 = 6.01mg **Add 0.006 g**

Table A.2: Design of Type 1 water for microcosm experiment

- Use a pestle and mortar to grind chemicals before use
- Incubate groundwater at 37 °C for 24 hours while dissolving chemicals into water
- Naphthalene: Require $2.15\,\mathrm{mg}/\mathrm{l} \times 2.5\,\mathrm{l} = 5.375\,\mathrm{mg} \times 1.13$ fudge factor =Add $0.0061073\,\mathrm{g}$. This bottle broke while incubating in the 37 °C incubator – was remade and stirred for approximately 7 hours
- 1-Methyl-naphthalene: Require $2.2728\,\mathrm{mg}/\mathrm{l} \times 2.5\,\mathrm{l} = 0.0057\,\mathrm{g}$ or Add $5.7\mu\mathrm{l}$
- Acenaphthene: Require $1.143214\,\mathrm{mg}/\mathrm{l} * 2.5\,\mathrm{l} = 2.858\,\mathrm{mg} * 1.217$ fudge factor = Add $0.0035\,\mathrm{g}$

A.4.4 Appendix D:

Oxygen Calculations:

As per Caitlin Martin's stoichiometric calculations. Oxygen available in microcosm would be 7 times the oxygen necessary to degrade naphthalene, 1-methyl-naphthalene and Acenaphthene.

5.32 mg of oxygen in microcosm – require 0.24 mg for naphthalene (at 2 mg / l- 40 ml), 0.2432 for 1- methyl-naphthalene (at 2 mg / l- 40 ml) and 0.120 mg for acenaphthene (at 1 mg / l -40 ml)

A.4.5 Appendix E:

Method for Analytical Analysis:

ORGANIC GEOCHEMISTRY LABORATORY

DEPARTMENT OF EARTH SCIENCES

Telephone: 519 888 4567 ext. 5180 / 6370

VOLATILE AND SEMI VOLATILE AROMATIC HYDROCARBON ANALYSIS (BENZENE, TOLUENE, ETHYLBENZENE, p+m-XYLENE, o-XYLENE, TRIMETHYLBENZENES (1,3,5; 1,2,4 AND 1,2,3), NAPHTHALENE, INDOLE+ 2-METHYL NAPHTHALENE, 1-METHYL NAPHTHALENE, BIPHENYL, ACENAPHTHYLENE, ACENAPHTHENE, DIBENZOFURAN, FLUORENE, PHENANTHRENE, ANTHRACENE, CARBAZOLE, FLUORANTHENE, PYRENE, BENZO (a) ANTHRACENE, CHRYSENE, BENZO (b+k) FLUORANTHENE, BENZO (a) PYRENE, INDENO (1,2,3,cd) PYRENE and DIBENZO (a,h) ANTHRACENE, AND BENZO (g,h,i) PERYLENE)

INTRODUCTION:

A gas chromatographic technique is described to determine volatile aromatic components of gasoline and some polycyclic aromatic components of creosote, in groundwater samples (the components are listed above). Typically, these compounds are determined by purge and trap or exhaustive extraction techniques. However, because the hydrogeologist may require many analyses to define the shape, movement and attenuation of a trace contaminant plume, purge and trap methods are too time consuming to use on a routine basis. Separatory funnel or continuous solvent extraction techniques are not only slow and labour intensive but can also suffer from volatilization losses. The methodology presented here was derived from an extraction previously described by Henderson et. al.(1976). The technique required that the partitioning of the analyte be at equilibrium between the two phases, as opposed to being exhaustively extracted from the water.

APPARATUS:

Aqueous groundwater samples and methanolic standards are extracted in 18 ml crimp-top hypovials with Teflon-faced silicone septa. The determinations are performed on a gas chromatograph equipped with a splitless injection port, a 0.25mm X 30M glass DB5 capillary column with a film thickness of 0.25um and a flame ionization detector. The chromatographic conditions are as follows: injection port temperature, 275°C; initial column temperature, 35°C; initial time, 0.5 min.; heating rate, 15°C/min.; final temperature, 300°C; final time, 10.0 min. ; detector temperature, 325°C; column flow rate, 3 ml/min helium.

PROCEDURE:

(i)SAMPLE BOTTLE PREPARATION. Bottles and other glassware are soaked in a commercial alkaline cleaning solution for several hours, then rinsed with deionized water, dilute nitric acid, and more deionized water. The bottles are then baked overnight at 110°C

(ii)SAMPLE COLLECTION AND HANDLING. Each 18 ml hypovial sample bottle is filled without headspace, quickly crimp sealed with a Teflon septa and then stored at 4°C until extracted (7-14 day time limit). Prior to capping, sodium azide (200ul of a 10 % solution) may be added to the sample bottle as a preservative, if analysis will not occur with 7days.

To solvent extract a sample (or standard), the septum cap of the vial is quickly removed and 2.0 ml of water is removed with a syringe. This is followed by the addition of 1.0 ml of dichloromethane, containing the internal standards m-fluorotoluene and 2-fluorobiphenyl. The vial is quickly resealed and agitated on its side at maximum speed (350 rpm) on a platform shaker for 15 min. After shaking, the vial is inverted and the phases are allowed to separate for 10 to 30 minutes. Approximately 0.7ml of the dichloromethane phase is removed from the inverted vial with a syringe (through the septum) and placed in a sealed autosampler vial for injection into the gas chromatograph.

(iii)QUALITY CONTROL. Samples and standards are equilibrated to room temperature (approx. 22°C) before extraction. A calibration is made in internal standard mode and standards are run in triplicate at four different levels (or more) covering the expected sample range. A multiple point linear regression is performed to determine linearity and slope of the calibration curve. Standards are prepared by spiking water with a concentrated methanolic stock standard, and are extracted in the same manner as samples. Three methanolic stock standards are used, each

Units are $\mu g / l$	MDL
naphthalene	2.18
1-methyl naphthalene	2.68
acenaphthene	2.27

Table A.3: Method Detection Limits (MDL)

an order of magnitude above the other. The methanolic stock standard is prepared gravimetrically, injecting the various pure compounds through a septum into one 60 ml aliquot of methanol, or are purchased commercially.

Matrix spikes are performed by spiking a known amount of mid-range standard into a duplicate field sample and then calculating the amount recovered after extraction. Reagent water blanks are run on a daily basis. The methanolic stock standards are stored in a freezer when not in use and are replaced when accuracy becomes unacceptable

LITERATURE CITED.

Henderson, J.E., G.R. Peyton and W.H. Glaze (1976). A convenient liquid-liquid extraction method for the determination of halomethanes in water at the parts-per-billion level. IN: Identification and analysis of organic pollutants in water. Keith, L.H. ed. Ann Arbor Science Publishers Inc., Ann Arbor, MI.

Appendix B

Sample BIONAPL input file

```
BIONAPL MODEL -
    80x30x17 elements - Borden 3D creosote model, flow & transport
    May 2004
    0 0 0 0 0 0 0 0 0 1 1 0 1
;kp,kcn,kwt,kint,kintv,kgo,kg,kranb,krans,kbio,mode,keqm,krtype
    2 5 1 ;ngx, ngy, ngz # of uniform sections per direction
    20. 60. ;xlim length of section
    3 4.5 10.5 12 15 ;ylim in [m]
    6.8 ;zlim Aquifer thickness
    40 40 ;nlx # of elements per section
    3 3 18 3 3 ;nly
    17 ;nlz
    0 00. 0.0 0.0 1810. ;nwtl,datum,gamma,sdecay,rhob
    30 1 1 17 -1 ;monitor well
    0 ;INIT
    1 81 1 31 1 18 10.00 +1 ; initial condition head
    1 1 1 31 1 18 10.234 +1 ; initial condition head left face
    81 81 1 31 1 18 10.00 -1 ; initial condition head right face
    1 1 0 0 0 2 ;B.C.'S (FLOW) fixed flow at upper
```

1 31 1 18 -1 ;node range:type-1 at face 1 (left)

1 31 1 18 -1 ;node range:type-1 at face 2 (right)

1 81 1 31 0.840E-08 -1 ;groundwater recharge 265mm/yr

1 40800 8.8e-5 8.8e-5 8.8e-5 -1 ;1-NEL,KX,KY,KZ (m/s)

0 0 0 0 0 0 0.e-4 0.e-4 0.e-5 -1 ;inner source K of source

4 4 9 14 10 13 0.05e-0 +1 ;initial sn by node: Source and Saturation

4 4 18 23 10 13 0.05e-0 -1 ;initial sn by node: Source and Saturation

11 11 1 31 1 18 ;fence definition

0.0e-3 0.33 0.05 1.5e-4 ;SS,POR,srw,gradius

6 1 xlam b Kc Km DD ;# of components,#ea

Naphthalene

1100 .12818 0.1505 55.46 0.002 0.0 2.2e-4 0.0 1.0e-10 0 0.
;rho,mw,aqs,#m,Sh,b,kc,km,D,kdp,xdp

XYLENE

860 0.10616 0.196 26.84 0.002 0.0 1.10e-4 0.0 1.0e-10 0 0.
;rho,mw,aqs,#m,Sh,b,kc,km,D,kdp,xdp

ONE-METHYL-NAPHTHALENE

1050 0.14219 0.0285 9.95 0.002 0.0 2.40E-4 0.0 1.0e-10 0 0.
;rho,mw,aqs,#m,Sh,b,kc,km,D,kdp,xdp

ACENAPTHENE

1100 0.1542 0.0198 34.11 0.002 0.0 1.03E-3 0.0 1.0e-10 0 0.
;rho,mw,aqs,#m,Sh,b,kc,km,D,kdp,xdp

GROW

1100 0.16871 0.0593 106.40 0.002 0.0 1.61e-3 0.0 1.0e-10 0 0.
;rho,mw,aqs,#m,Sh,b,kc,km,D,kdp,xdp

OTHER

1100 .260 0.001 150.19 0.002 0.0 2.5e-2 0.0 1.0e-10 0 0.
;rho,mw,aqs,#m,Sh,b,kc,km,D,kdp,xdp

0.05 0.002 0.004 3.24 0.5 9999. ;utils,uhs,uho,ros,ym,cinib NAPH

0.12 0.002 0.004 3.17 0.5 9999. ;utils,uhs,uho,ros,ym,cinib XYLENE

0.15 0.002 0.004 3.04 0.5 9999. ;utils,uhs,uho,ros,ym,cinib one-m-naph

0.001 0.002 0.004 3.01 0.5 9999. ;utils,uhs,uho,ros,ym,cinib ACENAPTHENE

0.10 0.002 0.004 2.93 0.5 9999. ;utils,uhs,uho,ros,ym,cinib GROW

0.05 0.002 0.004 3.20 0.5 9999. ;utils,uhs,uho,ros,ym,cinib OTHER

1. 9999. ;reto,xkin

1000. 1.00e-10 .014 ;retm,bm,ymmax

0.0200 0.001 ;BACKGROUND CONC. EA1,EA2...-M1,M2...

0.0200 0.001 ;INITIAL SOURCE CONC. EA1,M1, EA2,M2

0.000001 0.000001 ;threshold S,EA1,EA2...

1 81 1 31 1 18 1 0.0 0.0 +1 ;initial condition NAPH

1 81 1 31 1 18 2 0.0 0.0 +1 ;initial condition XYLENE

1 81 1 31 1 18 3 0.0 0.0 +1 ;initial condition one-m-naph

1 81 1 31 1 18 4 0.0 0.0 +1 ;initial condition ACENAPTHENE

1 81 1 31 1 18 5 0.0 0.0 +1 ;initial condition GROW

1 81 1 31 1 18 6 0.0 0.0 +1 ;initial condition OTHER

1 81 1 31 1 18 8 0.02 0.02 -1 ;initial condition Oxygen

1 0 0 0 0 0 ;B.C.'S (TRANSPORT) -

1 31 1 18 -1

1 0 0 0 0 0 ;B.C.'S (HA carrier TRANSPORT) -

1 31 1 18 -1

1 0 0 0 0 0 ;B.C.'s Oxygen

1 31 1 18 -1

0 1.0 .0 0.47 0.000 ;ka,n,xmtc,feqm,qha(kgHA/kgsol) (HA sorption)

0 0. 0. 0. ;IVEL,VX,VY,VZ

1 80 1 30 1 17 0.36 .108 .00036 0.000 -1 ;AL,ATH,ATV,decay(bckgnd)by elm

.01 .001 2 2 ;CCP,CCc(i)%,CCW,MAXIT1,MAXIT2

1.0 1.00 ;OVER-RELAX HEADS,temp

0 0 0 0 0 ;KNOX(1)(2)TRANSV. SECTION

5 0 0 0 0 ;KNOY(1),(2)LONG. SECTION

12 ;knoz

00. 00. 00. 00. 00. ;five 3d print times (days)

0. 5. 0.20 10 999 +1 ;t0,t1,dt,kplot(days),kmom

5. 5. 5. 5. 5. 5. 5. 5. ;new ccc

0.000 1. 1.0 0. 0 ;hinc,rinc,sfact,eqmfact,kha

1 1 1 1 1 -0.0 0. 0.0 -1 ;ix,iy,iz1,iz2,kcomp,q(m3/s)conc,rad,more

5. 100. 0.5 100 999 +1 ;t0,t1,dt,kplot(days),kmom

5. 5. 5. 5. 5. 5. 5. 5. ;new ccc

0.000 1. 1.0 0. 0 ;hinc,rinc,sfact,eqmfact,kha

1 1 1 1 1 -0.0 0. 0.0 -1 ;ix,iy,iz1,iz2,kcomp,q(m3/s)conc,rad,more

100. 278. 1.0 178 178 +1 ;t0,t1,dt,kplot(days),kmom

5. 5. 5. 5. 5. 5. 5. 5. ;new ccc

0.000 1. 1.0 0. 0 ;hinc,rinc,sfact,eqmfact,kha

1 1 1 1 1 -0.0 0. 0.0 -1 ;ix,iy,iz1,iz2,kcomp,q(m3/s)conc,rad,more

278. 300. 1.0 178 100 +1 ;t0,t1,dt,kplot(days),kmom

5. 5. 5. 5. 5. 5. 5. 5. ;new ccc

0.000 1. 1.0 0. 0 ;hinc,rinc,sfact,eqmfact,kha

1 1 1 1 1 -0.0 0. 0.0 -1 ;ix,iy,iz1,iz2,kcomp,q(m3/s)conc,rad,more

300. 626. 1.0 326 326 +1 ;t0,t1,dt,kplot(days),kmom

5. 5. 5. 5. 5. 5. 5. 5. ;new ccc

0.000 1. 1.0 0. 0 ;hinc,rinc,sfact,eqmfact,kha

1 1 1 1 1 -0.0 0. 0.0 -1 ;ix,iy,iz1,iz2,kcomp,q(m3/s)conc,rad,more

626. 700. 1.0 326 100 +1 ;t0,t1,dt,kplot(days),kmom

5. 5. 5. 5. 5. 5. 5. 5. ;new ccc

0.000 1. 1.0 0. 0 ;hinc,rinc,sfact,eqmfact,kha

1 1 1 1 1 -0.0 0. 0.0 -1 ;ix,iy,iz1,iz2,kcomp,q(m3/s)conc,rad,more

700. 1008. 1.0 308 308 +1 ;t0,t1,dt,kplot(days),kmom

5. 5. 5. 5. 5. 5. 5. 5. ;new ccc

0.000 1. 1.0 0. 0 ;hinc,rinc,sfact,eqmfact,kha

1 1 1 1 1 -0.0 0. 0.0 -1 ;ix,iy,iz1,iz2,kcomp,q(m3/s)conc,rad,more

1008. 1100. 1.0 308 100 +1 ;t0,t1,dt,kplot(days),kmom

5. 5. 5. 5. 5. 5. 5. 5. ;new ccc

0.000 1. 1.0 0. 0 ;hinc,rinc,sfact,eqmfact,kha

1 1 1 1 1 -0.0 0. 0.0 -1 ;ix,iy,iz1,iz2,kcomp,q(m3/s)conc,rad,more

1100. 1357. 1.0 257 257 +1 ;t0,t1,dt,kplot(days),kmom

5. 5. 5. 5. 5. 5. 5. 5. ;new ccc

0.000 1. 1.0 0. 0 ;hinc,rinc,sfact,eqmfact,kha

1 1 1 1 1 -0.0 0. 0.0 -1 ;ix,iy,iz1,iz2,kcomp,q(m3/s)conc,rad,more

1357. 1400. 1.0 257 100 +1 ;t0,t1,dt,kplot(days),kmom

5. 5. 5. 5. 5. 5. 5. 5. ;new ccc

0.000 1. 1.0 0. 0 ;hinc,rinc,sfact,eqmfact,kha

1 1 1 1 1 -0.0 0. 0.0 -1 ;ix,iy,iz1,iz2,kcomp,q(m3/s)conc,rad,more

1400. 2900. 1.0 1500 1500 +1 ;t0,t1,dt,kplot(days),kmom

5. 5. 5. 5. 5. 5. 5. 5. ;new ccc

0.000 1. 1.0 0. 0 ;hinc,rinc,sfact,eqmfact,kha

1 1 1 1 1 -0.0 0. 0.0 -1 ;ix,iy,iz1,iz2,kcomp,q(m3/s)conc,rad,more

2900. 3300. 1.0 400 400 +1 ;t0,t1,dt,kplot(days),kmom

5. 5. 5. 5. 5. 5. 5. 5. ;new ccc

0.000 1. 1.0 0. 0 ;hinc,rinc,sfact,eqmfact,kha

1 1 1 1 1 -0.0 0. 0.0 -1 ;ix,iy,iz1,iz2,kcomp,q(m3/s)conc,rad,more

3300. 3619. 1.0 319 319 -1 ;t0,t1,dt,kplot(days),kmom

5. 5. 5. 5. 5. 5. 5. 5. ;new ccc

0.000 1. 1.0 0. 0 ;hinc,rinc,sfact,eqmfact,kha

1 1 1 1 1 -0.0 0. 0.0 -1 ;ix,iy,iz1,iz2,kcomp,q(m3/s)conc,rad,more